

12-2013

Developmental And Molecular Functions Of Plakophilin-3

William A. Munoz

Follow this and additional works at: https://digitalcommons.library.tmc.edu/utgsbs_dissertations



Part of the [Cell Biology Commons](#), [Developmental Biology Commons](#), [Developmental Neuroscience Commons](#), [Laboratory and Basic Science Research Commons](#), and the [Medicine and Health Sciences Commons](#)

Recommended Citation

Munoz, William A., "Developmental And Molecular Functions Of Plakophilin-3" (2013). *Dissertations and Theses (Open Access)*. 405.

https://digitalcommons.library.tmc.edu/utgsbs_dissertations/405

This Dissertation (PhD) is brought to you for free and open access by the MD Anderson UTHealth Houston Graduate School at DigitalCommons@TMC. It has been accepted for inclusion in Dissertations and Theses (Open Access) by an authorized administrator of DigitalCommons@TMC. For more information, please contact digcommons@library.tmc.edu.

DEVELOPMENTAL AND MOLECULAR FUNCTIONS OF PLAKOPHILIN-3

by

William A. Muñoz, B.S.

APPROVED:

Supervisory Professor, Pierre D. McCrea, Ph.D.

Michelle C. Barton, Ph.D.

Fernando R. Cabral, Ph.D.

Michael J. Galko, Ph.D.

Malgorzata Kloc, Ph.D.

Gregory S. May, Ph.D.

APPROVED:

Dean, The University of Texas
Graduate School of Biomedical Sciences at Houston

DEVELOPMENTAL AND MOLECULAR FUNCTIONS OF PLAKOPHILIN-3

A

DISSERTATION

Presented to the Faculty of

The University of Texas

Health Science Center at Houston

and

The University of Texas

MD Anderson Cancer Center

Graduate School of Biomedical Sciences

in Partial Fulfillment

of the Requirements

for the Degree of

DOCTOR OF PHILOSOPHY

by

William A. Muñoz, B.S.
Houston, Texas

Date of Graduation (*December, 2013*)

DEDICATION

I would first like to dedicate this work to my sister Katherine, whom in her short time with us had such a major impact on the world, and was my inspiration for pursuing a biomedical research career.

I would also like to dedicate this work to my parents, Guillermo and Susan, and my wonderful wife, Jennifer. Without their love, support and consideration this work could not be and I would not be the person I am today.

ACKNOWLEDGEMENT

First, I would like to thank my mentor, Pierre D. McCrea, Ph.D. for his extreme patience and support. During my time in the lab, he has pushed me to excel, has been an invaluable resource in my education and has always encouraged my career progression. For this, I am truly appreciative.

I would like to thank the members of my current and past committees: Malgorzata Kloc, Ph.D.; Michael Galko, Ph.D.; Fernando Cabral, Ph.D.; Michelle Barton, Ph.D.; Jill Schumacher, Ph.D.; and Gregory May, Ph.D. I appreciate them for their guidance, kindness and insight.

I would also like to thank the current and past members of the McCrea lab: Rachel Miller, Ph.D.; Moonsup Lee; Hong Ji; Kyucheol Cho, Ph.D.; Dongmin Gu, Ph.D.; Ji-Yeon Hong, Ph.D. I will always appreciate the times I had with them in and out of the lab.

In addition, I would like to thank Sabrina Stratton and Kendra Allton for so often providing me with experimental protocols, and helping optimize those protocols in my hands.

There are numerous others that I would like to thank for their friendship and support that made graduate school a great experience.

I would like to thank the Genes & Development program, especially Elisabeth Lindheim, and the Department of Biochemistry and Molecular Biology at UT MD Anderson Cancer Center for providing me with wonderful support and a superb environment to learn.

Finally, I would like to thank my parents and wife for the love and encouragement to help finish my studies.

This work was supported by a Research Supplement to Promote Diversity in Health-Related Research, a Cancer Prevention and Research Institute of Texas Research Training Award (RP101502), and by The University of Texas Graduate School of Biomedical Science (GSBS) – Houston.

DEVELOPMENTAL AND MOLECULAR FUNCTIONS OF PLAKOPHILIN-3

William Muñoz, Ph.D.

Supervisory Professor: Pierre D. McCrea, Ph.D.

Plakophilin-3, the less studied member of the plakophilin-catenin subfamily, and the larger catenin family, binds directly to desmosomal cadherin cytoplasmic domains and enhances desmosome formation and stability. In mammals, plakophilin-3 is expressed at the highest levels in desmosome-enriched tissues such as epithelia, with the knock-out in mice producing corresponding reductions in ectodermal integrity. In tissue, cellular and intracellular contexts where plakophilin-3 is not at the desmosomal plaque, little is known about its functions in the cytoplasm or nucleus, where it also localizes.

My work employed embryos of the amphibian, *Xenopus laevis*, to examine plakophilin-3's developmental roles. I first evaluated the expression pattern of endogenous plakophilin-3 mRNA and protein, revealing two principal and differentially expressed isoforms, and an enrichment in neural tissues as well as various epithelial structures. Further, despite conflicting reports on plakophilin-3's nuclear localization, I showed that plakophilin-3 consistently localizes to the nucleus in both *Xenopus* naive ectoderm (animal caps) and mouse embryonic stem cells. To assess the *in vivo* functions of plakophilin-3, I employed sequence specific anti-sense morpholinos to knock-down its gene products. This resulted in developmental defects in the ectoderm, heart, the formation or maintenance of cilia, tactile sensation, neural crest establishment and migration, and the peripheral nervous system. These phenotypes were specific based upon the use

of distinct non-overlapping morpholinos, and in the case of neural crest, the use of rescue experiments with morpholino-resistant plakophilin-3 mRNA. As noted below, the delineation of which phenotypes result from plakophilin-3's functions at the desmosome, or in the cytoplasm, versus or in addition to those in the nucleus, is a point of continuing interest. My results in all cases point to plakophilin-3's essential roles in *Xenopus* development.

In probing for novel plakophilin-3 actions in the nucleus as well as elsewhere in the cell, I performed a yeast two-hybrid screening of a mouse brain cDNA library, resolving and then validating its interaction with ETV1. ETV1 is an ETS transcription factor family member with important roles in neural development as well as human disease progression. Plakophilin-3's interaction with ETV1 was confirmed using biochemical, functional, and developmental assays that centered ultimately upon plakophilin-3's ability to regulate ETV1 transcriptional activity. These findings reveal the first sequence specific transcription factor to bind a member of the plakophilin-catenin subfamily.

Together, my work supports plakophilin-3's essential roles in amphibian development, and shows plakophilin-3's biochemical and functional association with ETV1. In a wider context, it strengthens the view that many (perhaps all?) catenin proteins play key roles at both cell-cell junctions and in the nucleus, as well as elsewhere in the cell, and raises the longer-term question of if such relationships might assist in integrating information across distinct cellular compartments.

TABLE OF CONTENTS

Approval Page	i
Title Page	ii
Dedication	iii
Acknowledgements	iv
Abstract	vi
Table of Contents	viii
List of Illustrations	xi

Chapter I: Introduction

<i>Cadherins and catenins</i>	2
<i>Pkp-catenin sub-family</i>	7
<i>Pkp3</i>	9
<i>ETS transcription factor family</i>	10
<i>ETV1</i>	12
<i>Summary</i>	13

Chapter II: Results

Part One: Characterization of *Xenopus* Pkp3

<i>Identification of the <i>Xenopus</i> Pkp3 ortholog</i>	15
<i><i>Xenopus</i> Pkp3 temporal expression</i>	17
<i><i>Xenopus</i> Pkp3 spatial expression</i>	21
<i><i>Xenopus</i> Pkp3 subcellular localization</i>	24

<u>Part Two: Developmental Roles of Pkp3-catenin</u>	
<i>Knockdown of endogenous Pkp3 upon treatment with morpholinos</i>	31
<i>Pkp3 depletion results in ectodermal fragility</i>	32
<i>Touch hyposensitivity and neural phenotypes in</i>	
<i>Pkp3 depleted embryos</i>	41
<i>Pkp3 may have a role in neural crest cell induction and migration</i>	51
 <u>Part Three: Identification of the Pkp3-catenin:ETV1 complex</u>	
<i>Yeast two-hybrid screening identified a novel Pkp3-associated protein</i>	57
<i>ETV1 interacts with Pkp3 in cells</i>	59
<i>Interaction domain mapping of the Pkp3:ETV1 complex</i>	60
<i>xETV1 partially rescues molecular phenotypes resulting from</i>	
<i>xPkp3 depletion in Xenopus embryos</i>	71
<i>Pkp3 positively modulates ETV1-dependent transcriptional activation</i>	74
 <u>Chapter III: Discussion</u>	80
<i>Pkp3 isoforms, expression and subcellular localization</i>	81
<i>Developmental roles of Pkp3</i>	84
<i>Identification of the Pkp3:ETV1 interaction</i>	90
<i>Concluding remarks</i>	93
 <u>Chapter IV: Materials and Methods</u>	100

<u>References</u>	114
<u>Vita</u>	139

LIST OF ILLUSTRATIONS

Figure 1. Schematic diagram of the catenin family	4
Figure 2. The known roles of p120- and Pkp-catenin subfamily proteins and the predicted roles of Pkp-catenin subfamily proteins	5
Figure 3. Pkp3 domain structure and amino acid sequence alignment	16
Figure 4. <i>Xenopus</i> Pkp3 temporal expression profiles	18
Figure 5. Characterization of affinity purified rabbit polyclonal antibodies that are directed against the N-terminal domain of Pkp3 (amino acids 1-350).	20
Figure 6. <i>Xenopus</i> Pkp3 spatial expression profiles during development	22
Figure 7. Adult <i>Xenopus</i> Pkp3 spatial expression	25
Figure 8. Expression of exogenous Pkp3-Myc in <i>Xenopus</i> extracts	26
Figure 9. Pkp3 subcellular localization	28
Figure 10. Two independent morpholinos knockdown Pkp3 protein expression	33
Figure 11. Pkp3 depletion does not notably affect Pkp2 mRNA levels	34
Figure 12. Depletion of endogenous Pkp3 results in skin fragility	35
Figure 13. Depletion of endogenous Pkp3 results in loss of desmosomes, increased secretory vesicle size and relocalization of mitochondria	36
Figure 14. Pkp3 depletion alters the morphology of various cellular features	39
Figure 15. Pkp3 depletion results in reductions of multiciliated cells	

and neural tracts	40
Figure 16. Pkp3 depletion results in permanent kinked axes due to prolonged entrapment in Vitelline membrane	42
Figure 17. Pkp3 depletion results in tactile hyposensitivity	44
Figure 18. Pkp3 depletion does not appear to affect early muscle formation	45
Figure 19. Pkp3 depletion does not significantly affect motorneurites along the somite boundaries	48
Figure 20. Pkp3 depletion results in late developmental neural defects .	49
Figure 21. Pkp3 knockdown significantly affects certain peripheral neural structures	50
Figure 22. Neural crest derived tissues are disrupted upon Pkp3 depletion	53
Figure 23. Neural crest induction and migration is disrupted upon Pkp3 depletion	54
Figure 24. Expression of neural crest markers Twist and Foxd3 is affected by Pkp3 knockdown, but can be rescued by exogenous Pkp3 mRNA not targeted by Pkp3 morpholinos further indicating specificity of morpholinos	55
Figure 25. ETV1 and ETV5 are potential novel binding partners of Pkp3-catenin identified via yeast-two-hybrid	58
Figure 26. ETV1 and Pkp3 interact in cells	61
Figure 27. Pkp3 localizes to nuclei of mouse embryonic stem cells .	63
Figure 28. ETV1 overexpression promotes Pkp3 nuclear localization .	64
Figure 29. Ectopic mitochondrial outer membrane (MOM) localization of Pkp3	66

Figure 30. Ectopic mitochondrial outer membrane (MOM)	
co-recruitment of xPkp3 with xETV1 in HeLa cells and	
ETV1 binding domain mapping	67
Figure 31. Ectopic mitochondrial outer membrane (MOM)	
co-recruitment of xETV1 with xPkp3 in HeLa cells and	
Pkp3 binding domain mapping	69
Figure 32. Rescue of neural crest establishment defects, induced upon	
xPkp3-catenin depletion, through ectopic expression of xETV1	72
Figure 33. Pkp3-catenin regulation of ETV1 reporters	75
Figure 34. Pkp3-catenin regulation of ETV1 target genes in vivo	78
Figure 35. Potential molecular mechanisms regulating Pkp3 developmental	
functions in amphibians	87
Figure 36. Transcriptional activity of various catenin family members	95

Chapter I

Introduction

Cadherins and catenins

Cadherins are calcium-dependent cell adhesion molecules best known for their roles in mediating cell-cell adhesions [1]. While the cadherin family consists of more than a hundred members, most can be characterized by an extracellular domain, a single transmembrane domain and a cytoplasmic domain [2]. The cadherin family is divided into several sub-families including: the classical cadherins, the desmosomal cadherins, and the protocadherins, among others. The classical and desmosomal cadherins are the central cell-cell adhesive components of the adherens junctions and desmosomes, respectively, along with their associated catenins. Such cadherin-catenin complexes, and their associated larger cytoskeletal (etc.) structures, have significant effects on the formation and maintenance of tissue architecture throughout the body [3,4]. Further, defects in these components or their functions contribute to pathology, including tumor progression and metastasis [5-10].

Catenins were initially defined for their interaction with cadherins at cell borders [11], and all, with the exception of alpha-catenin, possess an Armadillo-domain composed of either nine or twelve repeats (each of approximately 42 amino acids) [12-18]. Based upon overall sequence similarity, the size of the Armadillo-domain and the region of the cadherin cyto-domain to which they bind, the catenin family has been divided into three sub-families: the beta-catenin subfamily (beta-catenin and plakoglobin/ gamma-catenin), the p120-catenin sub-

family [p120-catenin, ARVCF (Armadillo repeat gene deleted in velocardiofacial syndrome), delta-catenin, and p0071], and the Plakophilin (Pkp) subfamily (Pkps 1 to 3) (Figure 1) [19-21]. The catenins have evolved in some cases to have various other protein binding domains, such as a carboxyl-terminal PDZ motif (beta-catenin, ARVCF, delta-catenin, and p0071) and a coiled-coiled domain positioned upstream of the Armadillo domain (only in the p120 subfamily) [20]. Especially through the Armadillo-domain, various protein-protein interactions occur. The best characterized of these interactions are with the classical cadherins of the adherens junction (a site of cell-cell adhesion), where the Armadillo domain of a beta-catenin subfamily member associates with the membrane-distal cytoplasmic tail of the cadherin, and a p120-catenin subfamily member binds with the membrane-proximal region [22-27]. The Pkp catenins localize at desmosomes, specialized sites of cell-cell adhesion most prominent in mechanically stressed tissues, interacting through their amino terminal region (rather than their Armadillo-domain) to the cytoplasmic tail of desmosomal cadherins [16,20,28,29]. Interestingly, the plakoglobin-catenin (gamma-catenin) has been shown to bind cadherins of both the adherens and desmosomal junctions [21,30].

Catenins have numerous roles throughout the cell (Figure 2). At the cadherin complex they contribute to cadherin stability (p120- and Pkp sub-families) [5,28,29,31-34]. The p120 subfamily is predominately thought to promote cadherin stability by inhibiting clathrin-mediated endocytosis of the

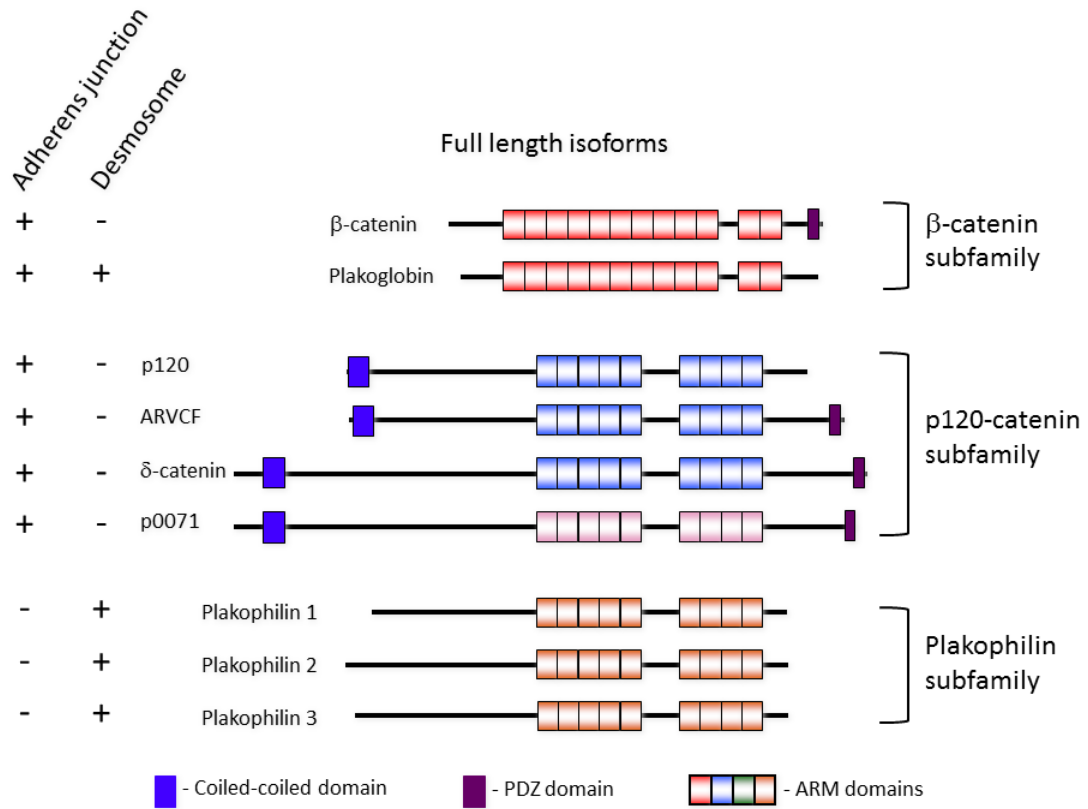


Figure 1. Schematic diagram of the catenin family.

Depicted are catenins divided into their individual sub-families including the beta-catenin, p120-catenin, and Pkp subfamilies.

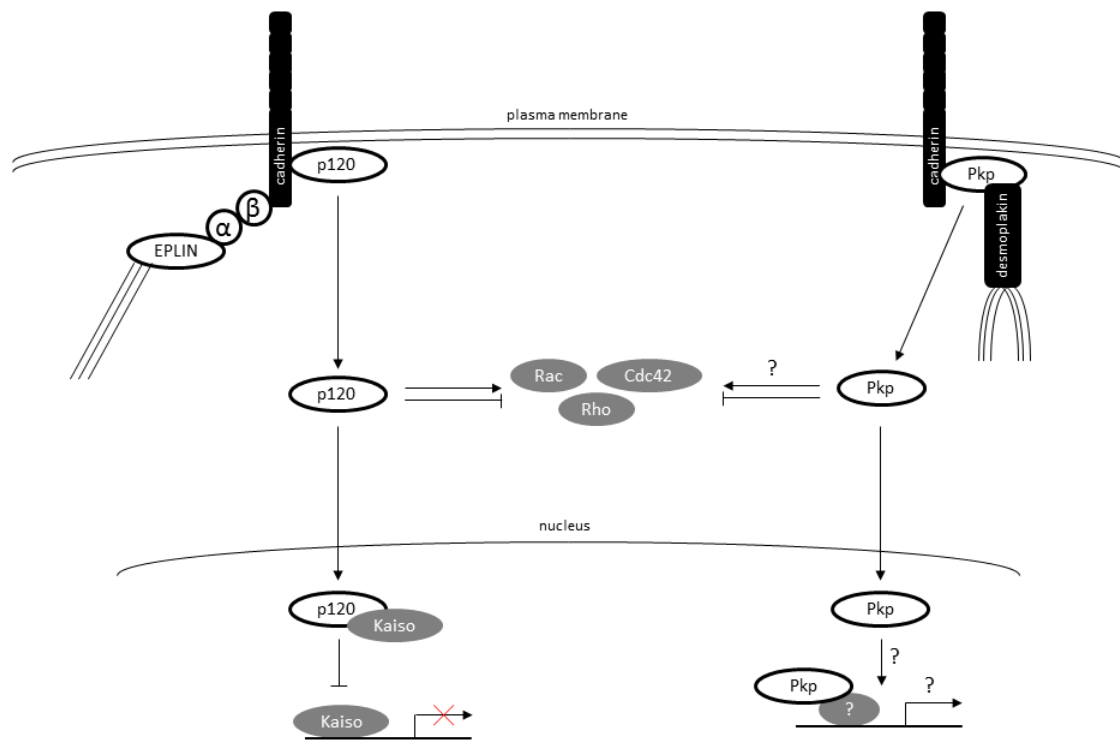


Figure 2. The known roles of p120- and Pkp-catenin subfamily proteins and the predicted roles of Pkp-catenin subfamily proteins.

At cell-cell contacts, the p120- and Pkp-catenin subfamily members stabilize the cadherin complexes at either the adherens junction or desmosome, respectively. p120 sub-family members also modulate small Rho GTPases with early evidence suggesting similar roles for Pkp sub-family members. P120-catenin binds to transcriptional repressor, Kaiso, de-repressing Kaiso target genes. The Pkps localize to the nucleus with nuclear binding partners now being characterized by several groups.

classical cadherin, where the cadherins are subjected to lysosomal degradation [35-37]. The Pkp subfamily members ensure desmosomal cadherin stability by promoting the transport of cadherins to the desmosome and providing a scaffold for the complex linking the various desmosomal components [16,17,29,32,38-42]. The catenins also indirectly link either the adherens junctions or desmosomal junctions to the cytoskeleton (beta-catenin and Pkp subfamilies), enhancing the strength of the junction leading to a junctional-cytoskeletal interdependence [16,28,29,32,43-47].

In the cytoplasm, the p120- and Pkp sub-families have been shown to modulate the activity of Rho-family GTPases [17,42,48-53]. The p120 subfamily modulates Rho family small G proteins, including RhoA, Rac1 and Cdc42- affecting cytoskeletal formation, cell motility, and endocytosis [34,48-50,52,54]. While not as well understood, Pkps also affect cell shape through a RhoA dependent mechanism [55,56]. Initial results indicate Pkp2 regulates RhoA activity through the relocation of active RhoA to intercellular interfaces upon cell-cell contact contributing to cortical actin remodeling, having downstream effects on desmosome assembly [42].

Finally, most if not all catenins localize to the nucleus [18]. For example, significant research has shown that beta-catenin relieves TCF/LEF-mediated transcriptional repression following canonical Wnt-pathway activation. p120-catenin has been shown to bind the transcriptional repressor Kaiso, Glis2 and the

REST/CoREST complex [57-60] (Moonsup Lee's unpublished results). p120-catenin (isoform1) also appears to respond to canonical Wnt signals by de-repressing Kaiso gene targets, including some shared with beta-catenin/TCF [58,61-66]. In comparison to members of the p120-catenin or beta-catenin subfamilies, very little is known about Pkp-catenins' interactions or roles in the cytoplasm or nucleus.

Pkp-catenin sub-family

Defects in Pkp expression or function have been linked to several developmental diseases, such as skin dysplasia resulting from Pkp1 mutations, where hyperkeratinosis and blistering follows impact trauma [7,67-72]. Pkp2 mutations have been found to contribute to arrhythmogenic right ventricular cardiomyopathy (heart failure), in which heart muscle is replaced by a fatty tissue [17,73-76]. Interestingly, cancer studies suggest that Pkps have roles as both tumor suppressors and oncogenes [10,55,77-80], indicating they may have multiple activities to produce these effects.

Pkps form a subfamily of catenins, each containing an Armadillo-repeat domain that is structurally homologous to those present in members of the beta-catenin as well as p120-catenin subfamilies [10,16-18,81,82]. The Pkps consist of Pkps-1, -2, and -3 and are characterized by nine Armadillo repeats, a highly variable amino terminal domain and a short or absent carboxy terminal domain.

Additionally, the Pkps have been identified in a variety of tissues with their localization rarely overlapping, suggesting that they may have independent, yet complementary roles.

As mentioned earlier, the Pkps assist in assembling and stabilizing desmosomal cell-cell junctions through interactions with the cytoplasmic tail of desmosomal cadherins (named desmocollins and desmogleins), that span the plasma membrane and interact with intracellular desmosomal components such as desmoplakin and intermediate filaments [16,32,76,83,84]. These interactions aid in connecting desmosomal junctions to the intermediate filament cytoskeleton, promoting the physical integrity of multiple tissues subjected to mechanical stress [7,28,29,39,45,46,84-87]. While their cytoplasmic functions are less clear at present, Pkps are involved in regulating mRNA expression, protein translation, the trafficking of desmosomal cadherins and insulin-induced cell proliferation [41,80,88,89]. In addition to junctional and cytoplasmic localizations and roles, Pkp-catenins have also been reported to localize to the nucleus in some contexts [18,40,90-96]. Conceivably, some Pkp roles might later prove to be analogous to those of the beta- and p120-catenin subfamily members, in that they may associate with transcription-factor partners (e.g. beta-catenin binds/ modulates TCF/LEF, and p120-catenin binds/ modulates Kaiso) [57-59]. Thus far, the nuclear associations of the Pkps have intriguingly included Pkp1 binding to single-stranded DNA and Pkp2 to the RNA polymerase III holoenzyme [97,98].

The functional roles of these particular nuclear interactions require future clarification.

Pkp3

Pkp3 is the least understood member of the Pkp sub-family. Mammalian systems have demonstrated that the highest levels of Pkp3 are found in tissues enriched for desmosomes, such as in simple epithelia or the living layers of stratified epithelia and the epidermis [93,99,100]. However, Pkp3 mRNA is expressed in most tissues of mammals [101]. The targeted whole-animal knockout of Pkp3 in mice resulted in hair shaft abnormalities, skin inflammatory responses, and disruptions of desmosome assembly in the epidermis. As no further effects were reported, Pkp3^{-/-} desmosomal defects in mice appear to predominate in skin. [102]. However, additional Pkp3 phenotypes may have been masked by partial compensation by Pkp1 or 2, given that they each showed increased expression in the Pkp3 knockout mouse.

In pathology, Pkp3 misexpression has been associated with non-small cell lung carcinomas, squamous cell carcinomas, gastric carcinoma, breast carcinoma and adenocarcinomas [55,77,79,103-105]. It has also been shown that reduction of Pkp3 levels in HCT116 cells enhances their metastatic potential in mice [78].

In addition to interactions shared among different Pkp proteins (desmosomal cadherins, desmoplakin and plakoglobin), Pkp3 exhibits some distinctions. For example, Pkp3 associates with a wider range of desmosomal proteins than the other Pkps and has been shown to interact with components of stress granules with strong localization to this structure [45,88]. In addition, Pkp3 has been found to localize to the nucleus under certain conditions in addition to other cellular structures [40,95,99]. Prior reports have been inconsistent in suggesting that Pkp3 localizes to the nucleus. However, as described below, my work demonstrates consistent localization of Pkp3 to the nucleus in two different developmental systems and suggests a novel nuclear function.

ETS transcription factor family

The E twenty-six (ETS) family of proteins, found only in metazoans, consists of 28 members in humans. This family is characterized by a conserved ETS DNA binding domain, which recognizes DNA with the specific core motif sequence 5'-GGA(A/T)-3' [106-108]. The ETS domain is a variant of the winged helix-turn-helix motif, consisting of three alpha-helices on a four beta-sheet scaffold forming direct contacts with the core 5'-GGA(A/T)-3' motif exclusively [109]. This family of proteins is divided into numerous sub-families based upon sequence similarities in the ETS domain and other conserved domains, including the Polyomavirus enhancer activator 3 (PEA3) subfamily described later [110].

The diverse functions of this family are reflected in the broad range of phenotypes resulting from knockouts in *C. elegans*, *Drosophila* and mouse (e.g. defects in neuronal connections, fertility, vasculature, hematopoiesis, etc.) (reviewed in Hollenhorst et al. 2011) [111-113]. Due to the strong conservation of the ETS domain and its structure, there is only minor variance in the DNA-binding motif preference amongst most of the ETS family *in vitro* [114], suggesting that the diverse roles of ETS proteins may arise from differences in their binding partners and changes in the highest-affinity consensus motifs. For example, an ETS family member PU.1 regulates a different gene set alone than when bound to Pip, a lymphoid-specific co-regulator. [115].

The PEA3 subfamily, consisting of PEA3, Ets variant gene 1 [ETV1/ER81 (Ets-related 81)] and ETS variant gene 5 (ETV5), is characterized by two autoinhibitory domains flanking the ETS DNA binding domain and an acidic domain near the amino-terminus [116]. The autoinhibitory domains are thought to fold on each other, obscuring the DNA binding domain from interacting with DNA. This autoinhibition can be disrupted by either addition of an antibody specific to one of the domains or deletion of one of the autoinhibitory domains, further supporting the hypothesis that they cooperate to inhibit DNA binding [111,117,118]. Interestingly, all three PEA3 subfamily members contribute to the development of neuronal structures [119-123].

ETV1

ETV1, a PEA3 subfamily member, is known to contribute to the formation of dopaminergic neurons through the transcriptional regulation of dopamine transport and synthesis genes, and it also contributes to the formation of proper connections between group 1a sensory afferents and motor neurons, which transduce sensory signals to and from the brain [120,123]. ETV1 knockout in mouse results in limb ataxia, loss of coordination, and death by six weeks post-natal, likely due to an unresolved neural defect [120]. Our work demonstrates that overexpression of ETV1 in *Xenopus* also results in later neurological defects, with a loss of eye structures following evagination of the rudimentary eye [124]. The results from both mouse and *Xenopus* suggest that ETV1 is necessary in the later stages of neuronal development.

Examination of tumorigenic cell lines have shown that ETV1 regulates the matrix metalloproteinase genes, which are involved in invasion of cells through the extracellular matrix and the basement membrane, promoting metastasis [125,126]. Also, ETV1 promotes Ewing's sarcomas through a fusion with the Ewing's sarcoma gene (EWS), and is implicated in promoting the metastasis of prostate cancer (reviewed in Oh et al., 2012) [127].

Summary

The Pkp-catenin subfamily has always been shown to have strong localization in various cellular compartments, including the desmosomes, the cytoplasm and the nucleus, but the functions of Pkps in these compartments have remained elusive. Contributing to this, the multiple mammalian Pkp proteins derived through evolution have overlapping functions, potentially masking knockout phenotypes that would otherwise be readily identified by compensating for each other. Altogether, my research has demonstrated the first interaction between a plakophilin-catenin (Pkp3) and a site-specific DNA-binding transcription factor, ETV1, while demonstrating the necessity of Pkp3 during amphibian development. This work should assist in providing an understanding of how Pkps influence development and possibly disease as a result of their actions in the nuclear compartment.

Chapter II

Results

Part One: Characterization of *Xenopus* Pkp3

Identification of the *Xenopus* Pkp3 ortholog

Xenopus Pkp3 shares strong similarity (71.2%) with human and mouse Pkp3 (Figure 3). The isoform isolated is encoded by 2472 base pairs, corresponding to 824 amino acids and a predicted protein molecular mass of 91 kDa. The sequence has been deposited online as Genbank ID: AF182522. Two potential alternative translational start sites were found in the predicted protein sequence that reside prior to the Armadillo domain and are conserved in mouse (but not human). In contrast to their known or putative relevance in p120-subfamily biology [81,128], it is unclear at this time if alternative translational start sites are employed to generate different Pkp isoforms in vivo. Also found in Pkp3, as we recently characterized in some detail for delta-catenin [129], is a conserved predicted caspase cleavage site that if employed would generate ~56 kDa and ~35 kDa Pkp3 fragments. The amino-terminus is serine rich, accounting for approximately 15% of the residues in this region, and includes numerous potential phosphorylation sites. Overall, *Xenopus* Pkp3 resembles in its primary structure its mammalian counterparts, with caspase cleavage and phosphorylation being among possible points of regulation.

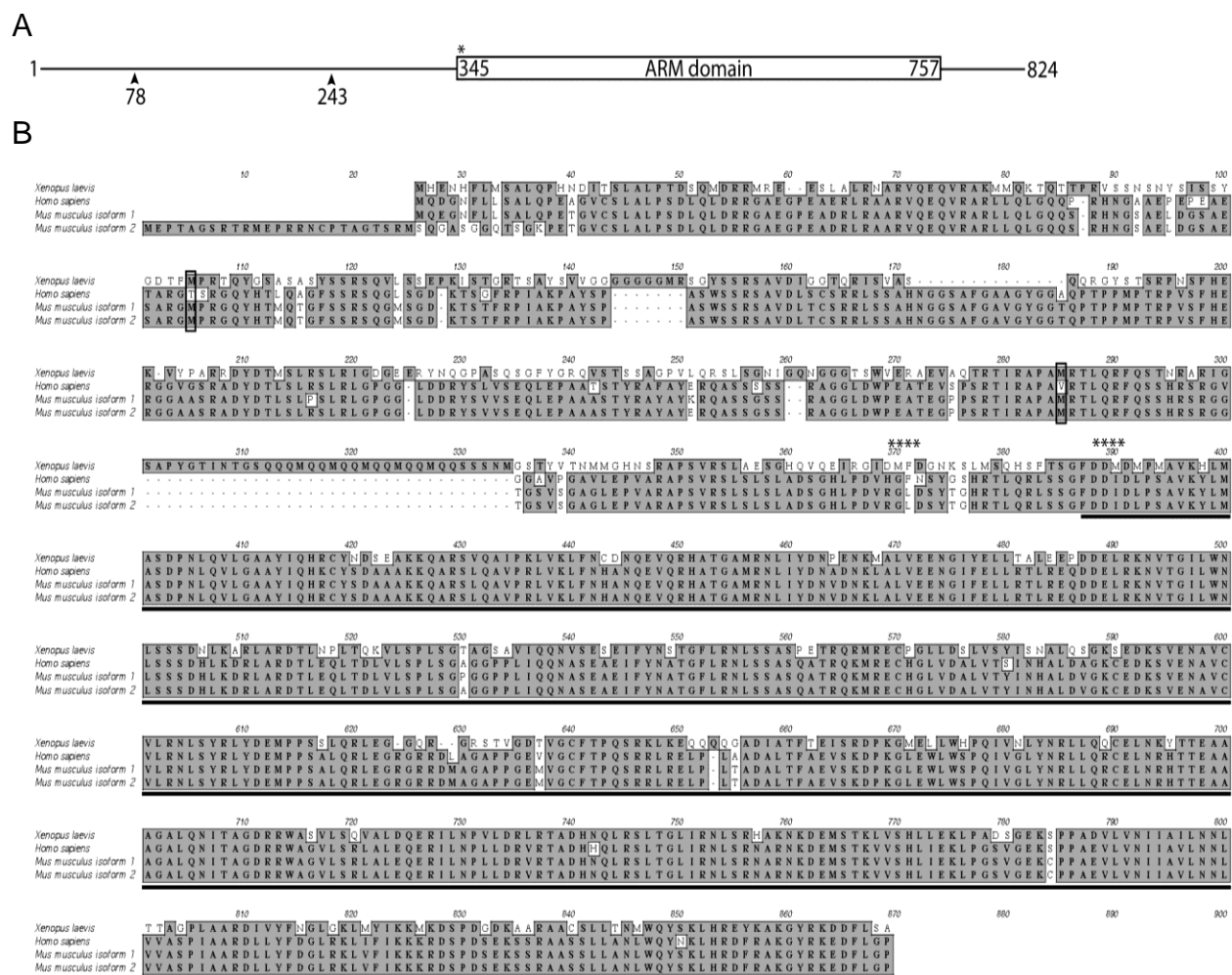


Figure 3. Pkp3 domain structure and amino acid sequence alignment.

(A) Diagram of Pkp3 protein characteristics. Potential alternative translation initiation start sites are indicated with arrows, while a conserved, potential caspase cleavage site is labeled with an asterisk. (B) Sequence alignment of *Xenopus laevis*, human and two isoforms of mouse Pkp3. Identical and similar residues are indicated by grey highlighting. The Armadillo domain is underlined. Black boxes indicate methionines conserved with mouse that might serve as alternative translation initiation sites. Potential caspase cleavage sites are labeled with asterisks.

***Xenopus* Pkp3 temporal expression**

To evaluate the temporal expression pattern of Pkp3, I performed semi-quantitative real-time RT-PCR utilizing total mRNA isolated from *Xenopus* embryos. Dissimilar from other characterized catenin mRNAs [34,130-133], *Xenopus* Pkp3 transcript levels appeared to increase rather dramatically (5-10 fold) following gastrula stages (Figure 4A), suggesting that Pkp3 may act predominately later in development. To examine *Xenopus* Pkp3 at the protein level, we generated a rabbit polyclonal antibody directed against its N-terminal domain (amino acids 1-350), that precedes the Armadillo domain (Figure 3A). The affinity-purified antibody recognizes two Pkp3 protein products migrating at approximately 110 kDa and 75 kDa, which are not detected using pre-immunization sera from the same rabbit (Figure 5). The 110 kDa migrating product is larger than predictions based upon the isolated Pkp3 mRNA, suggesting that our cloning procedures may have missed a larger alternatively spliced mRNA, possibly one including a more upstream translation initiation site. Within the p120 subfamily, such alternative splicing is well known to take place across various catenin domains [34,134,135]. Finally, a third and larger protein product is occasionally (and weakly) detected at approximately 120 kDa. It is likely to be a Pkp3 isoform and may arise from an unknown alternative RNA splicing event, translation from a more upstream start site, or post-translational modification. Via morpholino knockdown of Pkp3 with two independent morpholinos, the 110 and 75 kDa bands were demonstrated to be authentic

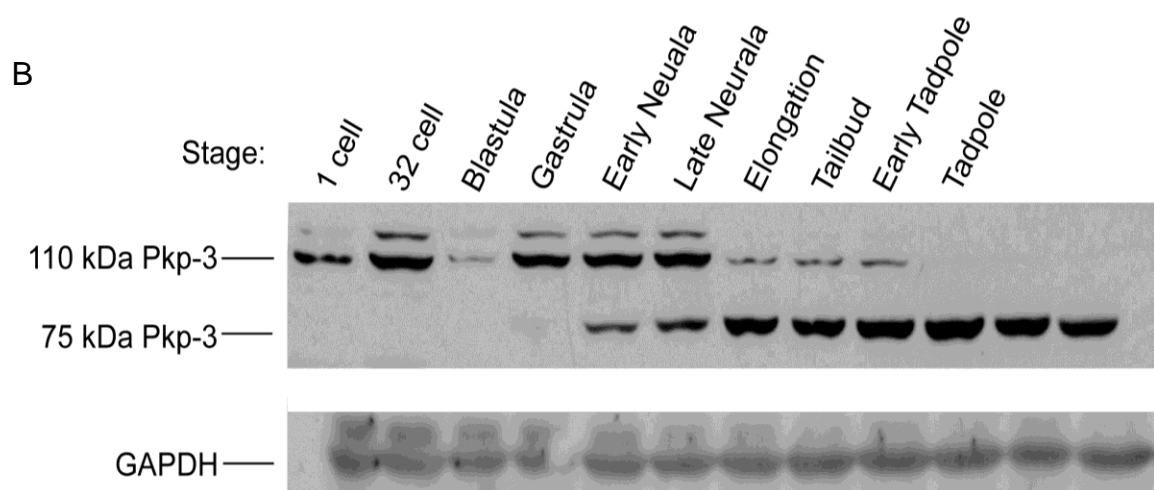
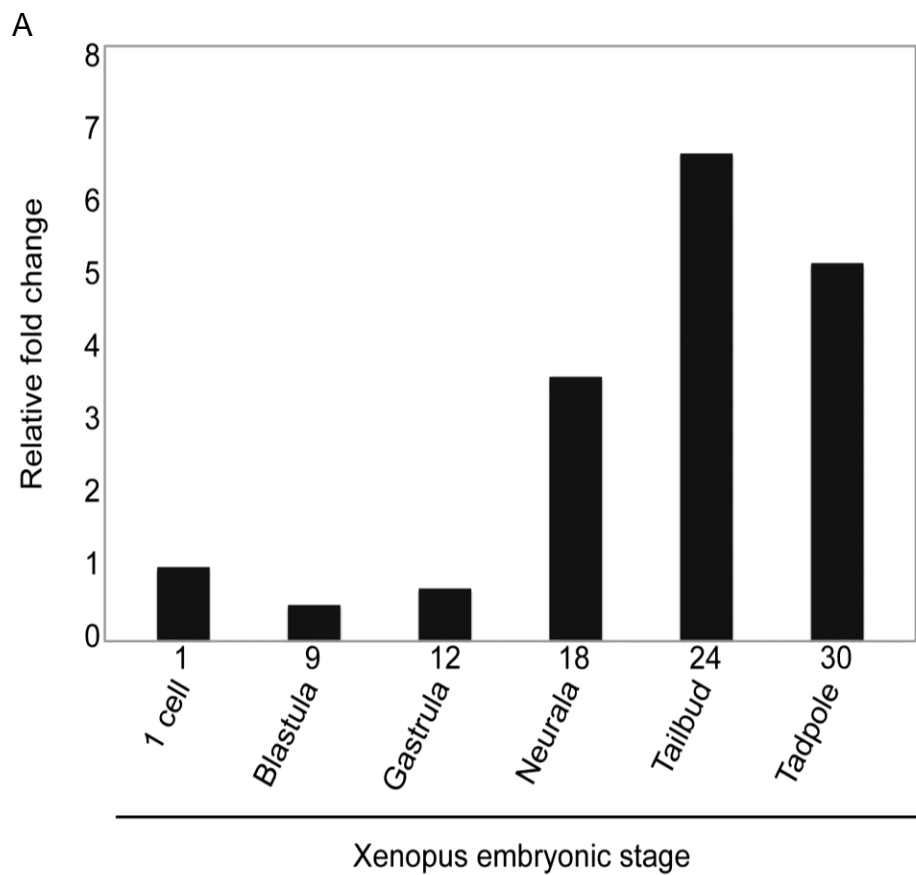


Figure 4. *Xenopus* Pkp3 temporal expression profiles.

(A) Semi-quantitative real-time RT-PCR analyses indicating Pkp3 transcripts are deposited maternally at a relatively low level and then levels increase following gastrulation. (B) The 75 kDa Pkp3 protein isoform increases following gastrulation, while the 110 kDa isoform exhibits an inverse pattern. The polyclonal antibody generated against *Xenopus* Pkp3 amino acids 1-350 (N-terminal domain) recognizes Pkp3 protein products migrating at approximately 110 kDa and 75 kDa. Further, in early development, a fainter and more slowly migrating band is detected at approximately 120 kDa. Immuno-blot detection of GAPDH serves as a loading control.

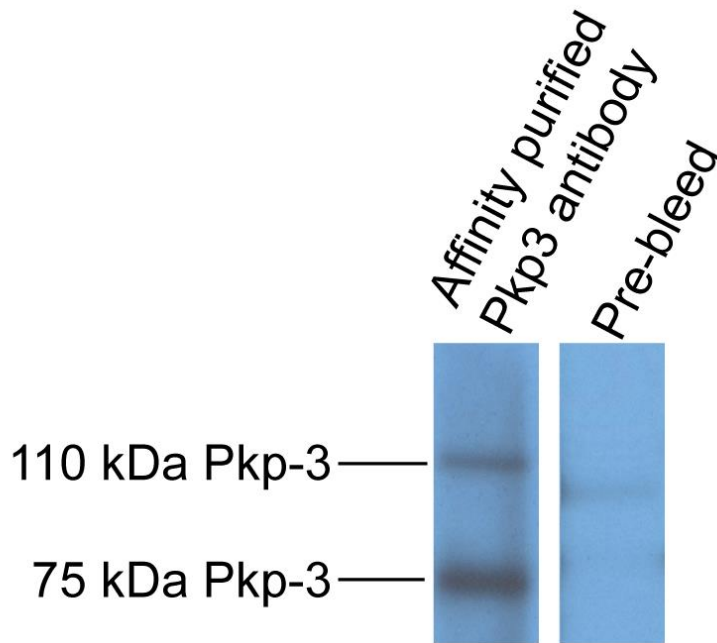


Figure 5. Characterization of affinity purified rabbit polyclonal antibodies that are directed against the N-terminal domain of Pkp3 (amino acids 1-350).

Immuno-blotting using the noted anti-Pkp3 antibodies specifically revealed 110 kDa and 75 kDa protein products in *Xenopus* embryo extracts (stage 25; also detected using whole sera). The same bands are not resolved using serum collected from the same rabbit prior to immunization.

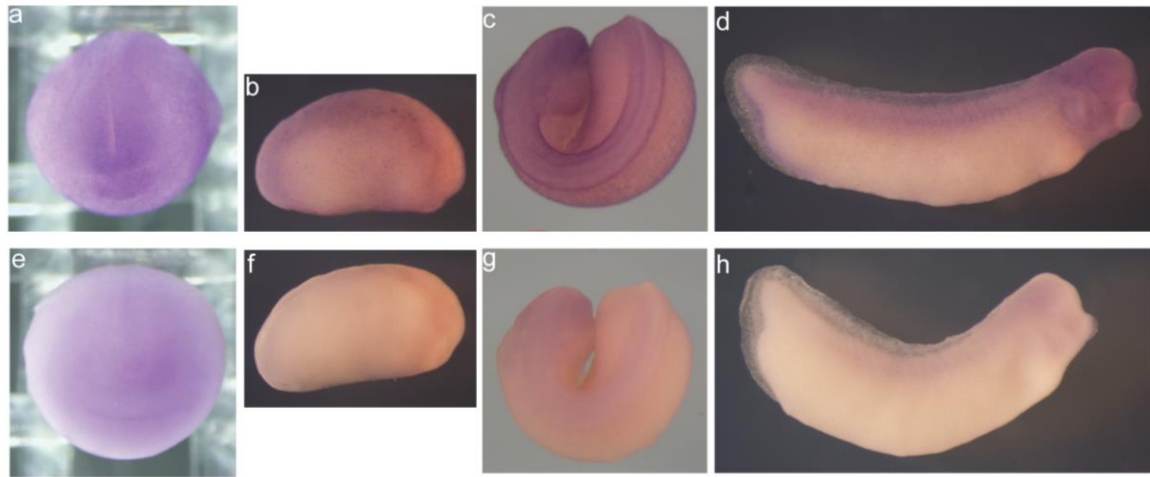
(Figure 10B). With regards to Pkp3 protein levels, I found that consistent with the relative abundance of Pkp3 transcripts across developmental stages (Figure 4a), the 75 kDa translation product of Pkp3 increases following gastrulation.

Complementing the temporally increasing expression profile of 75 kDa Pkp3, the 110 kDa protein product is instead maternally deposited and expression decreases following gastrulation (Figure 4B). This suggests the possibility of distinct functions of the two isoforms according to developmental stage in amphibian development.

***Xenopus* Pkp3 spatial expression**

The spatial expression profile of Pkp3 was obtained through whole-mount in situ RNA hybridization of *Xenopus* embryos at various stages. I used a digoxigenin-labeled antisense full-length RNA probe of Pkp3 (Figure 6A a-d). A sense negative-control probe was hybridized and processed in parallel, and as expected did not produce significant signal intensities (Figure 6A e-h). In agreement with my qRT-PCR (Figure 4A), Pkp3 transcripts were less apparent prior to neurulation (data not shown), but subsequently become evident in the dorsal and anterior regions of neurula stage whole-mount embryos. At tailbud stages, embryos show staining in neural and neural crest derived tissues, as well as within somites and broad expression across the ectoderm. In particular, I observed signals consistent with the brain, eye vesicle and spinal cord, as well as the branchial arches. While quite faint, sectioning of these embryos confirmed

A



B

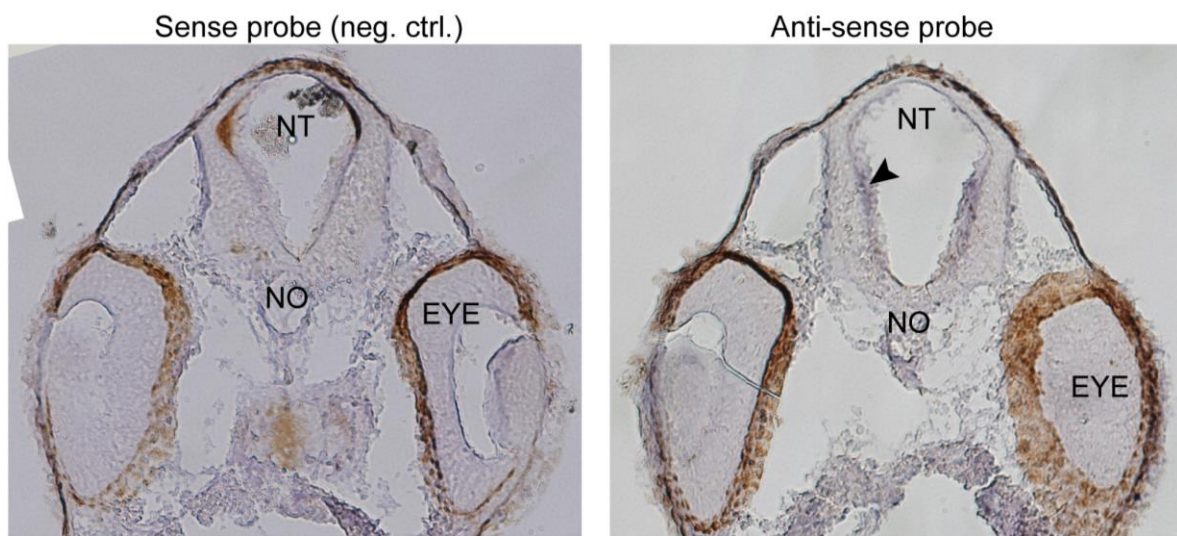


Figure 6. *Xenopus* Pkp3 spatial expression profiles during development.

(A) Whole-mount in situ RNA hybridization reveals Pkp3 mRNA signals in the anterior and dorsal neural fold regions of neurula embryos (subpanel a). At elongation stages (stage 22; subpanel b), staining of the skin remains apparent, as does a concentration in dorsal structures. At tadpole stages, neural derived tissues including the brain, branchial arches and the spinal cord are stained, as are somites (subpanels c-d). As a basis for comparison (negative controls), we undertook sense-probe hybridizations in parallel (subpanels E-H). (B) Whole mount anti-sense in situ staining of tadpole stage embryos, followed by cross-sectioning and agarose embedding, reveals faint Pkp3 signals in the neural tube (arrowhead) relative to the sense (negative) control stained embryos. NT, neural tube; NO, notochord.

Pkp3 expression in the ectoderm, branchial arches and neural tube (Figure 6B and data not shown).

To further examine the spatial profile of Pkp3 protein products, I performed immuno-blot analysis of adult *Xenopus laevis* tissues using our affinity purified polyclonal antibody. Consistent with Pkp3's predominant later expression in embryogenesis (Figure 4B), only the 75 kDa Pkp3 product was detected, being most prominent in tissues enriched for desmosomes, such as the heart, lung, muscle and skin (Figure 7). Following longer exposures of the ECL films, Pkp3 was also clearly present in the kidney and brain (results not shown). My findings indicate that *Xenopus* Pkp3 is most highly expressed at the mRNA and protein levels in desmosome-strengthened tissues, and is also found in tissues of neural derivation.

***Xenopus* Pkp3 subcellular localization**

Catenin family members have been shown previously to localize to differing subcellular compartments, consistent with even a single catenin's varied functions [17,18,20]. This includes interactions with cadherin cytoplasmic tails at cell-cell junctions, modulation of small GTPases and protein translation in the cytoplasm, and alterations of gene expression in the nucleus. To assist in assessing Pkp3's subcellular localization, I generated a Myc-Pkp3 fusion construct, expressed it at levels similar to endogenous Pkp3 (Figure 8) and

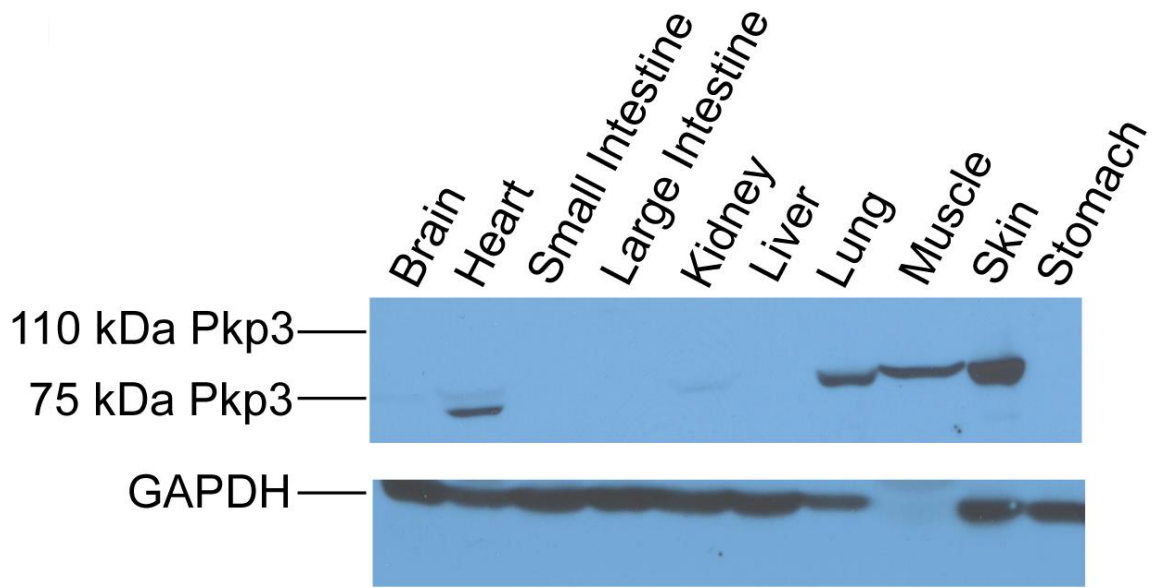


Figure 7. Adult *Xenopus* Pkp3 spatial expression.

Immuno-blotting on adult *Xenopus* tissue extracts. We used an affinity purified rabbit polyclonal antibody directed against the N-terminal domain of Pkp3, which clearly resolved the Pkp3 protein isoform migrating at approximately 75 kDa. This product was strongly expressed in heart, lung, muscle and skin. Weak, reproducible expression was detected in brain and kidney.

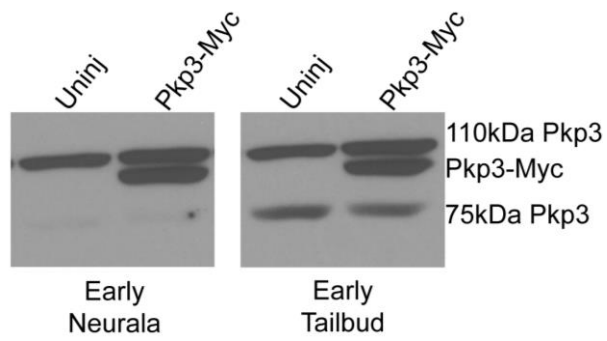


Figure 8. Expression of exogenous Pkp3-Myc in *Xenopus* extracts.

Immuno-blots of early neurula and tailbud extracts, showing the level of exogenous Myc-tagged Pkp3 relative to endogenous Pkp3 (500pg Pkp3 mRNA injection at one-cell stage).

examined its distribution in the *Xenopus* ectoderm of blastula stage embryos (animal caps), and late neurula stage embryos. At blastula stage, I found that Pkp3 is present at cell-cell borders, along fibrous cytoplasmic structures and in the nucleus (Figure 9Aa). In early tailbud, I consistently observed quite faint Pkp3 localization at cell borders, with even less intensity in the nucleus relative to blastula stages (Figure 9Aa’). Interestingly, I observed more intense punctate spots in select smaller cells within the same field that we later confirmed were within multiciliated cells intercalating from the sensoral layer of the ectoderm (Figure 9Aa’ and data not shown). Nuclear localization of endogenous Pkp3 was likewise easily detected in uninjected embryos (Figure 9B), while cell border localization was considerably fainter to absent. This latter observation might arise from lesser accessibility of the added antibodies to the endogenous Pkp3 antigen(s) within mature desmosomal structures. That is, since Pkp3 is known to bind multiple desmosomal proteins [45], the exogenous protein might more easily decorate desmosomal structures in a manner that leaves the Myc-tag exposed for antibody based detection. In summary, my results suggest that *Xenopus* may prove a good model for studying Pkp3’s junctional and/ or cytosolic contributions to vertebrate development, and perhaps also its currently understudied nuclear functions.

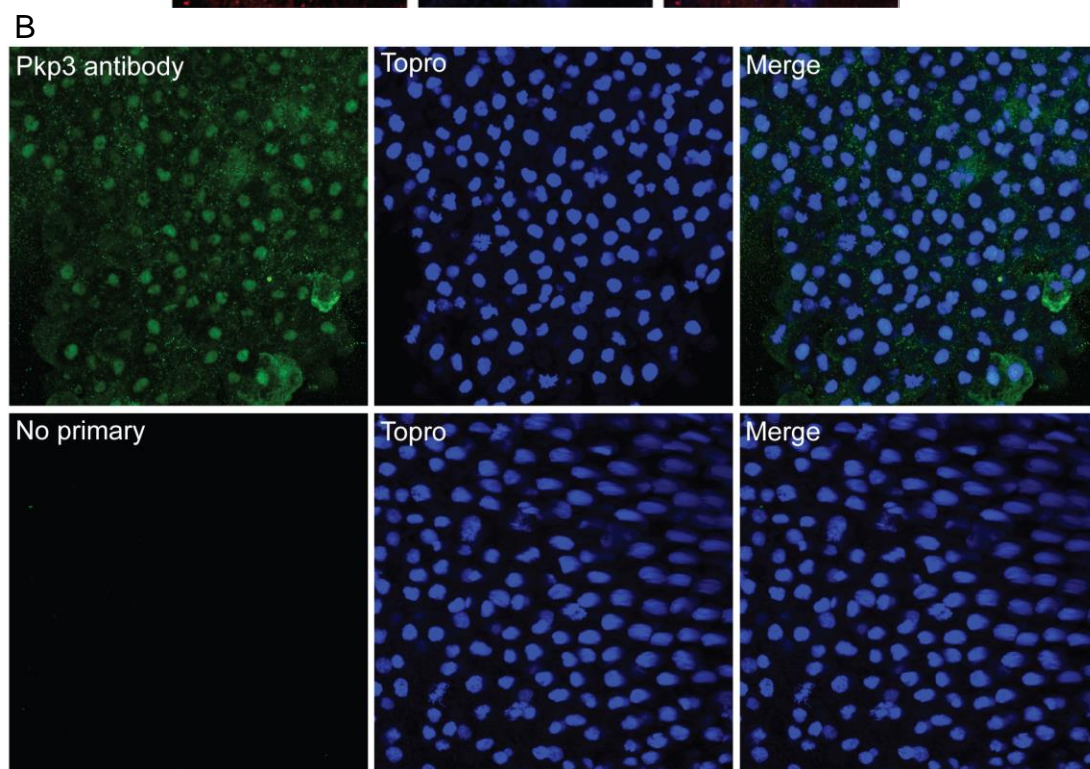
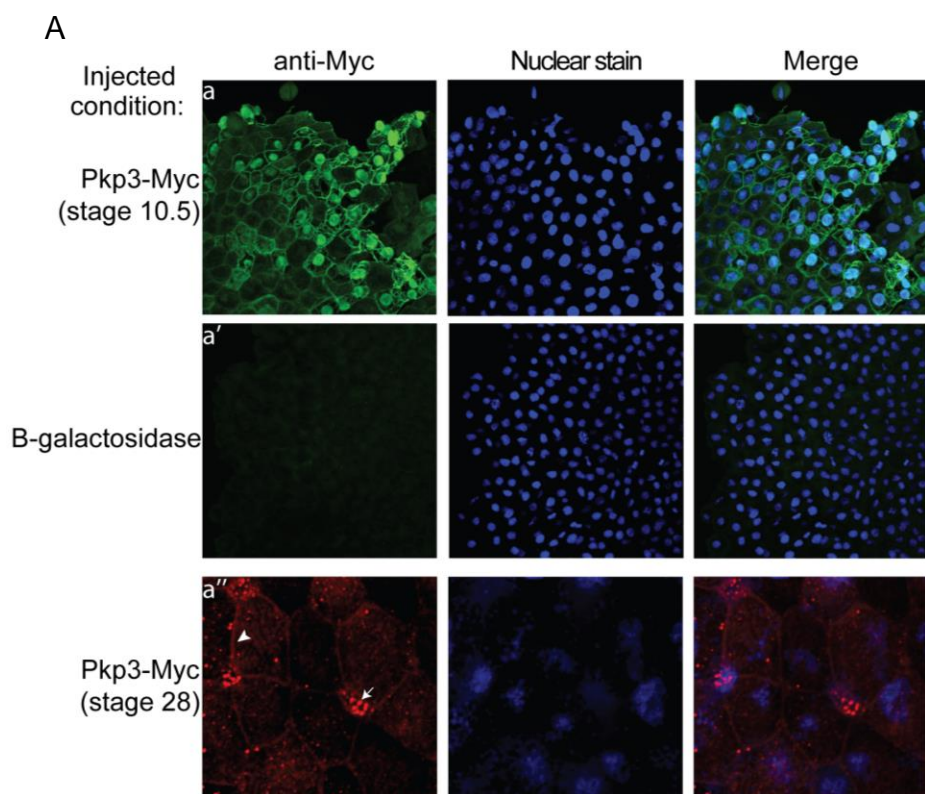


Figure 9. Pkp3 subcellular localization.

(A) Following earlier injection of exogenous Myc-tagged Pkp3 mRNA (0.5ng injected into one-cell stage embryo), Pkp3 was visualized in the naïve ectoderm (animal cap) cells of blastula embryos at the plasma membrane, in the cytoplasm along what appear to be fibrous structures (possibly the intermediate filament network), and in the nuclear compartment (subpanel a). At late neurula stage the exogenous Pkp3 was again detected at the plasma membrane (arrowhead), in the nuclear compartment (though much weaker), and as punctate apically disposed spots (conceivably basal bodies or other cilia associated structures, arrow), in multiciliated cells intercalating upwards from the deeper sensoral layer (subpanel a''). (B) Immuno-fluorescence detection of endogenous Pkp3, using the affinity purified rabbit polyclonal antibody we generated. Pkp3 is detected in the nucleus of non-dividing cells within blastula-stage ectoderm (animal caps), while the secondary antibody alone did not produce a detectable signal (nor did additional negative controls; data not shown).

This part is published work taken from Munoz WA, Kloc M, Cho K, Lee M, Hofmann I, Sater A, Vleminckx K, McCrea PD. (2012) Plakophilin-3 Is Required for Late Embryonic Amphibian Development, Exhibiting Roles in Ectodermal and Neural Tissues. PLoS ONE 7(4): e34342. doi:10.1371/journal.pone.0034342.

Open access agreement. Upon submission of an article, its authors are asked to indicate their agreement to abide by an open access Creative Commons license (CC-BY). Under the terms of this license, authors retain ownership of the copyright of their articles. However, the license permits any user to download, print out, extract, reuse, archive, and distribute the article, so long as appropriate credit is given to the authors and source of the work. The license ensures that the authors' article will be available as widely as possible and that the article can be included in any scientific archive.

Part Two: Developmental Roles of Pkp3-catenin

Knockdown of endogenous Pkp3 upon treatment with morpholinos

The temporal and spatial expression of Pkp3, noted above, suggested that Pkp3 might contribute to various embryonic stages and developmental processes. To assess this possibility, we designed antisense morpholinos to lower endogenous Pkp3 protein expression in *Xenopus*. Specifically, two independent oligonucleotide sequences were designed to compliment either the start ATG (MO3), or the proximal 5' UTR (MO1) of the Pkp3 mRNA (Figure 10A). Reducing the probability of off-target effects, the morpholinos employed had no discernable complementation to the mRNA of *X. laevis* Pkp2 or other sequences. Further, while *X. laevis* Pkp1 was not resolved in the existing databases, *X. tropicalis* Pkp1 likewise lacked sequence complementation. To characterize their efficacy, the Pkp3 morpholinos were injected at varying doses (1-40ng) into early cleavage stage embryos, which were then observed through tadpole stages. Immuno-blot assay of extracts obtained from embryos injected at the 1-cell stage confirmed that Pkp3 was reproducibly depleted by 40ng of either MO1 or MO3 or a mixture of the two morpholinos totaling 40ng, but not by the standard control (SC) morpholino (Figure 10B). Likewise, the translation of an exogenous Pkp3 mRNA, that included 90bp of the 5' UTR, was prevented upon the co-injection of either MO1 or MO3 (1ng; Figure 10C). Of note, Pkp2 mRNA and protein levels

were not affected by injection of morpholinos directed against Pkp3 (Figure 10B and 11).

Pkp3 depletion results in ectodermal fragility

To assess the developmental impact of Pkp3 depletion, I injected MO1 or MO3, or both together into the animal pole of 1-cell embryos, or into a single blastomere of 2-cell embryos. Based upon gross external observation, these MO-injected embryos did not present any significant phenotypes until early tailbud stages, when hatching from their protective Vitelline envelope normally occurs. In contrast to SC injections (negative control), MO1 or MO3 injected embryos experienced damage to their surface ectoderm during shedding of the Vitelline membrane, which exerts tension and presumably frictional effects upon the hatching embryo. The phenotypic penetrance following Pkp3 depletion varied from 30-100%, as a function of the particular batch of embryos, amount of morpholino and the morpholino employed (Figure 12). To obtain higher resolution views of the ectodermal phenotype, we turned to transmission electron microscopy. Following use of either of the Pkp3 targeting morpholinos, we observed reductions in the size and number of more basally localized desmosomal densities (Figure 13). Interestingly, while we do not presently understand the underlying basis, ectodermal cells of Pkp3 depleted embryos also displayed apically clustered mitochondria, as well as a significantly increased number and size of mucus secretory vesicles. Through the use of scanning

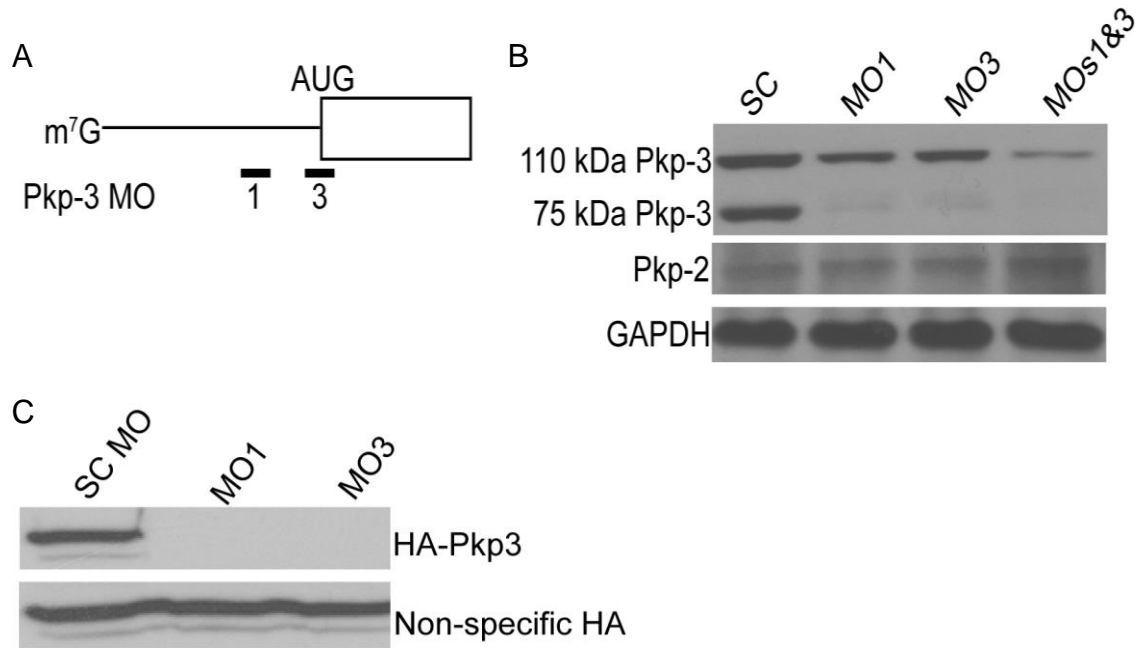


Figure 10. Two independent morpholinos knockdown Pkp3 protein expression.

(A) Diagram of morpholino-based depletion strategy. MO 3 targets the Pkp3 mRNA translational start site and MO 1 targets a non-overlapping upstream sequence in the 5' UTR. Both morpholinos were designed to block translation initiation. (B) Immuno-blotting of hatching embryo extracts (stage 27) confirmed reductions of both Pkp3 protein isoforms following morpholino injection, but no reductions of Pkp2 protein (40ng of each morpholino when injected individually or 20ng of each morpholino when injected together into one-cell stage embryos). GAPDH serves as a loading control. (C) Immuno-blotting of blastula extracts confirmed the reduced presence of exogenous HA-tagged Pkp3 protein following earlier co-injection (one-cell stage) of Pkp3 mRNA (250pg) with even low-doses of MO1 or MO3 (1ng of either morpholino). A non-specific band serves as a loading control.

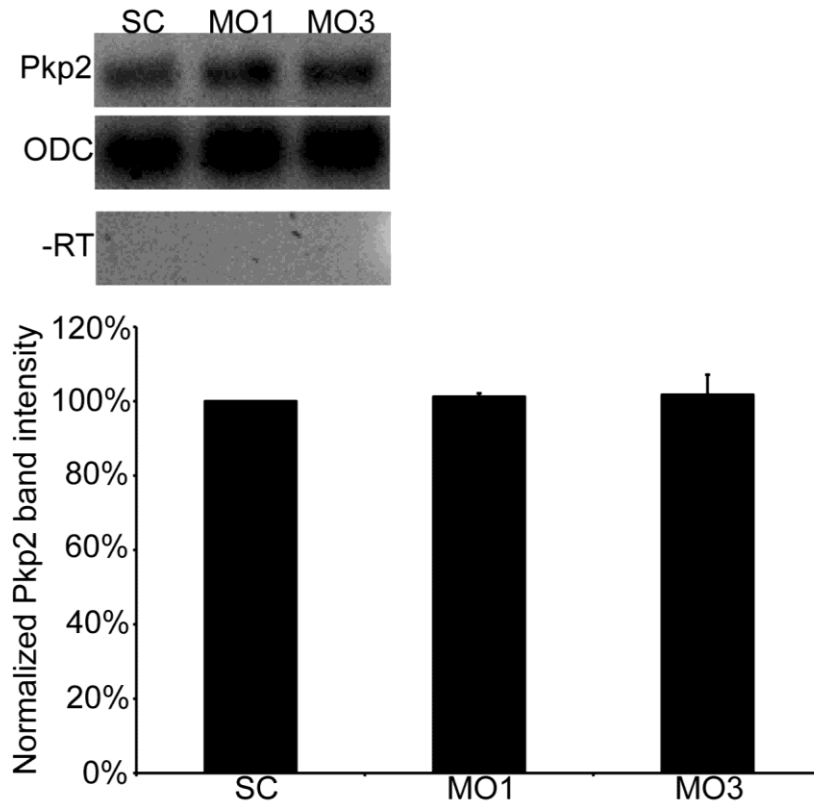


Figure 11. Pkp3 depletion does not notably affect Pkp2 mRNA levels.

Following depletion of Pkp3 (40ng MO1 or MO3 into one-cell stage embryos) RT-PCR was performed on cDNA derived from stage 27 embryos. No significant change was detected in Pkp2 mRNA levels, relative to embryos injected with standard control (SC) morpholino. Pkp2 bands were quantified and normalized relative to the ODC loading control, with no statistically significant differences found.

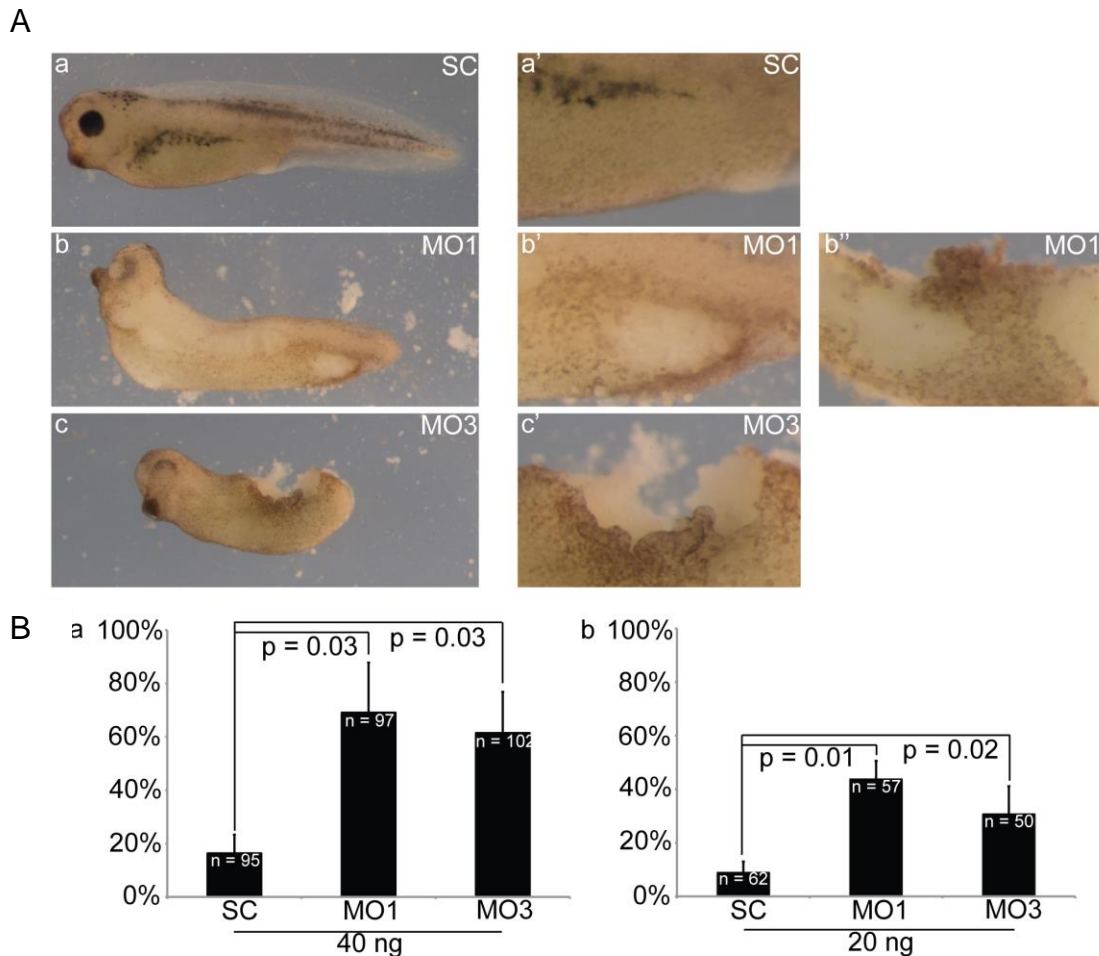
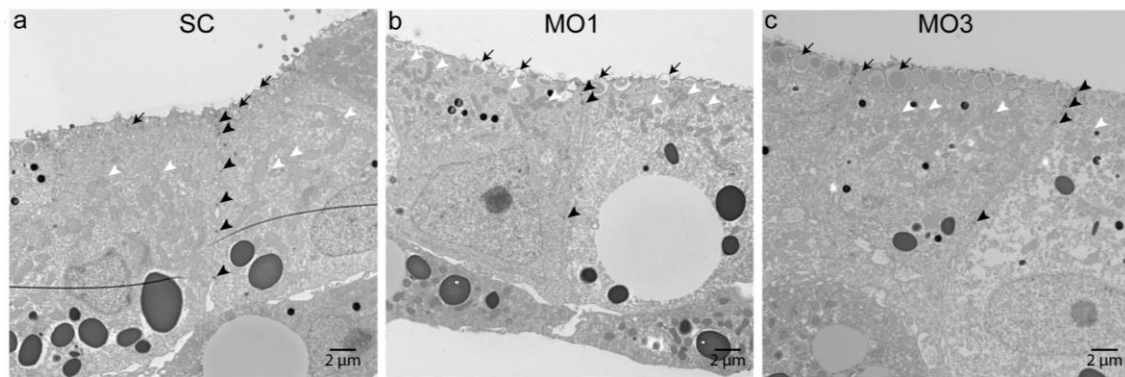


Figure 12. Depletion of endogenous Pkp3 results in skin fragility.

(A) Injection of MOs 1 or 3 (40ng into one-cell stage embryos) results in skin fragility (subpanels b and c, respectively), contributing to what can become lethal ectodermal damage sustained as the embryo hatches from the Vitelline membrane (higher magnification in subpanels b', b'', and c'). Negative control embryos injected with standard control morpholino (40ng) did not exhibit significant phenotypes (subpanels a-a'). (B) Quantification of the skin fragility effects are indicated in subpanel "b", where P-values indicate statistical significance. As indicated, either 40 or 20ng of each morpholino was injected into one-cell stage embryos.

A



B

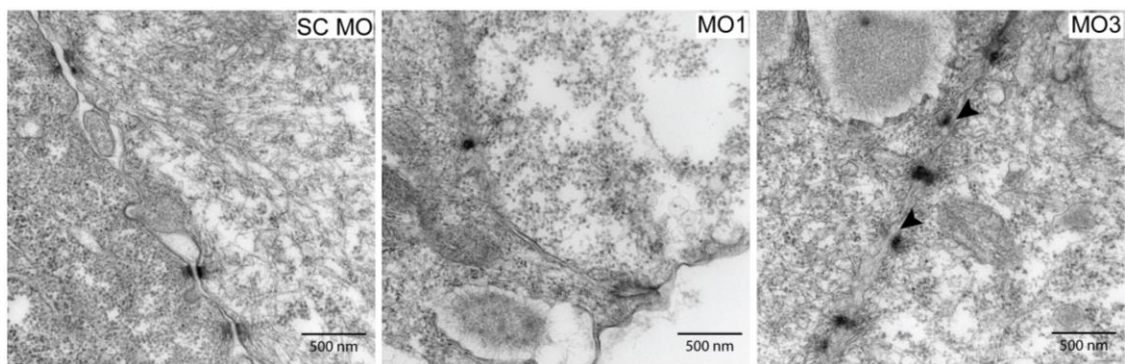


Figure 13. Depletion of endogenous Pkp3 results in loss of desmosomes, increased secretory vesicle size and relocalization of mitochondria.

(A) Skin of tailbud stage embryos injected at one-cell stage with 40 ng standard control morpholino (subpanel a) compared to 40 ng MO 1 or 3 injected embryos (subpanels b and c, respectively). Pkp3 depleted ectoderm contains fewer basally disposed desmosomes (black arrow heads), while in apical regions desmosomes appear equally abundant. Note also that in skin of Pkp3 knockdown embryos, mitochondria have become more apically disposed (white arrowheads), and secretory vesicles have become much larger along the apical surface (black arrows). (B) High-magnification transmitted electron microscopy revealed that the depletion of Pkp3 (subpanels MO1 and MO3) results in reduced desmosome size and appearance. For example, MO3 injected embryos exhibit some desmosome-like structures where equivalent densities are not always properly paired between contacting cells (see arrowheads).

electron microscopy (Figure 14), the more roughened surface features of embryos depleted of Pkp3 (using combined morpholinos), appeared to reflect the increased number and sizes of underlying mucus secretory vesicles making contact and then fusing with the plasma membrane (compare right-hand panels of Figure 14 that shows pocked/ roughened apical surface with panels b and c of Figure 13A, showing vesicles making surface contact). Additionally, scanning EM revealed defects in the motile cilia present upon multiciliated cells, as evident in Figure 14. Such reductions in motile cilia were further reflected in lessened immuno-fluorescent intensity when staining for acetylated alpha-tubulin, which is commonly used to resolve cilia as well as established neurons (Figure 15). Intriguingly, additional immuno-fluorescence analysis suggested that the multiciliated cells may themselves be reduced in number, or exhibit delays in intercalation upon Pkp3 depletion (data not shown). Finally, we noted that the very fine but observable surface demarcation of cell-cell borders within the ectoderm became less apparent following Pkp3 depletion (compare especially the lower panels of Figure 14).

To briefly survey another tissue dependent upon desmosome function, we looked at the heart. Here, we found that Pkp3 depleted embryos surviving ectoderm defects exhibited gross reductions in heart size as well as notable slowing of the beat rate at tadpole stages (data not shown). In summary, a number of phenotypes are apparent in *Xenopus* embryos depleted of Pkp3. While future study will be needed, some outcomes may not be the direct result of

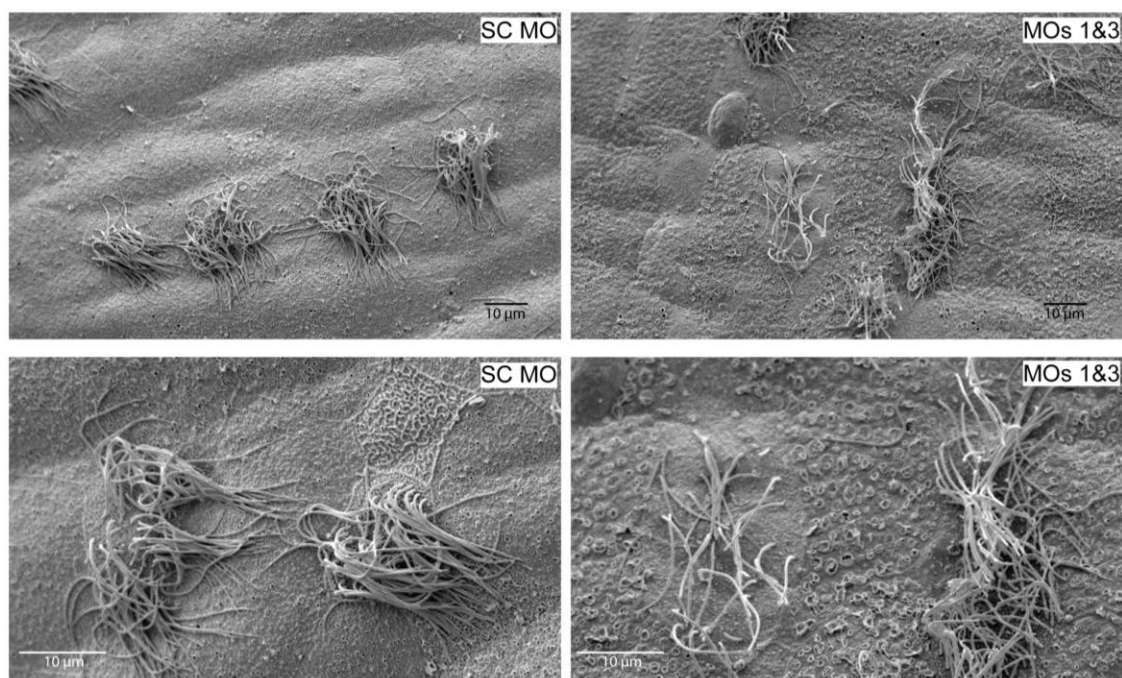


Figure 14. Pkp3 depletion alters the morphology of various cellular features.

Scanning electron microscopy revealed altered ectoderm surface features in Pkp3 depleted embryos. For example, whereas in control embryos fine demarcations can be seen upon close examination to reflect the borders between cells, such demarcations are more difficult to discern in Pkp3 depleted embryos. Further, we observed increases in the size of what we expect are mucus secretory vesicles (pits on the surface), a finding that was likewise reflected in transmission electron micrographs (see Figure 11A). Defects in the cilia of multiciliated cells were also apparent in Pkp3 morphants. 40ng of each morpholino was injected at the one-cell stage.

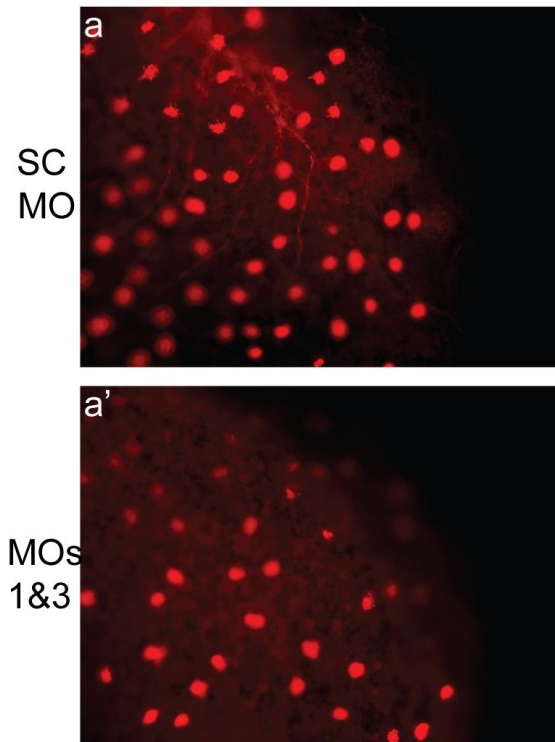


Figure 15. Pkp3 depletion results in reductions of multiciliated cells and neural tracts.

Neural processes present in the posterior region (tailbud) of control tailbud stage embryos (subpanel a) were reproducibly found to be less apparent and/ or foreshortened following Pkp3 depletion (subpanel a'). Morpholinos (40ng each) were injected at the one-cell stage.

altered desmosome function, such as the noted effects upon vesicle trafficking or cilia.

Touch hyposensitivity and neural phenotypes in Pkp3 depleted embryos

Skin fragility was found at varying penetrance in Pkp3 knock down embryos as noted, yet more detailed observation further revealed that depleted embryos hatch from the Vitelline membrane at later developmental stages than do controls. Upon hatching, MO1 or MO3 injected embryos maintained a laterally curled appearance, apparently the result of their prolonged entrapment. With possible reasons for their extended entrapment discussed below, such embryos exhibited a fixed lateral curvature or kink along the anterior-posterior axis (Figure 16A). Interestingly, if the Vitelline membrane was manually removed at an earlier developmental stage to reduce embryo entrapment times, the penetrance of this phenotype was significantly lowered (Figure 16B). A further obvious and unexpected phenotype was that depleted embryos, importantly including those with intact ectoderm, were not responsive to common laboratory stimuli such as gentle movement of their incubation dish or a light touch with a pipette tip (Figure 17 and data not shown). These observations suggested potential defects in neural or muscular development or function. Immuno-histochemical examination of the somites, early muscular structures, suggested that somite formation was not grossly altered (Figure 18). A further functional indication of normal muscle capability was that embryos appeared to swim normally following more robust

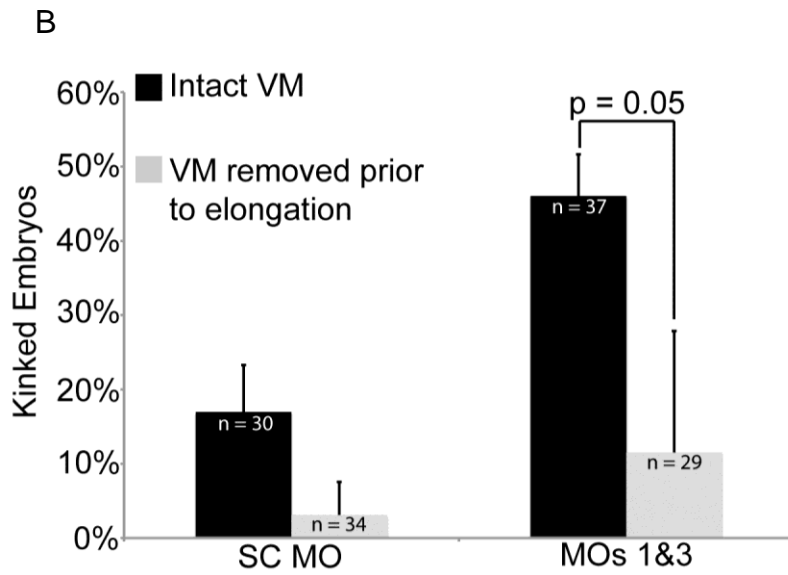
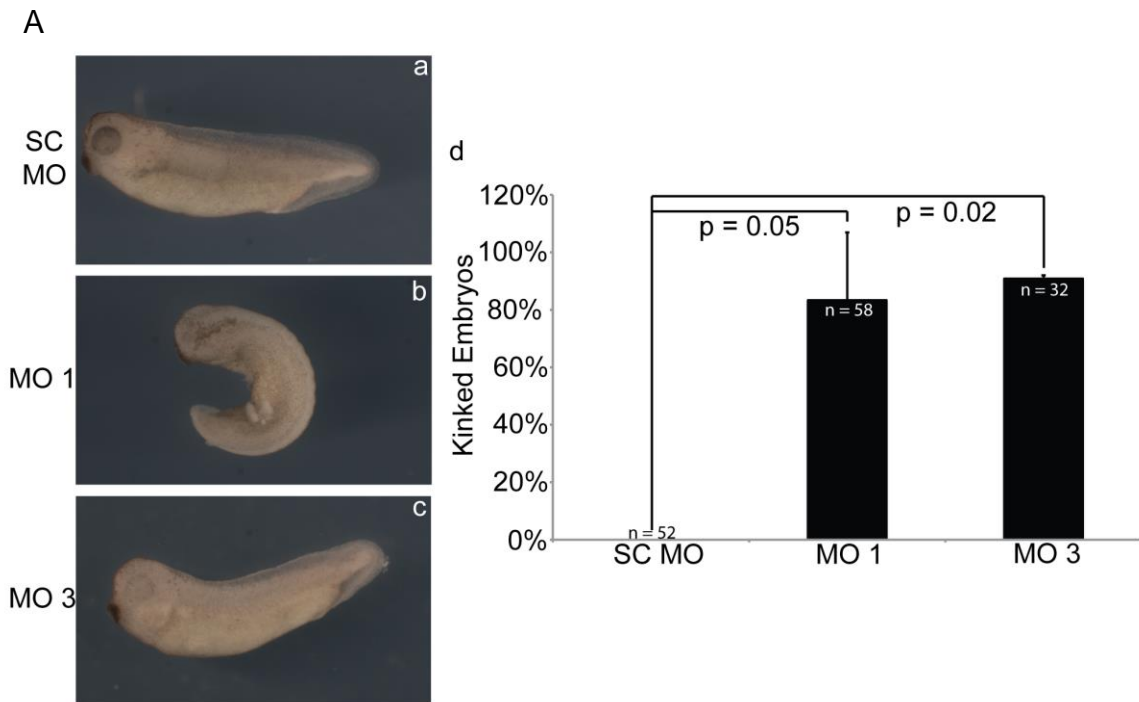


Figure 16. Pkp3 depletion results in permanent kinked axes due to prolonged entrapment in Vitelline membrane.

(A) MO 1 or 3 injected embryos that survive hatching have permanently kinked axes (subpanels b and c, respectively) (40ng at one-cell stage). This is quantified in subpanel d, where the P-values indicate statistical significance. (B) The kinked phenotype of embryos injected with MO 1 or MO3 was significantly rescued upon manual removal of the Vitelline membrane at neurula stage 19. Normally, the embryo hatches later through the Vitelline membrane, at stages 33/34. 40ng of each morpholino was injected at the one-cell stage. P-value indicates statistical significance.

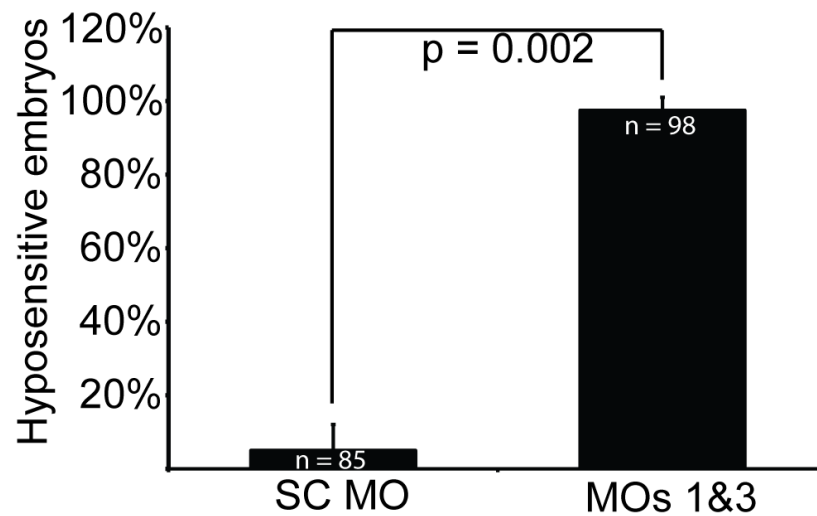


Figure 17. Pkp3 depletion results in tactile hyposensitivity.

Further observation revealed that Pkp3 depleted embryos were non-responsive to gentle tactile stimuli as observed by light shaking of their incubation dish, while controls attempted to escape from such stimuli. Upon more pronounced stimulation, it became evident that the embryos were able to swim normally, indicating retained muscle function (etc.) (data not shown).

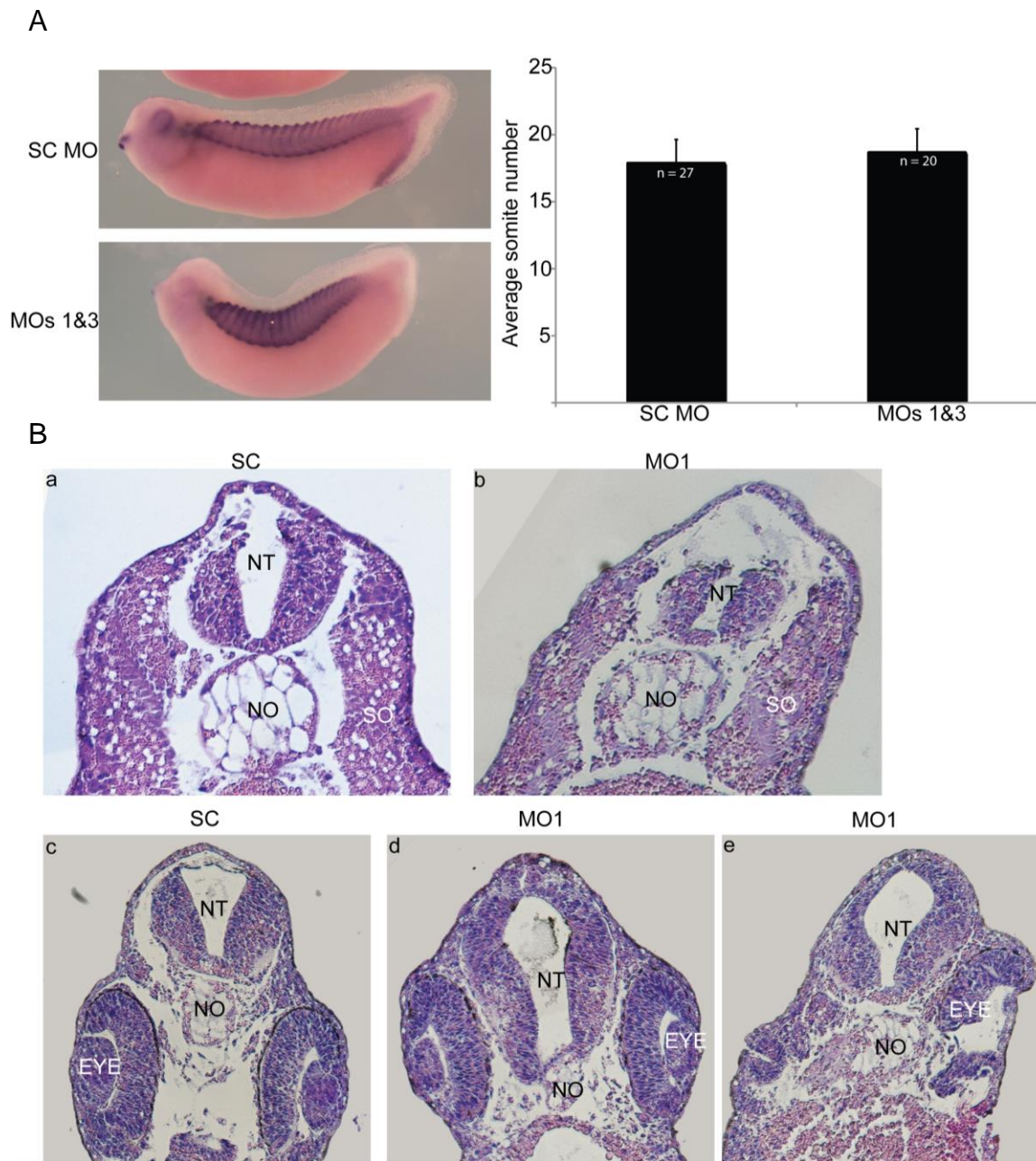


Figure 18. Pkp3 depletion does not appear to affect early muscle formation.

(A) Following injection with either standard control morpholino or a mix of MOs 1 and 3, the somites, an early muscle structure, do not appear disrupted. Note, the Pkp3 depleted embryo is laterally bowed towards the viewer, giving the false impression of compression of the somites. The number of somite segments was counted and compared, with no statistically significant differences found. 40ng of each morpholino was injected at the one-cell stage. (B) Sectioning and histological staining of Pkp3 knockdown embryos reveals no defects in main body somites (subpanel b, SC embryo image obtained from second series of sectioning and staining). However, defects in the head regions were observed in some cases. While possibly arising during sectioning due to reduced tissue integrity, there appeared to be overlaps in some embryos of the notochord and neural tube, as well as eye defects (subpanels d and e). NT, neural tube; NO, notochord; SO, somite.

mechanical stimulation, such as from firm prodding with a pipette tip (data not shown). Sectioning followed by H&E staining revealed that somites appeared grossly normal and oriented properly (Figure 18 and data not shown). It should be noted that the knockdown embryos were generally more fragile in head regions during sectioning procedures, with neighboring tissues not remaining as closely associated. Likewise, while possibly arising during sectioning, the boundary between the notochord and neural tube was altered in a proportion of Pkp3 depleted embryos (Figure 18 subpanel d).

To examine potential effects of Pkp3 depletion on neural structures that conceivably would influence embryo touch-responsiveness or the execution of embryo hatching, I used an antibody commonly used to mark differentiated neurons (directed against acetylated alpha-tubulin). While bundled motor neurons running within the inter-somitic regions appear unaffected by either MO1 or MO3 (Figure 19), I observed a loss of fine neural structures in the most posterior regions of early tailbud embryos (Figure 15). Additionally, I observed the consistent diminution in length of a lateral neural tract within tadpole stage embryos, which failed to extend into the tail region as far as those of SC injected controls (Figure 20 and Figure 21). Such altered neuronal morphologies may conceivably interfere with transducing or processing stimuli, possibly including neuro-muscular outputs to enable swimming or embryo hatching. Alternatively, or in addition, even small perturbations of the ectoderm may disrupt relationships

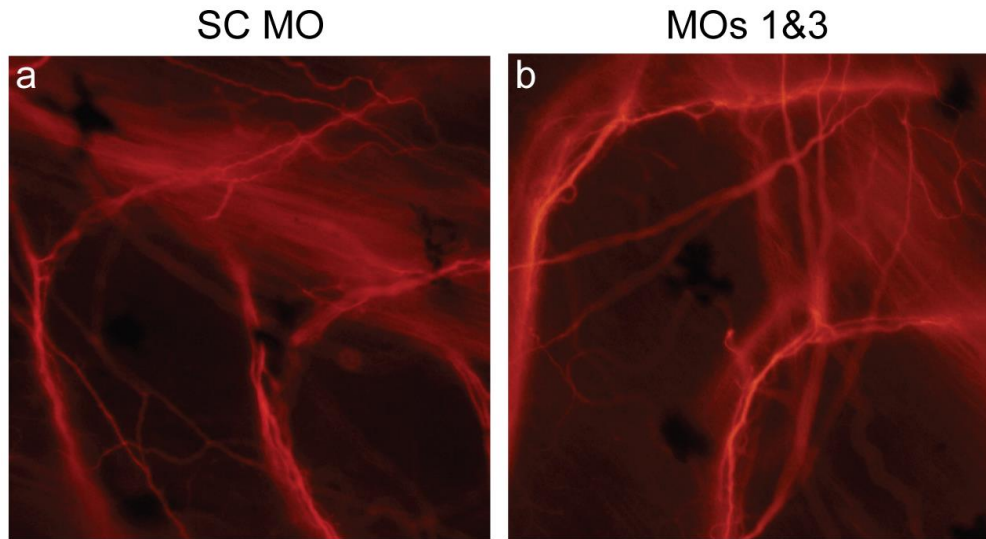


Figure 19. Pkp3 depletion does not significantly affect motoneurites along the somite boundaries.

Through the use of an established neural marker (acetylated alpha tubulin), examination of motoneurites arranged at somite boundaries revealed no large differences between controls and Pkp3 depleted embryos.

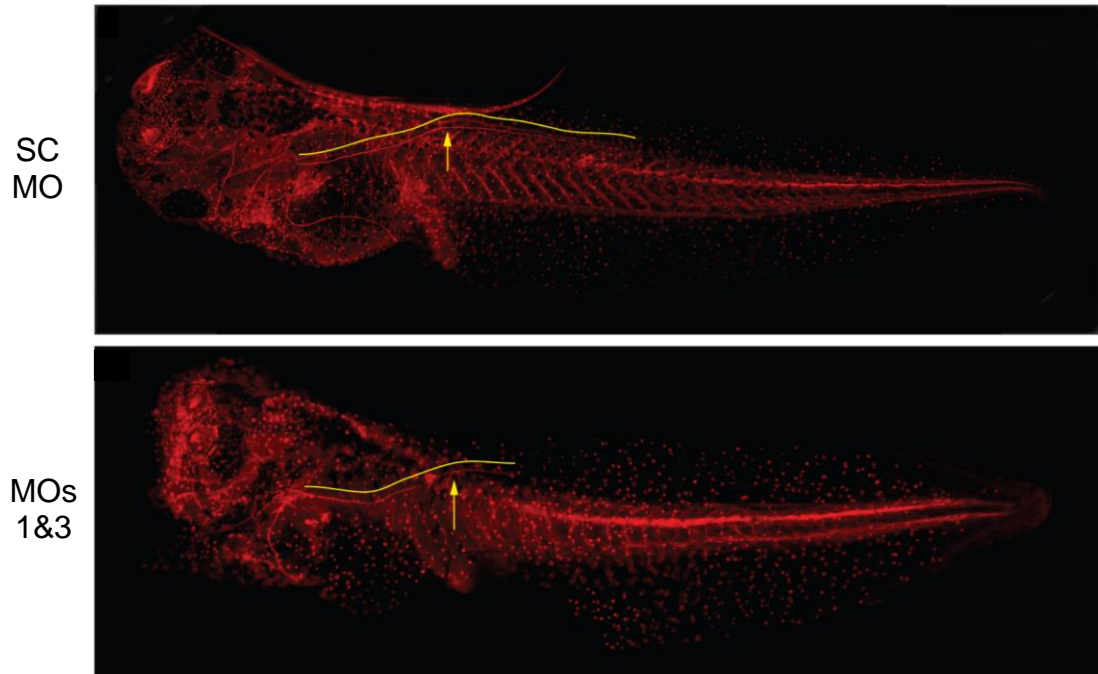


Figure 20. Pkp3 depletion results in late developmental neural defects.

Neural processes present in the tadpole stage lateral neural tract that contribute to the sensory network, were reproducibly found to be foreshortened following Pkp3 depletion. Morpholinos (40ng each) were injected at the one-cell stage.

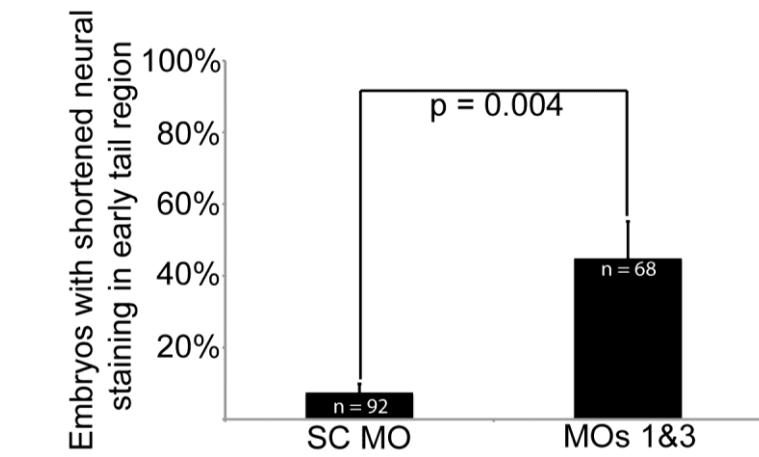


Figure 21. Pkp3 knockdown significantly affects certain peripheral neural structures.

Neural processes present in the posterior region (tailbud) of control tailbud stage embryos were reproducibly found to be less apparent and/ or foreshortened following Pkp3 depletion. Quantification of these results is shown here, where P-values indicate statistical significance. 40ng of each morpholino was injected at the one-cell stage.

between mechanosensory and signal transducing cells, thus having an impact upon responses such as touch.

Pkp3 may have a role in neural crest cell induction and migration

To assess the impact of Pkp3 depletion within the prospective neuro-ectoderm, especially given Pkp3's expression pattern as reflected in Figures 6 and 7 morpholino injections were made into a single dorsal blastomere at the 4-cell stage, with rhodamine dextran coinjected as a lineage tracer. At tadpole stages, these embryos exhibited reduced eye size (subpanels b and c of Figure 22). In embryos injected at the one-cell stage and later analyzed via sectioning, large segments of the eye were similarly found to be malformed (Figure 18B subpanel e). Also seen in embryo whole mounts (Figure 22), was a notable reduction in pigment cells throughout the embryo. As pigment cells are a neural crest derivative, Pkp3's possible contribution to neural crest was suggested. I thus tested an established marker of neural crest in embryos depleted of Pkp3 (versus SC injected). At early and late neurula stages (stages 16 versus 21; Figure 23), reporting respectively on inductive and migratory processes, the depletion of Pkp3 significantly reduced expression of Twist. FoxD3, another established neural crest marker, likewise exhibited disrupted expression at late neurula stages in response to Pkp3 depletion. Suggesting the specificity of these observations, we partially rescued the expression of both neural crest markers upon coinjection of exogenous Pkp3 (mRNA lacking the morpholino binding site;

Figure 24), but not with coinjection of exogenous beta-galactosidase. Based upon the pigment-loss and peripheral nervous system phenotypes, as well as the initial marker analysis, it appears that Pkp3 may contribute to forming at least some neural crest derived tissues. As additional tissues likewise depend upon the neural crest, future work will examine effects upon the craniofacial skeleton as well as the heart outflow tract.

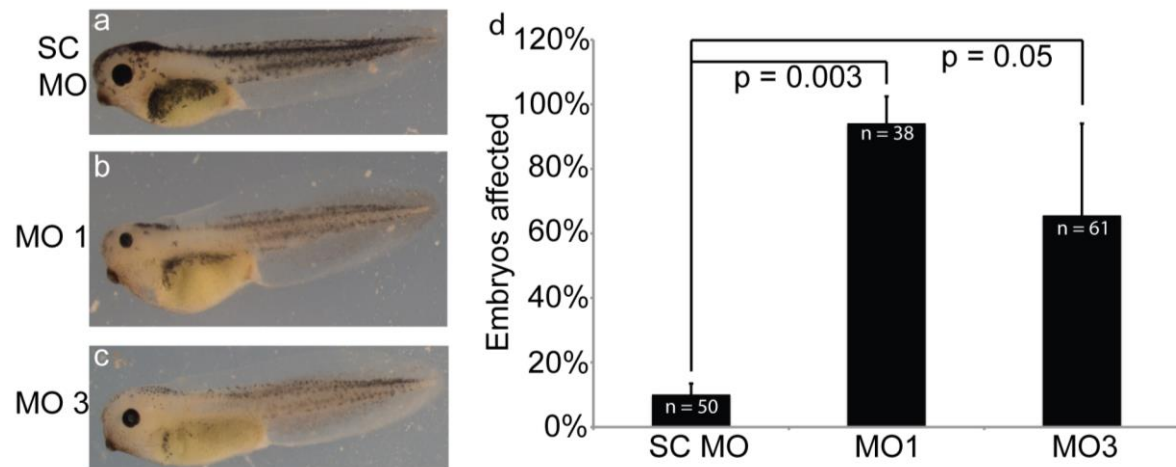


Figure 22. Neural crest derived tissues are disrupted upon Pkp3 depletion.

Embryos injected with either MO 1 or 3 resulted in loss of pigmentation and reduced eye size (panels b and c) compared to negative controls (panel a). 40ng of either morpholino was injected at the one-cell stage. Percent of embryos with reduced pigmentation is quantitated in panel d. p-values were obtained through Student's T-test.

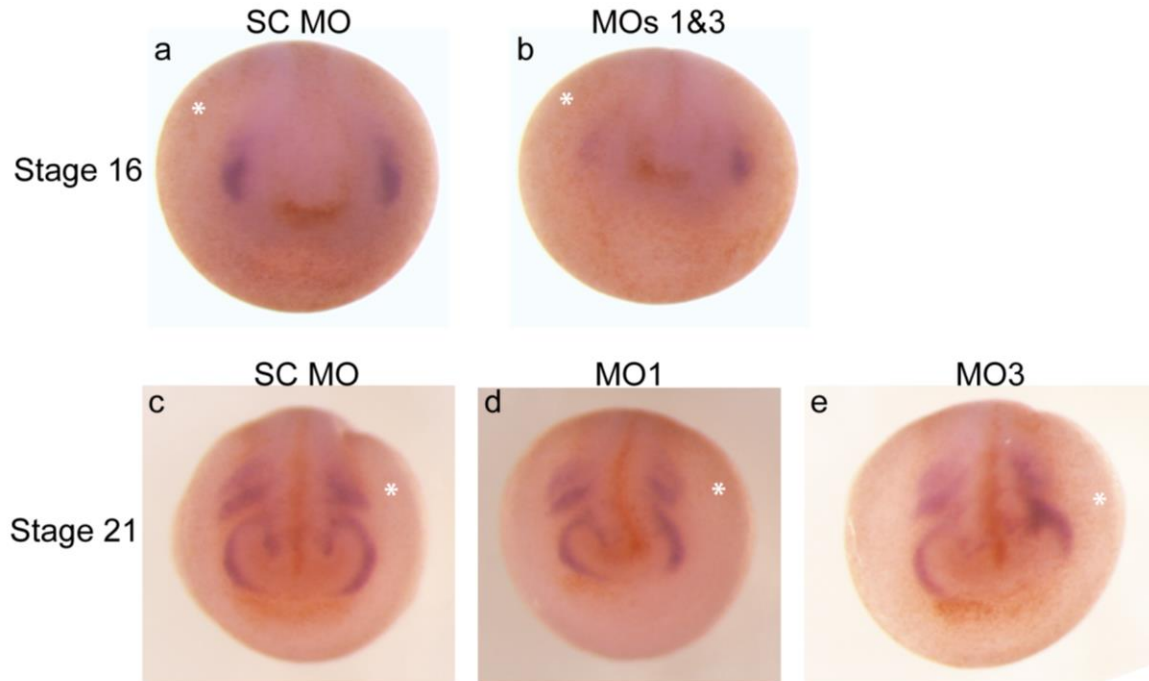


Figure 23. Neural crest induction and migration is disrupted upon Pkp3 depletion.

In situ hybridization of the neural crest marker, Twist, following morpholino injection (20ng total MO into a single dorsal blastomere at the four-cell stage). At neurula stage 16, early (inductive) neural crest expression of Twist is reduced or lost (subpanel b vs subpanel a). At neurula stage 21, later (migratory) neural crest expression likewise appears affected, as the tracts in Pkp3 depleted embryos do not extend (subpanel d-e) in the normal pattern (subpanel c).

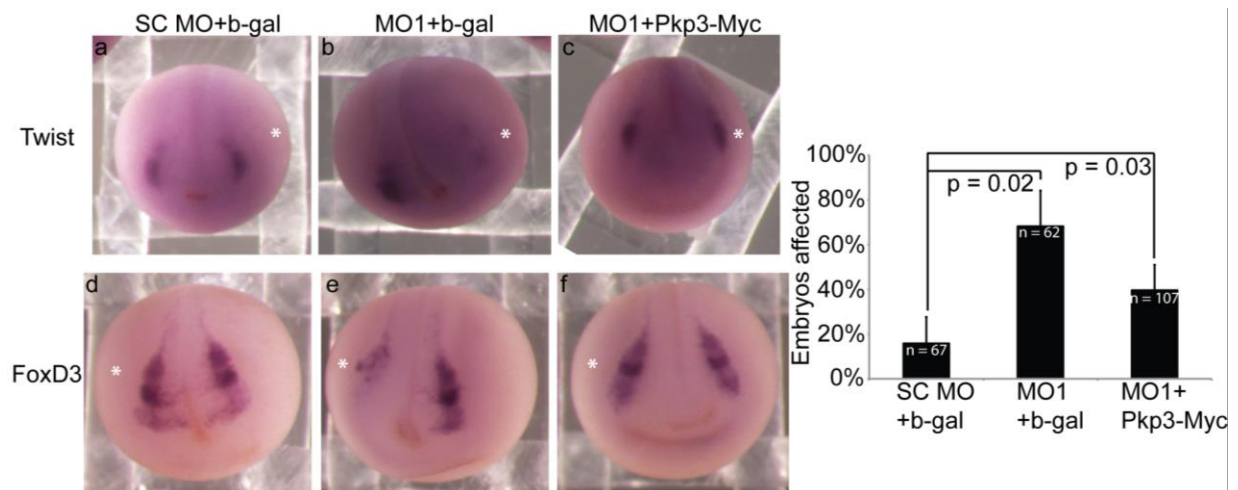


Figure 24. Expression of neural crest markers Twist and Foxd3 is affected by Pkp3 knockdown, but can be rescued by exogenous Pkp3 mRNA not targeted by Pkp3 morpholinos further indicating specificity of morpholinos.

Expression of the neural crest markers, Twist and FoxD3, was analyzed by in situ hybridization following knockdown of Pkp3. Pkp3 morphants showed reductions of both markers in the neural crest domain, that could be partially rescued upon co-injection of exogenous Pkp3 lacking the morpholino targeted sequence(s). 20ng of each morpholino and 100pg of either Myc-tagged beta-galactosidase or Myc-tagged Pkp3 mRNA was injected in a single dorsal blastomere. Quantification of these results is represented in the accompanying bar graph, where P-values indicate statistical significance.

This part is published work taken from Munoz WA, Kloc M, Cho K, Lee M, Hofmann I, Sater A, Vleminckx K, McCrea PD. (2012) Plakophilin-3 Is Required for Late Embryonic Amphibian Development, Exhibiting Roles in Ectodermal and Neural Tissues. PLoS ONE 7(4): e34342. doi:10.1371/journal.pone.0034342.

Open access agreement. Upon submission of an article, its authors are asked to indicate their agreement to abide by an open access Creative Commons license (CC-BY). Under the terms of this license, authors retain ownership of the copyright of their articles. However, the license permits any user to download, print out, extract, reuse, archive, and distribute the article, so long as appropriate credit is given to the authors and source of the work. The license ensures that the authors' article will be available as widely as possible and that the article can be included in any scientific archive.

Part Three: Identification of the Pkp3-catenin:ETV1 Complex

Yeast two-hybrid screening identifies a novel Pkp3-associated protein

Given the strong nuclear localization of *Xenopus laevis* Pkp3 in naïve ectoderm (“animal cap”) cells, and Pkp3’s suggested functional roles in *Xenopus* neural development (Figures 9, 15 and 22-24), we aimed to identify novel nuclear binding partners of Pkp3 involved in neural development. Employing *Xenopus laevis* Pkp3 as bait, we performed a yeast two-hybrid screen using an adult mouse brain cDNA library (Hybrigenics, Inc.). 351 clones were obtained, representing 156 distinct potential interactions. This screen suggested the Pkp3 has roles in varied cellular compartments, with potential binding partners suggesting roles in cell shape, intracellular trafficking, small GTPase regulation, the cell cycle, RNA processing and transcriptional regulation.

Included among the transcriptional regulators were ETV1 and ETV5, members of the large DNA-binding Ets-family, both falling within the much smaller (3-member) PEA3 sub-family. Clones of ETV1 and ETV5 identified in the screen suggested that homologous regions interact with Pkp3, namely a region just proximal to and partially including the Ets/DNA binding domain (Figure 25). I chose to validate the Pkp3:ETV1 interaction, due to shared spatial expression in *Xenopus* (see Figures 6 and 7 reference [136]), and their common roles in neural development [120,137,138]. Our yeast two-hybrid screen of mouse brain was not saturating as desmosomal cadherins, desmocollin and desmoglein, and

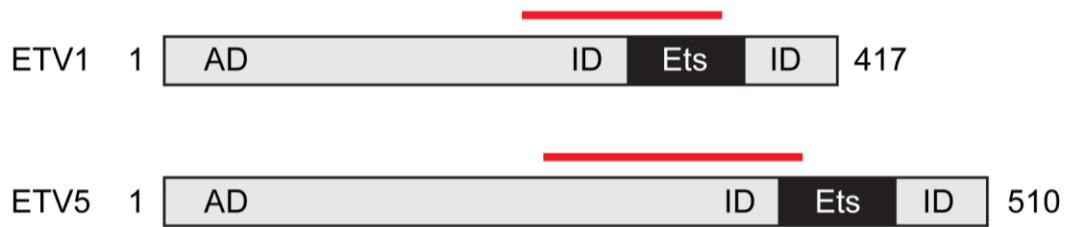


Figure 25. ETV1 and ETV5 are potential novel binding partners of Pkp3-catenin identified via yeast-two-hybrid.

Schematics of ETV1 and ETV5 protein structures identified from yeast-two hybrid screen. Red line indicates the binding region as suggested by sequenced prey clones.

previously identified RNA binding partners were not isolated [16,17,28,45,84,88,99]. This is likely due to the absence or low expression of desmosomal components in neural structures following neurulation [139]. Interestingly, β 2-spectrin, an ARVCF-catenin binding protein [140], was a strong candidate for interaction with Pkp3. This overlap may indicate a potential overlapping function between these and possibly other catenins, requiring further investigation. Given this potential overlapping binding partner and the homology between Pkp3 and ARVCF, especially in the armadillo repeats, ARVCF is an appropriate control to investigate binding partners that specifically interact with Pkp3, but not other catenin family members. In all cases, a homologous region of two closely related but independent members of the PEA3 subgroup of Ets-family transcription factors were implicated to associate with Pkp3-catenin.

ETV1 interacts with Pkp3 in cells

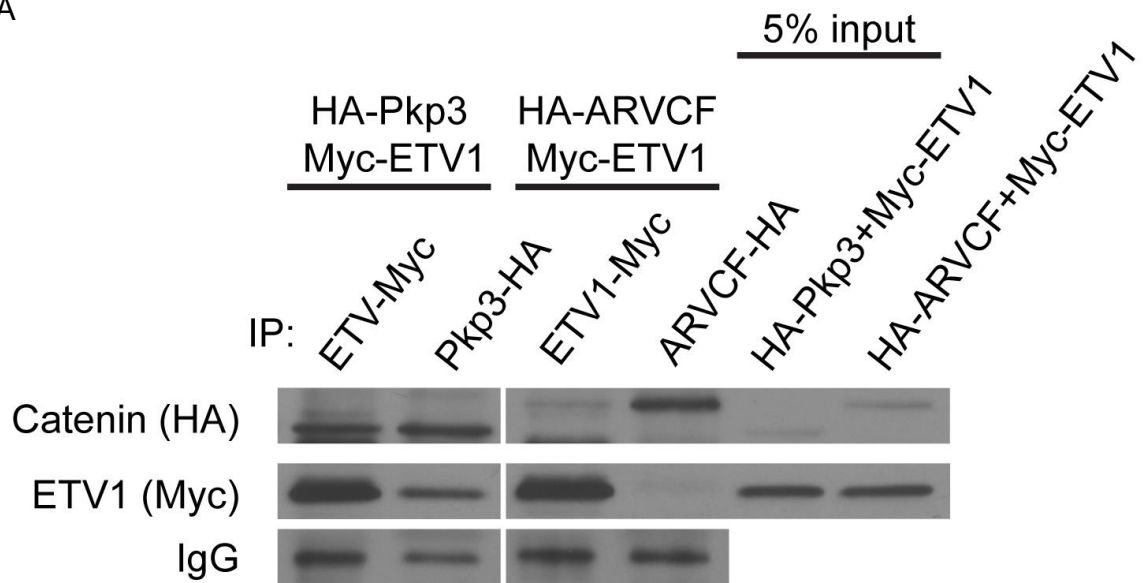
I first sought to confirm the Pkp3:ETV1 interaction using exogenously expressed *Xenopus* proteins. Antibodies are not available to precipitate endogenous *Xenopus* Pkp3 or ETV1, so HA-tagged xPkp3 (or negative control xARVCF) was coexpressed with Myc-tagged xETV1 in mammalian HEK 293T cells. HEK 293T cells provide the advantage of lacking detectable endogenous Pkp3 or ETV1 which could compete for exogenous interactions. In agreement with our yeast two-hybrid screen immuno-precipitation of HA-xPkp3 indicated that it interacts with Myc-xETV1, as did the reverse immuno-precipitation of Myc-

xETV1 (Figure 26A). Suggesting the specificity of the Pkp3:ETV1 interaction, ARVCF-catenin, which is structurally related to Pkp3-catenin (e.g. both contain a prominent Armadillo-domain), did not or only very weakly associated with Myc-xETV1. To test the conservation of the interaction across vertebrate species (*Xenopus* versus mouse), to confirm an endogenous interaction in a more developmental context, and confirm that Pkp3 and ETV1 interact in the nucleus I turned to the use of mouse embryonic stem cells (mESCs). mESCs exhibit easily detectable Pkp3 and ETV1 expression (Figure 26B), and we observed Pkp3's prominent presence in the nucleus (Figure 27), which was also observed when Pkp3 and ETV1 were over expressed in HeLa cells (Figure 28). Importantly, co-immunoprecipitation assays from nuclear lysates in this endogenous context further indicated that Pkp3 associates robustly with ETV1 (Figure 26B), whereas IgG control precipitations failed to resolve co-associations as expected.

Interaction domain mapping of the Pkp3:ETV1 complex

To investigate the interacting domain(s) of ETV1 with Pkp3, deletion constructs of ETV1 were utilized in conjunction with mitochondrial outer membrane (MOM) targeted Pkp3. The MOM localization domain of Bcl-X_L was carboxy-terminally fused to either xARVCF-catenin or xPkp3-catenin, as previously undertaken for p120-catenin [140]. These fusion proteins localize to the MOM in a punctate pattern when expressed in HeLa cells, which were used

A



B

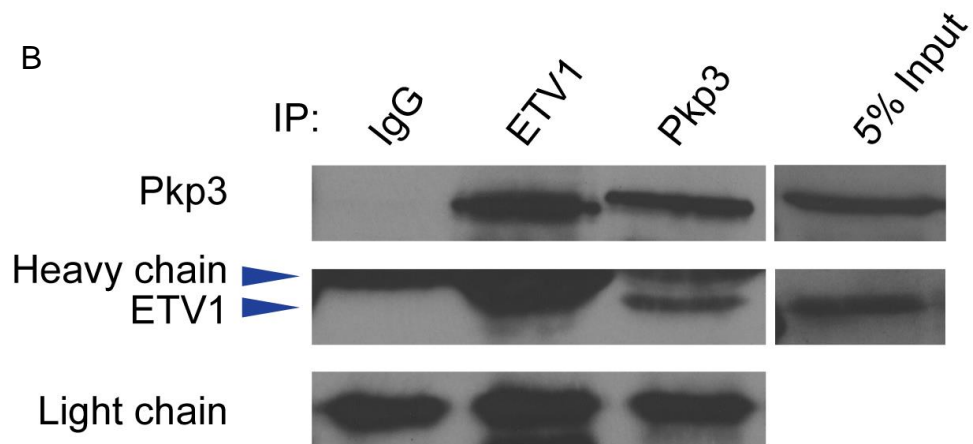


Figure 26. ETV1 and Pkp3 interact in cells.

(A) Either HA-Pkp3 or HA-ARVCF was co-transfected with Myc-ETV1 in HEK 293T cells. Anti-Myc (ETV1) or –HA (Pkp3 or ARVCF) immune-precipitates were subjected to immuno-blotting with anti-Myc (ETV1) and –HA (Pkp3 or ARVCF) antibodies. Pkp3-catenin co-precipitates ETV1, but the structurally homologous ARVCF-catenin does not (negative/ specificity control). ETV1 co-precipitates Pkp3, but does not co-precipitate ARVCF. (B) Untreated AB-1 wild type mouse embryonic stem cells were lysed at 90% confluency and endogenous Pkp3 or ETV1 was immuno-precipitated, followed by immuno-blotting for Pkp3 and ETV1. Five percent inputs were acquired separately due to the low levels of endogenous proteins.

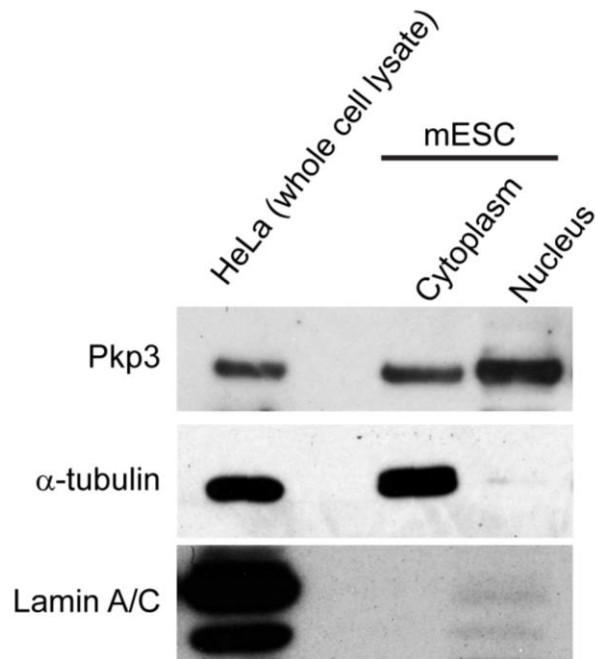


Figure 27. Pkp3 localizes to nuclei of mouse embryonic stem cells.

Mouse embryonic stem cells were fractionated into cytoplasm and nuclear pools, followed by immuno-blotting as indicated. Pkp3 fractionates to both the cytoplasmic and nuclear compartments. HeLa whole-cell extract was employed as a positive control. Fractionation efficiency of mouse embryonic stem cells was monitored via immuno-blotting for alpha-tubulin (cytoplasmic marker), or for lamin A/C (nuclear marker) (mouse embryonic stem cells exhibit low lamin A/C immuno-blot reactivity as compared to HeLa cells).

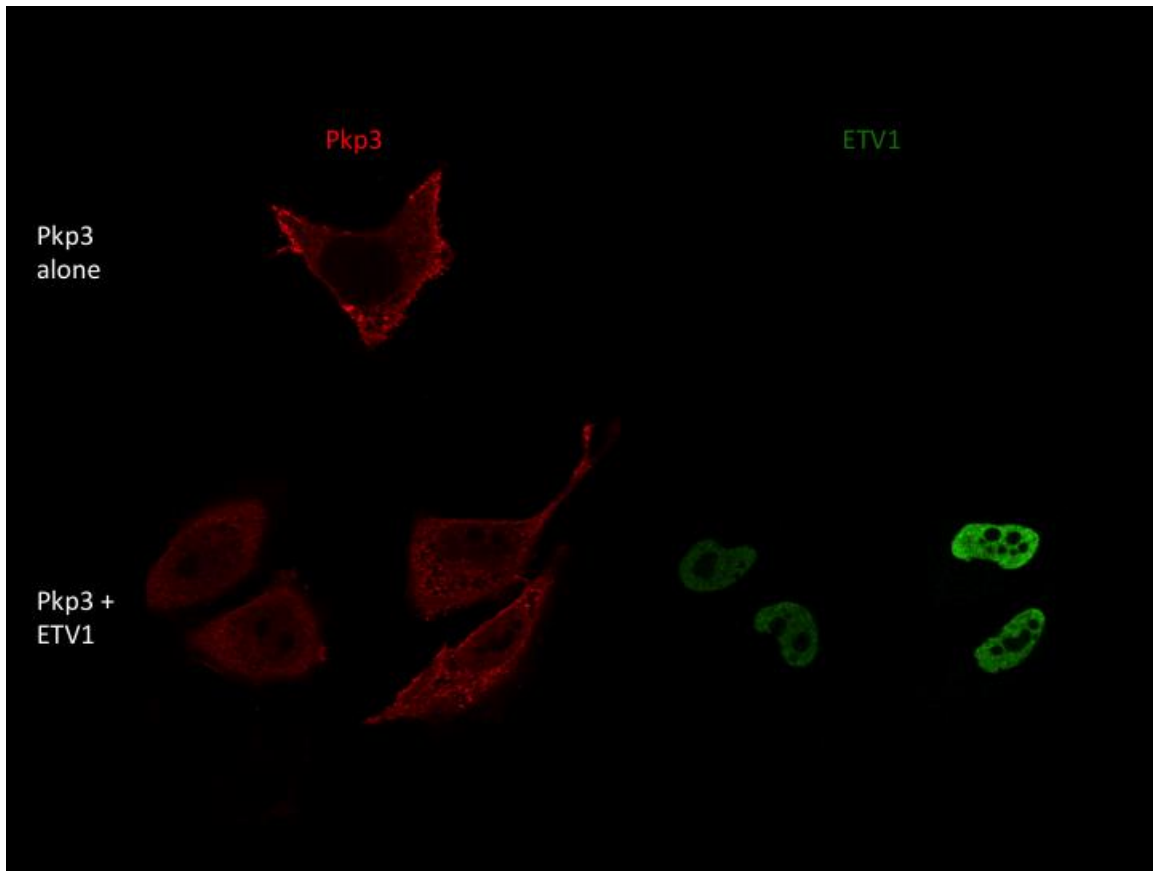


Figure 28. ETV1 overexpression promotes Pkp3 nuclear localization

HeLa cells were transfected with Pkp3-HA alone (top row) or Pkp3-HA with ETV1-MT (bottom row) and immune-stained for their respective epitope tag. Pkp3 transfection alone, causes little if any exogenous Pkp3 to enter the nucleus. However, when ETV1 is coexpressed with Pkp3 significant amounts of Pkp3 enter the nucleus.

for their ease of visualization (Figure 29; similar results were obtained using HEK 293T cells; data not shown). Four xETV1 deletion constructs expressed at similar levels were tested for interaction with xPkp3-MOM (Figure 30A and data not shown). While the relocalized Myc-ETV1 fluorescent signals were faint, I reproducibly found that full-length ETV1 relocalized in small part to the MOM when co-expressed with xPkp3-MOM, but demonstrating specificity, not when co-expressed with the structurally homologous xARVCF-MOM (Figure 29Aa' versus 30Af' and 30C) . Our yeast two-hybrid analysis had suggested that a proximal part of the ETS domain, plus an inhibitory region immediately upstream in the protein sequence, was necessary for the xPkp3:xETV1 interaction. Deletion of this region (and more) in ETV1 (Figure 30Ab and 30Ac; CT-ETV1 and Δ Y2H-ETV1, respectively, and 30C), abolished xETV1's recruitment to xPkp3-MOM. (Even as its general distribution led to the appearance of an overlap, close examination of CT-ETV1 showed that its signal was lost at sites of Pkp3-MOM relative to immediately adjacent areas). Interestingly, deletion of the ETS domain and C-terminus of ETV1 has no effect on ETV1's ability to relocalize with xPkp3-MOM. Consistent with suggestions from our initial yeast two-hybrid screen, these data point to a xETV1 region necessary for interaction with xPkp3 that include the proposed inhibitory domain (amino acid residues 257-335).

Additionally, using an ETV1-MOM construct, I demonstrate that the amino-terminus of Pkp3 is sufficient for interacting with ETV1 (Figure 31). However, while there is no strong relocalization of Pkp3's ARM domain in this assay, there

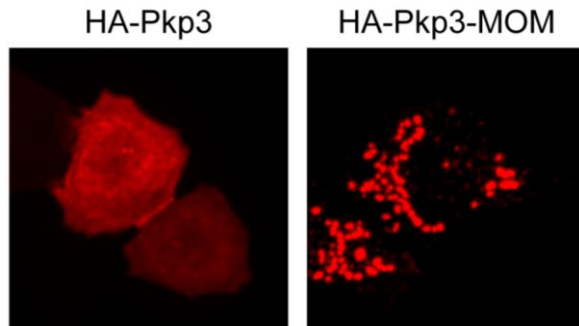


Figure 29. Ectopic mitochondrial outer membrane (MOM) localization of Pkp3.

Ectopic mitochondrial outer membrane (MOM) localization of Pkp3 was achieved by fusing a peptide sequence tag derived from human Bcl-XI [140], that directs the fusion product (HA-xPkp3-MOM) to the MOM, producing a distinctive punctate pattern surrounding the nucleus that is characteristic of mitochondrial localization (right panel). An HA-Pkp3 construct lacking a MOM fusion tag (left panel), shows an entirely different localization pattern (cell-cell junctions, cytoplasmic and nuclear presence). All transfected cells observed demonstrated this patterning.

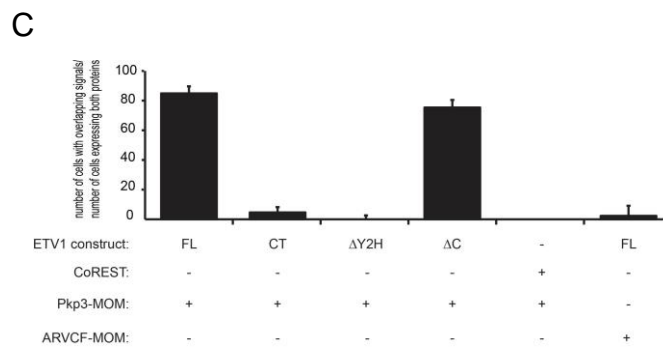
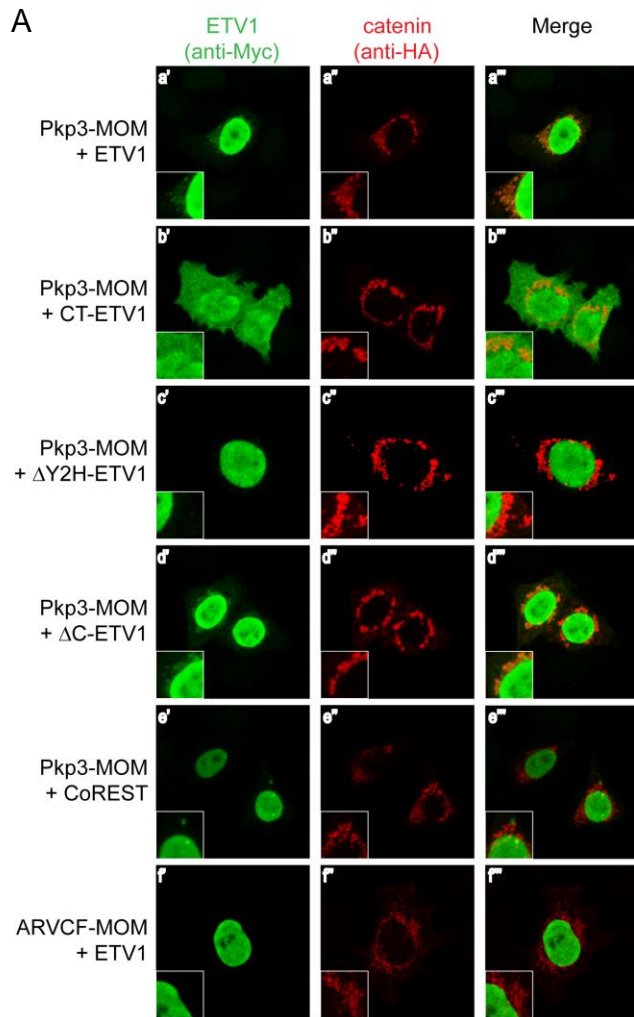
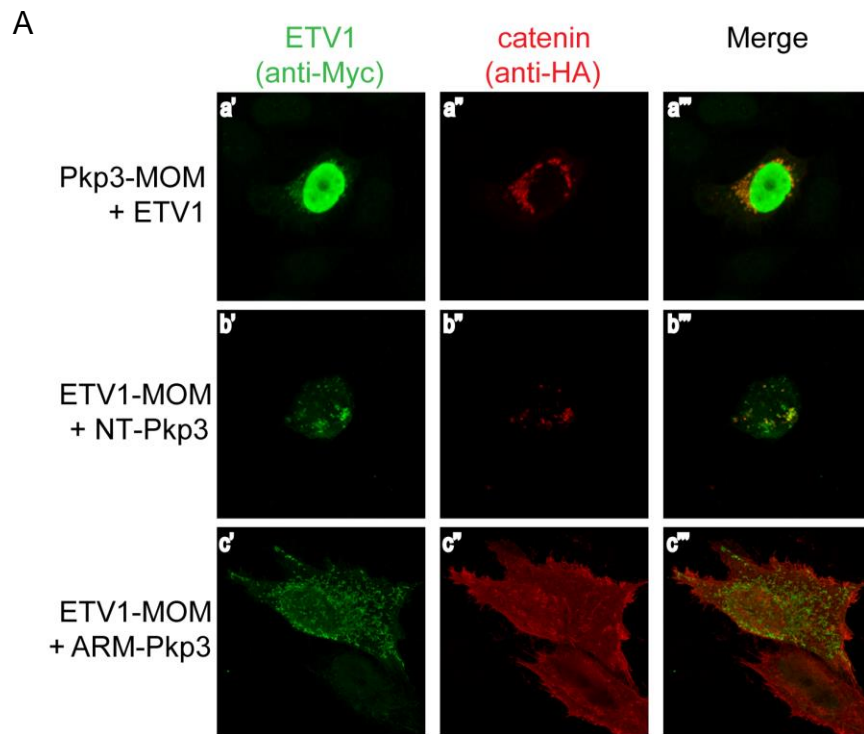


Figure 30. Ectopic mitochondrial outer membrane (MOM) co-recruitment of xPkp3 with xETV1 in HeLa cells and ETV1 binding domain mapping.

(A) Co-expression of Myc-xETV1 or Myc-CoREST (negative/ specificity-control transcription factor) with MOM-targeted HA-xPkp3 or MOM-targeted HA-xARVCF (negative/ specificity-control catenin). Cells were co-immunostained for the ectopic co-relocalization of xETV1 (Myc-epitope, left panels), as well as for the MOM-targeted catenin (HA-epitope, middle panels). Ectopic co-relocalization of xETV1 with MOM-targeted xPkp3 was only observed when amino acids 257-335 of xETV1 were present. Representative images from a minimum of sixty cells expressing both constructs analyzed are shown. (B) List of Myc-tagged (MT) xETV1 constructs, and their interaction status with MOM-targeted HA-xPkp3. A positive score (+) indicates that >75% of cells coexpressing the indicated xETV1 deletion construct showed co-relocalization of xETV1 with the MOM-targeted HA-xPkp3 construct. Our prior laboratory studies have shown that authentic partner proteins re-localize to the MOM (fusion protein), as visualized by their increased signal at the mitochondria [140]. (C) Quantification of cells processed for co-relocalization of indicated xETV1 deletion construct with the MOM-targeted HA-xPkp3 construct.



B

Construct		Interaction
HA Pkp3-MOM		+
HA NT-Pkp3		+
HA ARM-Pkp3		?

Figure 31. Ectopic mitochondrial outer membrane (MOM) co-recruitment of xETV1 with xPkp3 in HeLa cells and Pkp3 binding domain mapping.

(A) Co-expression of HA-Pkp3 with MOM-targeted Myc-ETV1. Cells were co-immunostained for the ectopic co-relocalization of MOM-targeted xETV1 (Myc-epitope, left panels), as well as for the Pkp3 fragment (HA-epitope, middle panels). Ectopic co-relocalization of xPkp3 with MOM-targeted xETV1 was observed when amino acids 1-325 of xPkp3 were present. Representative images from a minimum of sixty cells expressing both constructs analyzed are shown. (B) List of HA-tagged (HA) xPkp3 constructs, and their interaction status with MOM-targeted MT-ETV1. A positive score (+) indicates that >60% of cells coexpressing the indicated xPkp3 deletion construct showed co-relocalization of xPkp3 with the MOM-targeted MT-ETV1 construct. Our prior laboratory studies have shown that authentic partner proteins re-localize to the MOM (fusion protein), as visualized by their increased signal at the mitochondria [140].

is also no loss of its signal at the mitochondria making it unclear if any interaction exists between these molecules.

xETV1 partially rescues molecular phenotypes resulting from xPkp3 depletion in *Xenopus* embryos.

As shown earlier the morpholino-directed depletion of Pkp3 (>60% efficiency as shown in Figure 10B) in early *Xenopus laevis* embryos results in altered neural crest establishment, as well as ectodermal fragility, touch hyposensitivity and heart defects. Additionally, it has been reported that ETV1 localizes to neural crest cells during development and that other PEA3-subfamily members have roles in crest formation [136,141]. To test for an in vivo functional interaction between xPkp3 and xETV1, I attempted to rescue knock-down phenotypes following xPkp3 depletion through the exogenous expression of xETV1. Given the neural crest defects associated with Pkp3-catenin knockdown (Figure 24), we focused upon markers of neural crest establishment, namely Twist and FoxD3 (Figure 32). As shown in Figure 32B and 32C, xPkp3 depletion resulted in a reduction in Twist and FoxD3 expression. This xPkp3 depletion effect was significantly rescued upon the coordinate ectopic expression of xETV1. In agreement with findings presented below that were obtained using mammalian cell lines, these results are consistent with xPkp3 and xETV1 interacting positively at the functional level in vivo (embryos), in keeping with their noted biochemical association.

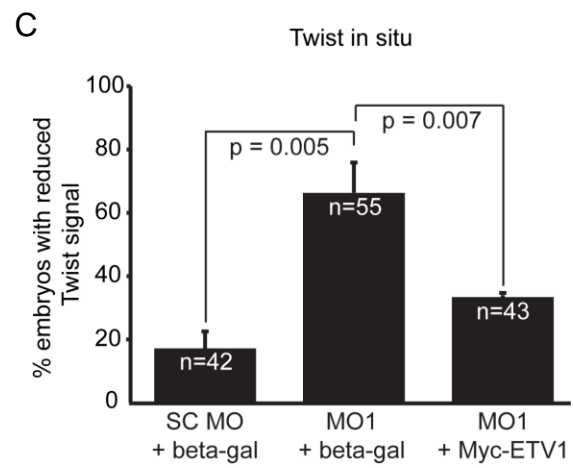
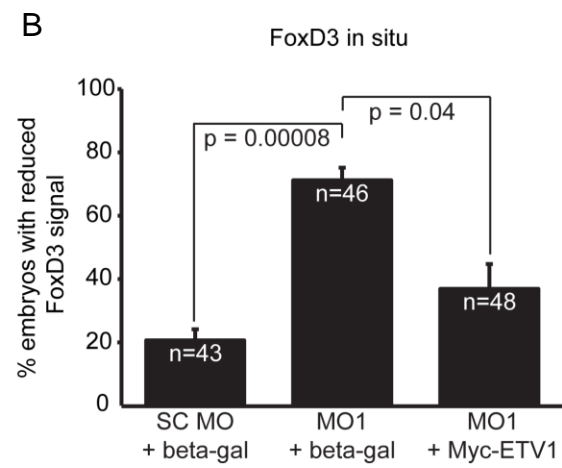
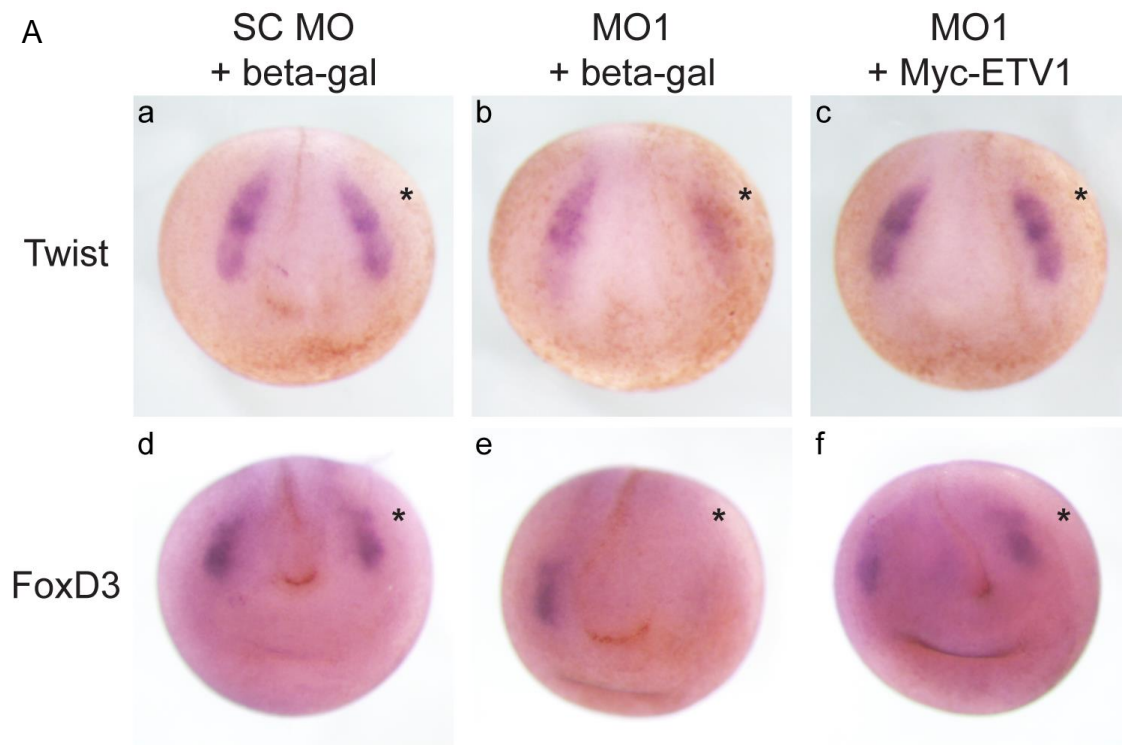


Figure 32. Rescue of neural crest establishment defects, induced upon xPkp3-catenin depletion, through ectopic expression of xETV1.

(A) The indicated morpholinos (20ng) and mRNAs (0.5ng) were co-injected into one dorsal blastomere at the four-cell stage with rhodamine dextran as a lineage tracer. After in situ hybridization for neural crest markers, Twist and FoxD3, embryos were imaged. The ectopic expression of ETV1-Myc largely rescued Twist and FoxD3 expression in embryos depleted for Pkp3-catenin (compare right-most images to middle images). (B) Quantification of embryos processed for Twist in situ hybridization, comparing the uninjected side to the injected side for reduction in signal. (C) Quantification of embryos processed for FoxD3 in situ hybridization, comparing the uninjected side to the injected side for reduction in signal. P-values indicate statistical significance.

Pkp3 positively modulates ETV1-dependent transcriptional activation

Based upon the in vivo rescuing activity of ETV1 following Pkp3 depletion (see above), I expected that ETV1 and Pkp3 might positively interact to regulate gene activity. I first addressed this possibility using an established artificial ETV1 reporter plasmid containing a *fes* gene promoter fragment encoding the ETV1 consensus sequence (CAGGAAAG), repeated in triplicate (Fes3xWT-Luc) [142-144]. As shown in Figure 33A, xPkp3 transfection alone resulted in a subtle effect upon the reporter (compare bars 1&2). This effect is significant ($p < 0.05$), however, and might result from xPkp3 binding to endogenous (even if undetectable in immuno-blots) ETV1 associated with the Fes3xWT-Luc reporter. More obvious is xPkp3's positive impact when exogenous ETV1 is co-expressed (compare bars 3&4). A less obvious, but still statistically significant effect ($p = 0.005$), was reproducibly observed when assessing an independent natural reporter of ETV1 activity, employing the control element of matrix metalloproteinase-1 (MMP1-Luc; Figure 33B). When the primary ETV1 binding site in MMP1-Luc is mutated to reduce ETV1 binding (in Figure 33B, compare bar 3 from the wild-type promoter to bar 3 in Figure 33C from the mutant promoter; note Figures 33B and 33C were performed in parallel, but presented graphically separate for ease of readership), xPkp3 no longer induced promoter activity by itself (Figure 33C, compare bars 1&2), and only weakly enhanced an already weak ETV1 activation (compare bars 3&4). This suggests that xPkp3's effects are dependent on ETV1 binding to the promoter and possibly that minimal

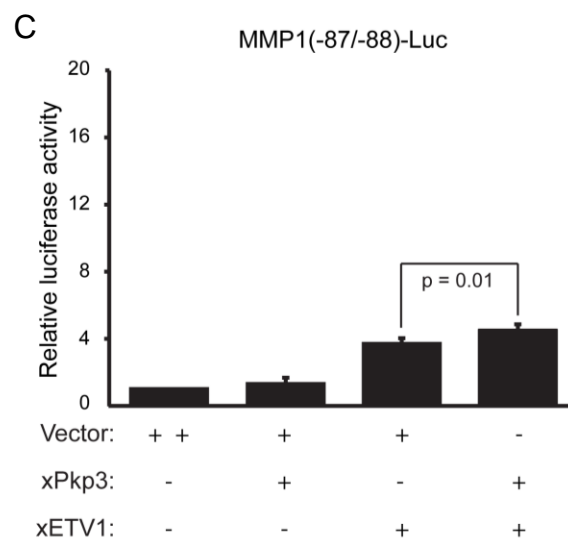
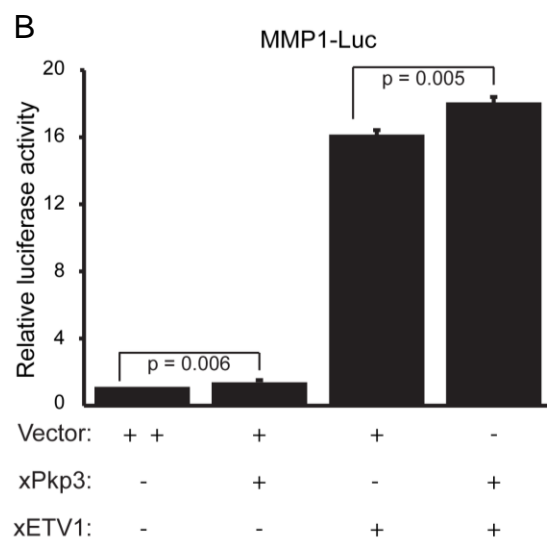
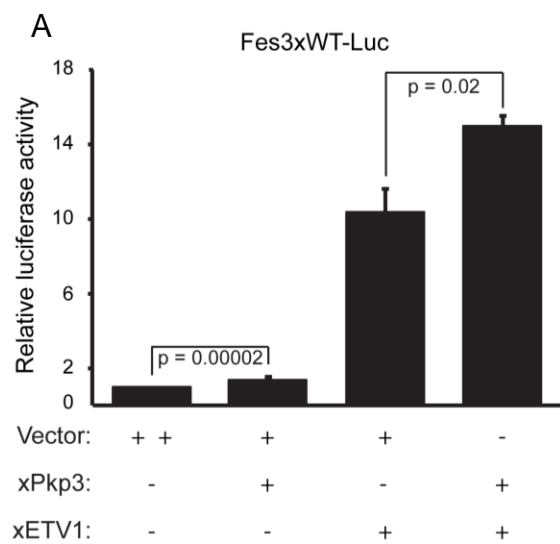


Figure 33. Pkp3-catenin regulation of ETV1 reporters.

HEK 293T cells were transfected with expression plasmids for Myc-xETV1 or HA-xPkp3 in the indicated combinations. (A) Pkp3's functional relationship with ETV1 was tested using an established luciferase reporter for Ets family member transcriptional activity harboring a *fes* gene promoter fragment in triplicate (Fes3xWT-Luc,[143]). (B) Pkp3's functional relationship with ETV1 was tested using a second established ETV1 reporter construct harboring a native matrix metalloproteinase-1 (MMP1) promoter fragment (MMP1-Luc,[142,145,146]). (C) MMP1(-87/-88)-Luc is a negative-control construct containing a non-functional ETV1 consensus binding site. Performed in parallel to Figure 30B. P-values indicate statistical significance.

reporter activation upon xPkp3 transfection alone arises due to the presence of low levels of endogenous ETV1.

Next, I evaluated the impact of xPkp3 upon endogenous ETV1 target genes [123]. As shown in Figure 34, xPkp3 knockdown in *Xenopus* embryos significantly reduced expression of established ETV1 targets involved in the dopamine transport and synthesis pathways, including dopa decarboxylase (DDC), tyrosine hydroxylase (TH), solute carrier family 18 member 2 (SLC18A2), and GTP cyclohydrolase I (GCH). These effects could be partially rescued upon the coordinate expression of ectopic ETV1. These findings continue to be consistent with the existence of a Pkp3:ETV1 functional interaction and Pkp3 being a positive modulator of ETV1 in vivo.

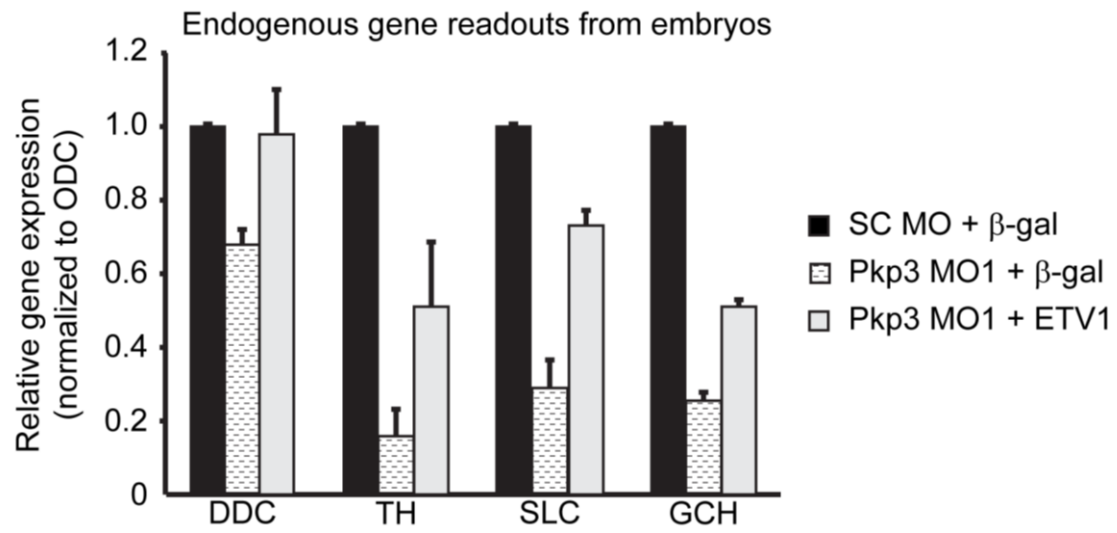


Figure 34. Pkp3-catenin regulation of ETV1 target genes in vivo.

The indicated morpholinos (40ng) and mRNAs (0.5ng) were injected into one-cell (cleavage) stage *Xenopus* embryos followed by RNA extraction at late neurula stages, DNase treatment, reverse transcription, and real-time PCR to assess Pkp3- depletion effects upon ETV1 target-gene transcription. The co-injection of ETV1 mRNA with Pkp3 morpholino (MO) significantly rescued the impact of Pkp3-catenin depletion. The ETV1 gene targets assessed are each components of the dopamine synthesis and transport pathways and include: DDC = dopa decarboxylase; TH = tyrosine hydroxylase; SLC = solute carrier family 18 member 2; and GCH = GTP cyclohydrolase I. All real-time PCR was repeated more than three times with samples tested in triplicate with similar outcomes. Error bars represent the standard deviation from three independent experiments. Differences between negative control (SC MO + β -gal) and Pkp3 knockdown (Pkp3 MO1 + β -gal) are all statistically significant based on the Student's T-Test, demonstrating p-values < 0.05. Differences between Pkp3 knockdown (Pkp3 MO1 + β -gal) and its rescue with ectopic ETV1 (Pkp3 MO1 + ETV1) are all statistically significant based on the Student's T-Test, demonstrating p-values < 0.05.

Chapter III

Discussion

In my study, I have evaluated the expression, subcellular localization, developmental roles and association of Pkp3 with ETV1. My work is the first to show Pkp3 is necessary for amphibian development, with depletions resulting in reductions of ectodermal integrity and heart defects, most likely from a reduction in desmosome number. Additionally, I find that xPkp3 plays important roles in neural crest development, with depletions causing various neurological defects of the peripheral nervous system. Distinct from reported protein interactions of Pkps at desmosomes, in stress granules and bound to single-strand DNA, I identified the first sequence-specific DNA binding partner of a Pkp, known as ETV1. ETV1 is an Ets-family transcription factor, involved in various aspects of neural development and maintenance. I observe that this biochemical interaction is functionally relevant (based upon rescue analysis) to embryonic neural development in amphibians. My results form an initial outline of Pkp3's role in amphibian development as well as revealing the first transcription factor to bind a Pkp.

Pkp3 isoforms, expression and subcellular localization

I observed that Pkp3 mRNA levels increase in *Xenopus* following gastrulation, congruent with available sequence-tag data from mice (<http://www.ncbi.nlm.nih.gov/UniGene/ESTProfileViewer.cgi?uglist=Mm.350037>). Expression of a 75 kDa Pkp3 protein isoform coincides with this mRNA profile and further the protein persists in the adult frog. Presumably due to maternal

protein deposits made to the oocyte and passed onwards to the egg and embryo, I did not observe Pkp3 protein levels drop immediately following morpholino injection (data not shown). At such early stages (prior to gastrulation), I resolved a Pkp3 protein isoform migrating at 110 kDa, with a reduction in expression following gastrulation, and no detectable presence in adult tissues. This complementary expression of the Pkp3 protein isoforms leaves open the possibility of a switch in function between the two isoforms in early versus later embryonic development. The two isoforms of Pkp3 might originate from alternative translation initiation sites, as is well known to occur for p120-catenin [19,128]. Alternatively, while speculative, a conserved, potential caspase-3 site in Pkp3, which would produce ~75 and ~ 35 kDa fragments, may make it sensitive to caspase-3 (or other) cleavage, as we recently revealed for delta-catenin [147]. As was shown for delta-catenin, we would expect that this potential cleavage would result in fragments with differing functions and/or localizations. Whole-mount in situ and immunoblot analyses indicate that Pkp3 is present in the skin and lungs of *Xenopus* and absent from the liver, consistent with previous expression data obtained from mouse tissues and mammalian cell lines [55,79,93,99,103]. However, distinct from prior reports, we further observe Pkp3 localization in neural derivatives, heart, kidney and muscle, but not in the intestine or stomach. Interestingly, certain structures of the central nervous system and the peripheral nerves are connected to surrounding sheaths of epitheloid cells via desmosome structures [148], providing a potential function for Pkp3 in these tissues. However, I show Pkp3 to be acting outside the

desmosome in conjunction with ETV1 in the development of these tissues. Interestingly, the closely related p120-catenin subfamily has been shown to have widespread expression in adult *Xenopus* tissues [34,131,132]. The more restricted although partially overlapping expression profile of Pkp3 suggests that it might fulfill specialized functions.

At the intracellular level in both *Xenopus* and mouse embryonic stem cells, Pkp3 localizes to a number of cell compartments including the nucleus, which had previously been ascribed as potentially exceptional or artifactual in mammalian systems [45]. However, my findings regarding Pkp3 are based upon both endogenous and exogenous detection, and coincide with detailed descriptions of nuclear Pkp1 and Pkp2, as well as of multiple other catenin family members [92,94,95,147,149]. Indeed, we have preliminarily resolved a number of nuclear proteins in association with Pkp3 that are now being characterized (data not shown) in addition to my confirmed interaction with ETV1. One possibility for the prior discrepancies, while requiring further investigation, may be explained through closer examinations of nuclear Pkp3 in *Xenopus* animal cap cells (*Xenopus* embryonic stem cells), and mouse embryonic stem cells. As the nuclear localization of Pkp3 is not readily discernible in adult mammalian tissues, the nuclear localization in these stem cell lineages may be transient. This would suggest a significance in early development that decreases as the animal matures and certain nuclear functions are possibly no longer required. I expect that plasma membrane-associated Pkp3 in *Xenopus* contributes to desmosome

formation and/or stability, as has been well characterized in mammalian systems [45,78,93,99,102]. In conjunction with Pkp3's structural capacity at desmosomes, the presence of Pkp3 at desmosomal junctions, and in the cytoplasm and nucleus, provides the possibility that this catenin may assist in a signaling capacity in cross-talk between junctional, cytoplasmic and nuclear compartments. These signaling roles might, for example, include Wnt signaling and small GTPase modulation as has been shown for other catenins [48,150-152].

Developmental roles of Pkp3

Amphibian embryos have provided a number of instances where depletion of genes of interest generate more obvious phenotypes than does their corresponding knockout in mammals/ mice. This has been true for various catenins, with more pronounced developmental effects following either *Xenopus* ARVCF or delta-catenin knockdown than found in knockout mice [34,49,153] (R. Kucherlapati, personal communication). Therefore, to uncover potentially novel development roles of Pkp3 relative to what had been reported in the mouse, I took advantage of the experimental advantages of the amphibian system [154], using knockdown approaches in *Xenopus laevis*.

To examine Pkp3 functions in vivo, I used Pkp3 sequence specific antisense morpholinos to block ribosome binding and translational initiation of the

Pkp3 transcript. This standard depletion approach, using either of two distinct sequence specific morpholinos, revealed a number of consistent phenotypic outcomes. Interestingly, in Pkp3 knockout mice, Pkps 1 and 2 were upregulated most likely as a compensatory mechanism [102], while in *Xenopus*, I found that Pkp3 depletion did not appear to alter Pkp2 mRNA or protein levels. Thus, this less pronounced compensation among Pkps in amphibians may allow for the more severe effects I observed following Pkp3 knockdown in *Xenopus* relative to losses of Pkp3 in mammals.

In evaluating targeted tissues such as neural crest, where one dorsal cell within a 4-cell embryo was injected with morpholino, I supported the specificity of the Pkp3 depletion phenotype by using an add-back approach. We observed consistent if partial rescues through expression of morpholino-resistant Pkp3. Self-rescues were more difficult to obtain in embryos injected with morpholinos at the 1-cell stage (or both cells of a 2-cell embryo), since essentially the entire embryo must be coordinately rescued. To address this concern, I employed the standard in the field, reproducibly obtaining similar phenotypes using independent (non-overlapping) morpholinos.

MO 1, targeting a region upstream of the translational start site, exhibited the highest phenotypic and Pkp3-protein knockdown penetrance. Each morpholino caused skin fragility, heart deformation, tactile hyposensitivity and a delayed escape from the Vitelline membrane. Increased skin fragility was

correlated with a decrease in the number and size of basally disposed desmosomes within the outer ectoderm, phenocopying prior Pkp3 depletion studies, and studies of patients with Pkp1 mutations that exhibit skin fragility ectodermal-dysplasia [68,70,102,155]. Mutations or loss of desmosomal components, including Pkp2 but not the other Pkps, are known to compromise desmosome structure and lead to arrhythmogenic right ventricular dysplasia and heart failure in patients [73,75,156]. Our results in *Xenopus* likewise suggest that Pkp3 is needed for heart formation and/or maintenance in *Xenopus*, possibly participating in a desmosomal context similar to that of Pkp2 in human heart, and/ or conceivably as an indirect consequence of effects upon neural crest, which contributes to the heart outflow tract [157]. The effects of *Xenopus* Pkp3 knockdown effects on ectoderm and desmosomes confirms the prior phenotypes identified in other models (Figure 35), but the impact upon heart is interesting, since reports from mouse and human have indicated that Pkp1 or 3 loss or mutation does not result in heart effects. It thus appears that this species distinction warrants future investigation.

In addition to the noted heart phenotypes in *Xenopus*, Pkp3 depletion caused defects in the multiciliated cells of the ectoderm. In overexpression studies, a punctate Pkp3 localization was observed in the same apical region where cilia are organized within these cells, suggesting a novel role for Pkp3 in cilia establishment or maintenance. Interestingly, we have identified a number of intracellular trafficking and motor proteins that we have preliminarily

Molecular Function

Developmental role

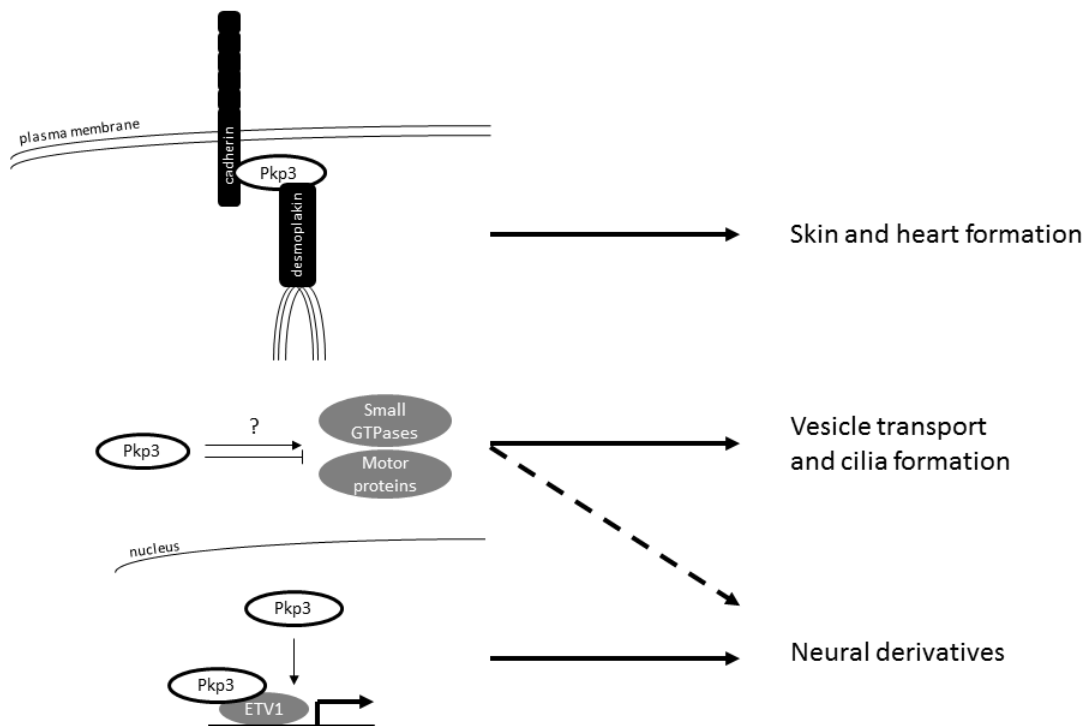


Figure 35. Potential molecular mechanisms regulating Pkp3 developmental functions in amphibians.

Pkp3 is depicted with known or likely activities indicated, and how these activities are expected or conjectured to relate to observed developmental functions in *Xenopus*. I expect that Pkp3's desmosomal roles contribute to proper formation of the skin and heart in *Xenopus*. Additionally, the potential role of Pkp3 as suggested from other Pkps and p120-catenin subfamily members in the modulation of small GTPases or trafficking motor proteins, may underlie the Pkp3's observed roles in vesicle transport and/ or cilia formation. It must also be considered that the regulation of small-GTPases and trafficking motor proteins would affect neural development, given the significant contributions these pathways provide to neural cytoskeletal structures and vesicle transport. However, given that ETV1 expression significantly rescues loss of neural crest cells due to Pkp3 knockdown, I expect that a major developmental role of Pkp3 in neural tissues occurs through the Pkp3:ETV1 nuclear interaction I resolved.

identified in association with Pkp3. These proteins were found previously by others to participate in cilia formation, cilia activity, vesicle transport or mitochondrial localization (Figure 35 and data not shown). Consistent with potential Pkp3 contributions to vesicle transport and cilia formation, the structurally related Pkp2 was found in mammalian cells to affect kinesin dependent intracellular transport of Dsg2 along microtubules. Additional catenin family members (p0071-, p120- and ARVCF-catenin) have been shown to have roles in actin organization [41,49,50,52,54,158].

We further uncovered an unexpected role for Pkp3 in amphibian sensitivity to tactile stimuli. The observed hyposensitivity that followed Pkp3 depletion can be partially attributed to the reduction or compromised function of certain sensory (and/ or motor?) neural tracts along the length of the animal, including the lateral tract that is responsible for transduction of tactile responses from the ectoderm to brain [159]. The requirement of Pkps in neural function has not been previously noted, and might prove to be an interesting area for future investigation. Tactile sensory pathways are mostly derived from neural crest cells [160,161], where we found indications that Pkp3 plays a necessary role. The neural crest molecular markers (Twist & FoxD3) and neural crest derived pigment cells were each notably reduced following Pkp3 depletion. Numerous signaling pathways, including the canonical and noncanonical Wnt pathways, act in neural crest cell specification and migration [160,162]. While speculative, since canonical Wnt signals are transduced by beta-catenin, recent evidence regarding the

involvement of vertebrate p120-catenin [152] supports that more distant members of the catenin family such as Pkp3 may additionally contribute to Wnt mediated processes in neural crest. Indeed, our preliminary results suggest a stabilization of Pkp3 by positive Wnt pathway modulators (data not shown). Additionally, small GTPases and intracellular trafficking proteins play important roles in the differentiation and stability of neural tissues through their effects on cell shape and motility, and positioning of various molecules necessary for proper neural synapses, respectively. Thus, Pkp3's potential regulation of these groups of proteins identified in our yeast-two-hybrid could also contribute to the observed phenotypes of Pkp3 depletions.

Identification of the Pkp3:ETV1 interaction

Our yeast two-hybrid screen using full-length Pkp3 as bait revealed multiple potential binding partners, including several nuclear/ gene-regulatory proteins such as ETV1 and 5. The mouse brain cDNA library used in this screen was chosen because of my earlier observations of xPkp3's possible roles in neural development [90], and because of the lack (or lower expression) of desmosomal components in brain that otherwise might dominate the screen and interfere with resolution of less obvious, but important nuclear interactions.

I confirmed the Pkp3:ETV1 association in co-immunoprecipitation experiments involving both exogenous and endogenous proteins. In conjunction

with such co-immunoprecipitations, we showed that Pkp3 localizes to both the nucleus and cytoplasm of mouse embryonic stem cells, similar to our earlier observations of Pkp3 in *Xenopus* naïve ectoderm (“animal cap”) cells [90]. Additionally, the relocalization of Pkp3 to the nucleus when ETV1 is overexpressed, and the co-immunoprecipitation of endogenous proteins from purified nuclear lysates, show that this interaction is most likely occurring in the nucleus.

The Pkp3:ETV1 interaction was further supported in functional assays, where ETV1 expression was able to significantly rescue the loss of neural crest markers that are otherwise diminished upon Pkp3 knockdown (Figure 35). Additionally, my data shows that Pkp3 can modulate ETV1 transcriptional activity, as measured by both reporter gene assays and endogenous gene expression. Based upon depletion and rescue analyses, Pkp3 acts positively at known dopaminergic ETV1 target genes. As the dopaminergic neurons are necessary for somatosensory responses [163], this relationship might account for the earlier phenotypic effects I observed in developing *Xenopus* embryos, where Pkp3 depletion led to clear perturbations of sensory neural tracts and to the reduction of responsiveness of early and tailbud stage embryos to touch [90].

With respect to the reporter assays, Pkp3's positive effect when co-expressed with ETV1 was obvious when using the artificial (3x) Fes Ets-binding element, while a more marginal but still significant effect arose using the natural

MMP-1 promoter fragment. Pkp3's ability to activate the reporter on its own or in conjunction with exogenous ETV1 was largely eliminated upon mutation of the ETV1 consensus binding site. This suggests, as we would predict, that Pkp3's effects are dependent upon ETV1's direct association with DNA. Interestingly, Pkp3 appears to be a stronger inducer of the artificial (3x) Fes Ets-binding element reporter in a cell-free system, relative to ETV1. In this cell-free system, Pkp3 may promote the activity of the RNA Polymerase III complex as has been suggested for Pkp2 [97], a possibility that requires future studies. Regarding my analysis of endogenous gene expression, it is noteworthy that Pkp3 knockdown reduces expression of ETV1 targets, and that this can be rescued by expression of ectopic ETV1.

All of these results are consistent with the view that Pkp3 acts as a co-activator in association with ETV1.

Concluding remarks

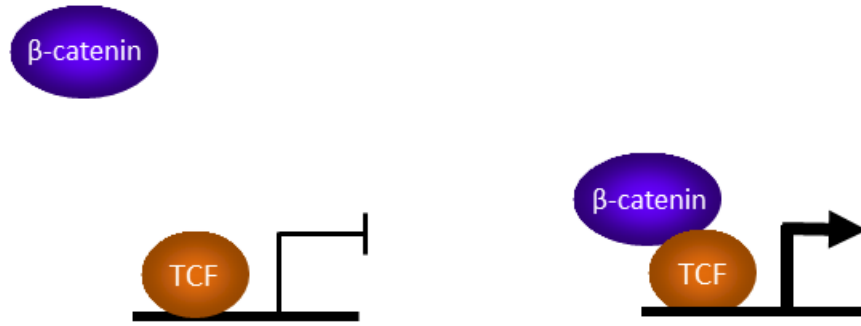
My work indicates that Pkp3 is necessary for various aspects of amphibian development including ectoderm integrity, heart formation or maintenance, and neural development. While the ectoderm and heart contributions are significant, they have been previously characterized for the Pkps in general, which exhibit some inter-compensatory properties, and found to relate to desmosome formation and stability [68,70,73,75,102,155,156]. In contrast, the Pkp3 contributions to neural development that I uncovered represent a novel area of Pkps' biology, with *Xenopus* providing a way to investigate Pkp3's functions that may otherwise be compensated for by Pkp1 or 2 in other species. Additionally, my work establishes ETV1 as the first nuclear binding partner of Pkp3, and to our knowledge, the first site-specific DNA-binding transcription factor binding to any of the plakophilin/ Pkp-catenins.

Xenopus Pkp3's role in ectoderm integrity and desmosome size and number is consistent with previous reports showing that Pkp3 contributes to desmosome stability, with loss of Pkp function in humans leading to ectoderm fragility and arrhythmogenic right ventricular disease as a consequence of desmosomal defects [17,28,68,70,73,75,76,93,102,155,156,164]. While the desmosomal roles of Pkp's have been reasonably well studied, their cytoplasmic and nuclear functions are poorly defined [17,18,40,41,88,89,92]. Individual catenins appear to have distinct interactions with transcription factors,

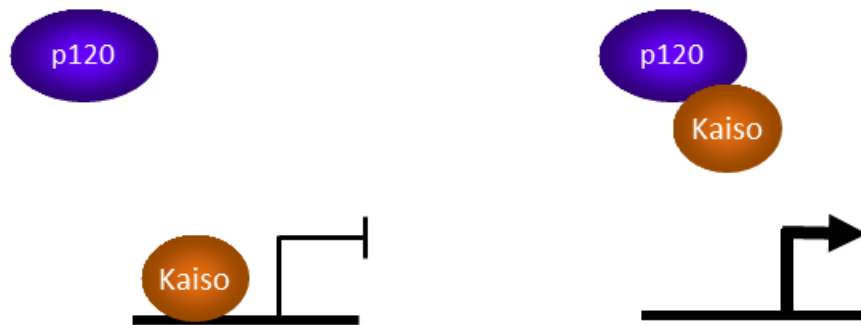
even as some interactions may be shared. For example, beta-catenin binds/modulates the TCF/LEF transcriptional repressor, while p120-catenin binds/modulates the Kaiso transcriptional repressor [57-59]. Intriguingly, some gene targets appear to be regulated coordinately by beta-catenin:TCF/LEF and p120-catenin:Kaiso, with upstream canonical-Wnt signals regulating the nuclear activity of both beta-catenin and p120-catenin (isoform1) [62,65,152,165,166]. Recent evidence has suggested that Pkp1 and Pkp2 may have differing roles in the nucleus, with Pkp1 binding to single-stranded DNA and Pkp2 associating with RNA polymerase III [92,97]. I have yet to test if Pkp1 or 2 associates with ETV1 (or ETV5), as reported here for Pkp3, though preliminary results suggest Pkp2 may enhance ETV1 transcriptional activity as well (data not shown). In resolving Pkp3's interaction with ETV1, we demonstrate for the first time to our knowledge that a Pkp-catenin functions in association with a site-specific DNA-binding transcription factor. In this regard, Pkp3's nuclear role(s) may be analogous in concept to those previously established for catenins of the beta- and p120-subfamilies (Figure 36).

Future work will be required to determine whether Pkp1 and Pkp2 also associate with ETV1, and thus potentially compensate in part for Pkp3 loss. Additionally, other potential Pkp3 binding partners identified in our screen will require further validation such as ETV5, with its strong similarity to ETV1, and HNRNPK, which is interesting because of its role in both transcription and translation possibly bridging the Pkp3 roles inside and outside the nucleus.

A



B



C

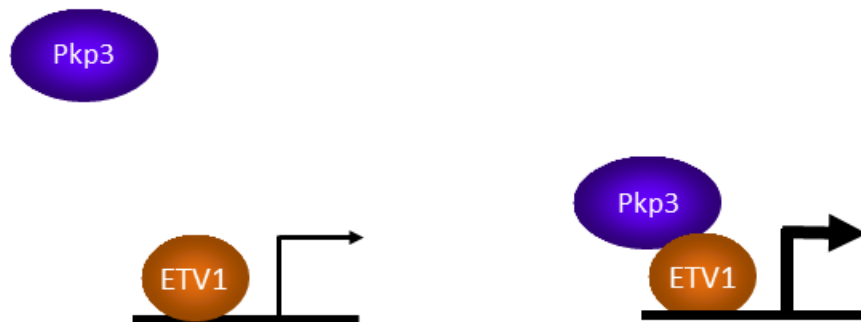


Figure 36. Transcriptional activity of various catenin family members.

(A) When beta-catenin is not bound to the transcription factor TCF, TCF acts as a transcriptional repressor. Once beta-catenin is bound to TCF, the complex promotes transcription. (B) p120-catenin de-represses (activates) Kaiso target genes by removing Kaiso from its target DNA sequence. (C) ETV1 activity is enhanced by the co-activator Pkp3.

Future work will also address how Pkp3-catenin confers positive gene-regulatory effects in association with ETV1, possibly for example, through assisting with the recruitment of transcriptional co-activators such as shown for beta-catenin in association with TCF/ LEF (reviewed in Saito-Diaz et al., 2013 and Mosimann et al., 2009) [167,168]. To further test how Pkp3 confers this regulation, individual ChIP-seqs of Pkp3, ETV1 and various chromatin modifications should be performed. This would reveal regions bound by both Pkp3 and ETV1 while also revealing how the chromatin is being modified at these sites. RNA-seq performed in parallel, comparing the impact upon the transcriptome of varying levels of Pkp3 and ETV1 (perhaps additionally comparing forms of Pkp3 or ETV1 incapable of binding the other), could also be used to help characterize genes regulated by the Pkp3:ETV1 association. I also demonstrated that an inhibitory region (amino acids 257-335), previously characterized in ETV1 and like-members of the PEA3 Ets-subfamily [117,127,169], is required for Pkp3's association with ETV1. Work from others has shown that when this region is bound by an antibody, the DNA binding region is unmasked to more readily bind DNA [118]. We speculate that Pkp3 binding to ETV1 may act similarly, unmasking ETV1's DNA binding domain and therefore promoting ETV1's transcriptional activity. In addition, I found that the amino-terminus of Pkp3 is required for ETV1 association. This region is known to be necessary for interaction with the desmosomal cadherins [20]. While requiring future investigation, the requirement for this same region of Pkp3, albeit in differing

cellular compartments (junctions versus nucleus), may result in competition between ETV1 and cadherins for Pkp3 binding.

In addition, the possible pleiotropic effects of the Pkp3 knockdown must be addressed. This could be examined using transplantation experiments in *Xenopus*. Naïve ectoderm from negative control or Pkp3 depletion (or Pkp3 expression, etc.) donor embryos ubiquitously expressing GFP would be tested for its ability to contribute to the various structures in host animals that were affected in my previous Pkp3 depletion studies. This would largely reduce concerns of Pkp3 manipulation of larger regions of the embryo producing secondary effects upon regions of interest. Of further use to more selectively define Pkp3's effects is to better map the regions of Pkp3 necessary for each molecular function, perhaps even extending to a co-crystal structure of Pkp3:ETV1. Point or other refined mutants of Pkp3 could then be devised to abrogate selected functions of Pkp3, to be used in add-back experiments where Pkp3 has been depleted (via MOs, etc.), generating host embryos for the above transplantation experiments. This would help to resolve how each Pkp3 biochemical interaction relates to its developmental roles in vivo. For example, I expect that when a Pkp3 point mutant that no longer interacts with ETV1 is used in add-back experiments in donor embryos depleted for ETV1, the transplanted naïve ectoderm would no longer differentiate into neural crest or the peripheral nervous system.

In a more clinical regard, ETV1 has been shown to have a role in

regulating matrix metalloproteinases during tumorigenesis [125-127,170], and it may prove worthwhile to test ETV1 target gene expression in human patients with elevated Pkp3 levels [77,105]. Likewise, we anticipate that Pkp3 loss or gain might prove relevant in certain neurological contexts, given ETV1's established roles in the dopaminergic pathway (etc.) of differentiating neurons.

Another question is how Pkp3 itself is regulated, and how such regulation would affect ETV1 activity. In conjunction with prior reports showing stabilization of the closely related p120-catenin sub-family members by Wnts, we have strong preliminary results that suggest Wnt signals likewise stabilize Pkp3 in *Xenopus* [65,152]. Once stabilized by Wnt signals, I speculate that the signaling pool of Pkp3 would be enhanced to interact with ETV1. This would then be expected to alter ETV1-modulated gene regulation and have an impact upon events, such as the specification of neural crest cells, and in later development, the differentiation of posterior neurons. Finally it would be of interest to examine the molecular differences between the Pkps across species to identify what may have given rise to the functional distinctions throughout evolution, especially given that a recent analysis of the Pkp-subfamily suggested that it evolved recently and rapidly [19].

Overall, my study revealed novel developmental roles of Pkp3 and identified the first transcription factor to bind a Pkp, thus broadening our understanding of the Pkp-subfamily of proteins.

Chapter IV

Materials and Methods

Embryo manipulations and Ethics

Xenopus laevis embryos were obtained, fertilized and microinjected as previously described [171], except that microinjections were performed in 5% Ficoll in 0.3X MMR (Marc's modified ringers solution), and cultured in solution for at least one hour. Embryos were then transferred to 0.3X MMR with 50 µg/mL Gentamycin for culture at 14-18°C. Phenotypes were visually scored at various embryonic stages using a standard binocular stereoscope (Olympus SZX12).

This study was carried out in strict accordance with the recommendations in the American Association for Laboratory Animal Science Learning Library. The protocol was approved by the Institutional Animal Care and Use Committee of the The University of Texas-M.D. Anderson Cancer Center (ACUF Protocol #09-93-05717). All efforts were made to minimize animal discomfort.

***Xenopus laevis* Pkp3 cDNA isolation**

In collaboration with Kris Vleminckx a Pkp3-specific cDNA fragment from *Xenopus laevis* was identified via screening of a cDNA library (embryonic stage 30; Stratagene), using a labeled human Pkp3 cDNA fragment. Further Pkp3 sequence was obtained using 5' RACE of mRNA extracted from *Xenopus laevis* XTC cells, and the assembled clone entered into the pGEMTeasy vector.

Histological sections

Histological sections were prepared by embedding embryos in paraplast using standard methods. Sections were then obtained at 10 μ m thickness and stained with hematoxylin and eosin and mounted [172].

Touch sensitivity assay

Embryos from stage 26-45 were subjected to a tactile stimulus. Using either gentle displacement of the incubation dish or the light touch of a pipette tip, a mild physical stimulus was applied to the embryo and its reaction was observed. Control embryos at earlier stages are not very active, but when a tactile stimulus is applied they swim away from the stimulus.

Electron Microscopy

In collaboration with Malgorzata Kloc at Houston Methodist Hospital, embryos were fixed in 2% formaldehyde, 3% glutaraldehyde (EM grade from Ted Pella Inc., glutaraldehyde 8% stock, 18421; formaldehyde 16% stock, 18505) in 1x phosphate buffered saline (PBS).

For transmitted electron microscopy, samples were dehydrated in ethanol at increasing concentrations, infiltrated and embedded in LX-112 medium (Epon

substitute; Ladd Research Industries). Ultrathin sections (70-100 nm) were contrasted with uranyl acetate and lead citrate according to standard protocols [173]; the sections were then examined in a JEOL 100SX transmission electron microscope (JEM, Japan) at an accelerating voltage of 80 kV.

For scanning electron microscopy, fixed samples were washed with 0.1 M cacodylate buffer, pH 7.3 for 3 x 10 min. The samples were then post fixed with 1% cacodylate buffered osmium tetroxide for 1 hour, washed with 0.1 M cacodylate buffer for 3 x 10 min, and then in distilled water, 2 x 5 min. The samples were sequentially treated with Millipore-filtered 1% aqueous tannic acid for 30 min in the dark, washed in distilled water 3 x 10 min, and then in Millipore-filtered 1% aqueous uranyl acetate for 1 hour in the dark. Samples were rinsed with distilled water for 2 x 5 min, and were then dehydrated with a graded series of increasing concentrations of ethanol for 5 min each. The samples were transferred to graded series of increasing concentrations of hexamethyldisilazane (HMDS) for 5 min each and air dried overnight. Samples were mounted on double-stick carbon tabs (Ted Pella. Inc., Redding, CA), which had been previously mounted on aluminum specimen mounts (Electron Microscopy Sciences). The samples were then coated under vacuum using a Balzer MED 010 evaporator (Technotrade International) with platinum alloy for a thickness of 25 nm, and immediately flash carbon coated under vacuum. The samples were transferred to a desiccator for examination at a later date. Samples were examined in a JSM-5910 scanning electron microscope (JEOL USA, Inc.) at an

accelerating voltage of 5 kV.

Antisense morpholinos

Two independent *Xenopus* Pkp3 translation-blocking morpholinos (Pkp3 MO 1 5'-CTCTCTCTCTGTCCCTGAGAGGCTT-3' and Pkp3 MO 3 5'-GCTTTAGTGTAGGCTCGGACCCCTC-3'), and a standard morpholino (5'-CCTCTTACCTCAGTTACAATTATA-3') were obtained from Gene Tools.

DNA constructs

pCS2-HA(CT)/xPkp3, pCS2-HA(CT)/xPkp3+5'UTR, pCS2-myc/xPkp3 and xPkp3 fused to a Bcl-XI MOM targeting sequence were made by PCR amplification of xPkp3 cDNA from pGEM11XLPKP3 and cloning into the pCS2 vector with the indicated epitope tag. *Xenopus* ETV1 cDNA was purchased from Open Biosystems (Thermo Fisher Scientific) and cloned into pCS2-myc. ETV1 fragments used for mapping of interactions with Pkp3 were cloned from pCS2-myc/xETV1 into pCS2-myc. Subsequent production of in vitro transcribed RNAs was done using the mMESSAGE SP6 kit (Ambion), with capped mRNAs synthesized in vitro following Not1 linearization. Transcripts were then acidic-phenol/chloroform extracted and unincorporated nucleotides were removed using Sephadex G-50 Quick Spin Columns (Roche). mRNA was ethanol precipitated at -80°C, and mRNA integrity then examined via agarose gel electrophoresis and

ethidium bromide staining. Other constructs were reported previously and kindly provided by Dr. L. Shemshedini (Fes3xWT-Luc and MMP1-Luc) and Dr. R. Janknecht (MMP1 -87/-88) [142,145,146].

RNA isolation and semi-quantitative real time PCR

RNA isolation and semi-quantitative real time PCR were performed as previously described [90]. Briefly, total RNA was extracted from *Xenopus* embryos using Trizol (Invitrogen). DNA was removed with RQ1 DNase (Promega M610A). Constant amounts of total RNA were reverse-transcribed into cDNA pools using oligo-dT (Invitrogen 18418-012) and SuperScript III Reverse Transcriptase (Invitrogen 18080-044). cDNA was then used as template for either real time PCR with SYBR Green Master Mix or PCR amplification. To control for DNA contamination, reactions were performed in the absence of reverse transcriptase. PCR primers are as follows: DDC 5'-TGGAGAGGGCTGGACTGATC-3', DDC-R 5'-AGCCTGACCACGAGCTACAAA-3', TH-F 5'-GCCGGATTGTTGCCATGA-3', TH-R 5'-GGCCCCCAAAGATGCTAAAC-3', SLC18A2-F 5'-GGCCCCCGCTATCAACTT-3', SLC18A2-R 5'-ACCTCCGATTTTTTGTGCAA-3', GCH-F 5'-TCTGGTGTGGAGTGGTTGTTG-3', GCH-R 5'-CCCCTAGCATGGTACTCGTTACA-3', ARM-F 5'-ATGGCATTATGAACTGTTGACCGCTTT-3', ARM-R 5'-TCTGCGTGAGTGGGTTTAAGGTGTCC-3', HH4-F 5'-

CGGGATAACATTCAGGGTA-3', HH4-R 5'-TCCATGGCGGTAAGTGC-3',
Pkp2-F 5'-TCGGCTGTTGCTCACATGATT-3', Pkp2-R 5'-
ATTTCTCTCGCGATCTCATTTTGG-3', ODC-F 5'-AAAAAGCATGTGCGTTGGT-
3', ODC-R 5'-ACGGCATAAAACGGAGTGA-3'.

Whole-mount in situ RNA hybridization

Whole-mount in situ RNA hybridizations were performed as previously described [154]. Briefly, digoxigenin-labeled sense and antisense RNA probes were prepared through in vitro transcription (DIG RNA Labeling Kit, Roche 11175025910). Probes were detected with anti-digoxigenin antibody conjugated to alkaline phosphatase (Roche 11093274910), and NBT/BCIP (Roche 11697471001) was used as a reaction substrate. Sections of stained embryos were obtained using previously described methods [174].

Immunostaining and fluorescent imaging of embryos

Embryos were fixed in 1X MEM and 4% Formaldehyde at specified stages for 1-2 hours followed by dehydration in 100% methanol at -20°C overnight. Rehydration was done in 1X PBS with 0.1% Tween-20 (PTw) followed by blocking in 20% goat serum in PTw. Primary antibody (Myc 1:500; Pkp3 1:12.5; 12/101 1:500; acetylated alpha tubulin 1:500) incubation was performed overnight at 4°C in 10% goat serum in PTw. Samples were washed in PTw (5X

over 5 hours), and then incubated overnight with secondary antibody (Alexa-488 or -555 conjugated to anti-rabbit or mouse specific antibody) in PTw, and washed again (5X over 5 hours). For experiments involving the detection of acetylated alpha-tubulin, 25-45 overlapping images were obtained per embryo sample using a Leica DM4000B, and then photomerged using Adobe Photoshop CS4. Sub-cellular localization was assessed via confocal microscopy using an Olympus IX70 microscope and images analyzed with Fluoview 500 software.

Yeast two-hybrid

Full-length *Xenopus* Pkp3 was used to screen an adult mouse brain and human keratinocyte cDNA library in collaboration with Hybrigenics ULTimate Y2H [175]. We obtained 351 positive clones that were then sequenced and analyzed. We were attracted to two clones in particular, ETV1/ER81 and ETV5/ERM, given that they fall within the same PEA subgroup of Ets-family members, which are known to have wide ranging roles in transcriptional control [127,144,176].

Nuclear Fractionation, Immunoprecipitation, and Immunoblotting

Nuclear fractionation of mouse embryonic stem cells required a 10 cm plate of AB-1 wild type cells at 80% confluency for 3 immuno-precipitating conditions. One plate of cells was collected by scraping, and then washed with

10 mL PBS and pelleted by centrifugation at 200xg for 2 minutes. The pellet was resuspended by gentle pipetting in 600 ul ice-cold buffer A (20 mM HEPES, pH 7.9; 10 mM KCl; 0.2 mM EDTA; protease inhibitors). The cells were allowed to swell for 15 minutes on ice. Following, 37.5 ul of 10% NP-40 was added and the tube vortexed 10 seconds. Nuclei were collected by centrifugation at 200xg for 10 minutes (supernatant contains cytoplasm, and the pellet contains nuclei). The nuclei were resuspended in 300 ul ice-cold buffer C1 (20 mM HEPES, pH 7.9; 400 mM NaCl; 10 mM EDTA; 1 mM EGTA; protease inhibitors) and were rocked at 4°C for 1 hour, prior to centrifugation at 16,100xg (microfuge maximum speed) at 4°C for 10 minutes (supernatant contains the nuclear extract). For immunoprecipitations, extracts were transferred to new tubes and diluted with one volume of ice-cold buffer C2 (20 mM HEPES, pH 7.9; 10 mM EDTA; 1 mM EGTA; protease inhibitors). One aliquot was set aside for whole nuclear lysate detection. Extract was diluted to a final volume of 1.5 mL with cold buffer C3 (20 mM HEPES, pH 7.9; 200 mM NaCl; 10 mM EDTA; 1 mM EGTA; protease inhibitors).

Protein A/G PLUS-Agarose (Santa Cruz Biotechnology SC-2003) (10 ul packed agarose/condition) was washed three times in cold buffer C3. After the last wash, the precipitating antibody was added to the beads (e.g. anti-Pkp3 hybridoma supernatant 11F2 – 300uL; anti-ETV1 – 3ug; mouse IgG – 3ug) and was rocked 45 minutes at 4°C. The beads were centrifuged at 1,000xg for 2 minutes and washed 3x with cold buffer C3 containing 0.5% Triton X-100.

Following agarose bead preparation and nuclear lysate dilutions, 500 uL of lysate was added to the beads and rocked gently for 1 hour at 4°C, centrifuged at 1,000xg for 2 minutes, and washed 3x with cold wash buffer (20 mM HEPES, pH 7.9; 200 mM NaCl; 10 mM EDTA; 1 mM EGTA; 0.5% Triton X-100; 0.5% sodium deoxycholate; 0.1% SDS). The final bead pellet was resuspended in 30 ul of 2x protein sample buffer and the entire sample loaded. Immunoblotting was carried out following standard protocols.

Antibodies

Anti-human Pkp3 hybridoma supernatant clone 11F2 was kindly provided by Dr. JK Wahl, 3rd. All other antibodies were purchased from commercial suppliers (mouse anti-c-myc, DSHB 9E 10; rabbit anti-myc, Santa Cruz SC-789; mouse anti-HA, 12CA5; rabbit anti-HA Santa Cruz SC-805; ETV1, Thermo Scientific MA5-15461; Pkp3, Progen 651113, GAPDH, Santa Cruz sc-25778, skeletal muscle, DSHB 12/101, and acetylated alpha-tubulin, Sigma T7451). Secondary antibodies were Alexa Fluor 488 labeled goat anti-rabbit antibody (Invitrogen), Alexa Fluor 555 labeled goat anti-mouse antibody (Invitrogen), HRP-conjugated goat anti-rabbit IgG (Bio-Rad) and HRP-conjugated goat anti-mouse IgG (Bio-Rad).

Antibodies generated against the recombinant (GST-tagged) N-terminal domain of *Xenopus* Pkp3 (amino acids 1-350; PTG labs), were affinity-purified

from rabbit crude serum. The *Xenopus* PKP2 antiserum was raised in guinea pigs using a cocktail consisting of three peptides (EWRSECDTRRPTL+C, RYRTASRARQNLSQQFRQDT+C, QDLHSTYKKSYKK+C) coupled to keyhole limpet hemocyanin.

Immunoblotting of *Xenopus* extracts

Embryos were harvested at the indicated developmental stages and immuno-blotting was performed following standard procedures using 1-0.2X 0.2% KPL Block (KPL 71-83-00) [177].

Cell culture

Human HeLa and HEK 293T cells were cultured in DMEM (Invitrogen), using standard mammalian cell culture conditions [140]. Cells were transfected using either Lipofectamine-2000 (Invitrogen) or polyethylenimine (Polysciences, Inc. 9002-98-6) following the manufacturer's instructions. Mouse wild type AB-1 embryonic stem cells were cultured as previously described [178].

Immunostaining and fluorescent imaging of cell lines

HeLa cells were plated on glass coverslips and grown to either 60 or 90% confluence 24 hours post-transfection. Cells were washed three times in 1X PBS

at room temperature (RT) and then fixed in PBS with 4% paraformaldehyde for 10 minutes at 4 C. Cells were then washed three times in 1X PBS at RT, before neutralizing the paraformaldehyde with 50mM NH₄Cl for 10 minutes at RT. Following two additional washes with 1X PBS, the cells were permeabilized with 0.5% Triton X-100 in PBS for 10 minutes at RT. Two 1X PBS washes preceded a one-hour RT incubation in blocking buffer (10% goat serum, 2mg/ml BSA, 0.1% Triton X-100 in 1X PBS). Cells were then incubated overnight at four degrees Celsius in blocking buffer containing primary antibody (1:500 dilutions of either anti-HA or anti-Myc). The next day, samples were washed 3X for 10 minutes each in 1X PBS. They were then incubated for 1 hour at RT with Alexa Flour® 488 or 555 conjugated secondary antibodies (1:500). Three washes were performed prior to mounting with Vectashield® mounting medium (Vector Laboratories Cat. No. H-1000).

Images were obtained with a Zeiss Observer Z1 confocal designed by 3i, Inc using Slidebook 5.5 software. To ensure loss of relocalization, images were adjusted for brightness in select cases using Adobe Photoshop software.

Luciferase assay

HEK 293T cells were co-transfected with the indicated plasmids and pRL-SV40 renilla reporter plasmid (internal control). Cells were lysed and assayed 24 hours later for luciferase activity using the Dual Luciferase® Reporter Assay

System, in accordance with the manufacturer's protocol (Promega). All experiments were repeated a minimum of three times.

Statistical Analysis

Data presented is in percentages to account for differences in total numbers between each experimental condition. Graphs produced were based on the average percentages of triplicate experiments. To analyze the significance of our phenotypes, we used the Student's T-test. To obtain P-values, we hypothesized that the two groups are statistically identical (null hypothesis), and analyzed the data using the Student's T-test (TTEST) within the Microsoft Excel software program.

This chapter contains published work taken from Munoz WA, Kloc M, Cho K, Lee M, Hofmann I, Sater A, Vleminckx K, McCrea PD. (2012) Plakophilin-3 Is Required for Late Embryonic Amphibian Development, Exhibiting Roles in Ectodermal and Neural Tissues. PLoS ONE 7(4): e34342. doi:10.1371/journal.pone.0034342.

Open access agreement. Upon submission of an article, its authors are asked to indicate their agreement to abide by an open access Creative Commons license (CC-BY). Under the terms of this license, authors retain ownership of the copyright of their articles. However, the license permits any user to download, print out, extract, reuse, archive, and distribute the article, so long as appropriate credit is given to the authors and source of the work. The license ensures that the authors' article will be available as widely as possible and that the article can be included in any scientific archive.

1. Takeichi M (1995) Morphogenetic roles of classic cadherins. *Curr Opin Cell Biol* 7: 619-627.
2. Shapiro L, Weis WI (2009) Structure and biochemistry of cadherins and catenins. *Cold Spring Harb Perspect Biol* 1: a003053.
3. Gumbiner BM (2005) Regulation of cadherin-mediated adhesion in morphogenesis. *Nat Rev Mol Cell Biol* 6: 622-634.
4. Harris TJ, Tepass U (2010) Adherens junctions: from molecules to morphogenesis. *Nat Rev Mol Cell Biol* 11: 502-514.
5. Reynolds AB, Carnahan RH (2004) Regulation of cadherin stability and turnover by p120ctn: implications in disease and cancer. *Semin Cell Dev Biol* 15: 657-663.
6. Jeanes A, Gottardi CJ, Yap AS (2008) Cadherins and cancer: how does cadherin dysfunction promote tumor progression? *Oncogene* 27: 6920-6929.
7. Brooke MA, Nitoiu D, Kelsell DP (2012) Cell-cell connectivity: desmosomes and disease. *J Pathol* 226: 158-171.
8. Chidgey M, Dawson C (2007) Desmosomes: a role in cancer? *Br J Cancer* 96: 1783-1787.
9. McGrath JA (2005) Inherited disorders of desmosomes. *Australas J Dermatol* 46: 221-229.
10. Thomason HA, Scothern A, McHarg S, Garrod DR (2010) Desmosomes: adhesive strength and signalling in health and disease. *Biochem J* 429: 419-433.

11. Ozawa M, Baribault H, Kemler R (1989) The cytoplasmic domain of the cell adhesion molecule uvomorulin associates with three independent proteins structurally related in different species. *EMBO J* 8: 1711-1717.
12. Heid HW, Schmidt A, Zimbelmann R, Schafer S, Winter-Simanowski S, Stumpp S, Keith M, Figge U, Schnolzer M, Franke WW (1994) Cell type-specific desmosomal plaque proteins of the plakoglobin family: plakophilin 1 (band 6 protein). *Differentiation* 58: 113-131.
13. Huber AH, Nelson WJ, Weis WI (1997) Three-dimensional structure of the armadillo repeat region of beta-catenin. *Cell* 90: 871-882.
14. Peifer M, Berg S, Reynolds AB (1994) A repeating amino acid motif shared by proteins with diverse cellular roles. *Cell* 76: 789-791.
15. Choi HJ, Weis WI (2005) Structure of the armadillo repeat domain of plakophilin 1. *J Mol Biol* 346: 367-376.
16. Bass-Zubek AE, Godsel LM, Delmar M, Green KJ (2009) Plakophilins: multifunctional scaffolds for adhesion and signaling. *Curr Opin Cell Biol* 21: 708-716.
17. Hatzfeld M (2007) Plakophilins: Multifunctional proteins or just regulators of desmosomal adhesion? *Biochim Biophys Acta* 1773: 69-77.
18. McCrea PD, Gu D, Balda MS (2009) Junctional music that the nucleus hears: cell-cell contact signaling and the modulation of gene activity. *Cold Spring Harb Perspect Biol* 1: a002923.

19. Carnahan RH, Rokas A, Gaucher EA, Reynolds AB (2010) The molecular evolution of the p120-catenin subfamily and its functional associations. *PLoS One* 5: e15747.
20. McCrea PD, Gu D (2010) The catenin family at a glance. *J Cell Sci* 123: 637-642.
21. Peifer M, McCrea PD, Green KJ, Wieschaus E, Gumbiner BM (1992) The vertebrate adhesive junction proteins beta-catenin and plakoglobin and the *Drosophila* segment polarity gene armadillo form a multigene family with similar properties. *J Cell Biol* 118: 681-691.
22. Mariner DJ, Wang J, Reynolds AB (2000) ARVCF localizes to the nucleus and adherens junction and is mutually exclusive with p120(ctn) in E-cadherin complexes. *J Cell Sci* 113 (Pt 8): 1481-1490.
23. Ohkubo T, Ozawa M (1999) p120(ctn) binds to the membrane-proximal region of the E-cadherin cytoplasmic domain and is involved in modulation of adhesion activity. *J Biol Chem* 274: 21409-21415.
24. Ozawa M, Ringwald M, Kemler R (1990) Uvomorulin-catenin complex formation is regulated by a specific domain in the cytoplasmic region of the cell adhesion molecule. *Proc Natl Acad Sci U S A* 87: 4246-4250.
25. Thoreson MA, Anastasiadis PZ, Daniel JM, Ireton RC, Wheelock MJ, Johnson KR, Hummingbird DK, Reynolds AB (2000) Selective uncoupling of p120(ctn) from E-cadherin disrupts strong adhesion. *J Cell Biol* 148: 189-202.

26. Yap AS, Niessen CM, Gumbiner BM (1998) The juxtamembrane region of the cadherin cytoplasmic tail supports lateral clustering, adhesive strengthening, and interaction with p120^{ctn}. *J Cell Biol* 141: 779-789.
27. Meng W, Takeichi M (2009) Adherens junction: molecular architecture and regulation. *Cold Spring Harb Perspect Biol* 1: a002899.
28. Chen X, Bonne S, Hatzfeld M, van Roy F, Green KJ (2002) Protein binding and functional characterization of plakophilin 2. Evidence for its diverse roles in desmosomes and beta -catenin signaling. *J Biol Chem* 277: 10512-10522.
29. Hatzfeld M, Haffner C, Schulze K, Vinzens U (2000) The function of plakophilin 1 in desmosome assembly and actin filament organization. *J Cell Biol* 149: 209-222.
30. Knudsen KA, Wheelock MJ (1992) Plakoglobin, or an 83-kD homologue distinct from beta-catenin, interacts with E-cadherin and N-cadherin. *J Cell Biol* 118: 671-679.
31. Ireton RC, Davis MA, van Hengel J, Mariner DJ, Barnes K, Thoreson MA, Anastasiadis PZ, Matrisian L, Bundy LM, Sealy L, Gilbert B, van Roy F, Reynolds AB (2002) A novel role for p120 catenin in E-cadherin function. *J Cell Biol* 159: 465-476.
32. Bass-Zubek AE, Hobbs RP, Amargo EV, Garcia NJ, Hsieh SN, Chen X, Wahl JK, 3rd, Denning MF, Green KJ (2008) Plakophilin 2: a critical scaffold for PKC alpha that regulates intercellular junction assembly. *J Cell Biol* 181: 605-613.

33. Davis MA, Ireton RC, Reynolds AB (2003) A core function for p120-catenin in cadherin turnover. *J Cell Biol* 163: 525-534.
34. Gu D, Sater AK, Ji H, Cho K, Clark M, Stratton SA, Barton MC, Lu Q, McCrea PD (2009) *Xenopus* delta-catenin is essential in early embryogenesis and is functionally linked to cadherins and small GTPases. *J Cell Sci* 122: 4049-4061.
35. Bryant DM, Stow JL (2004) The ins and outs of E-cadherin trafficking. *Trends Cell Biol* 14: 427-434.
36. Xiao K, Oas RG, Chiasson CM, Kowalczyk AP (2007) Role of p120-catenin in cadherin trafficking. *Biochim Biophys Acta* 1773: 8-16.
37. Xiao K, Garner J, Buckley KM, Vincent PA, Chiasson CM, Dejana E, Faundez V, Kowalczyk AP (2005) p120-Catenin regulates clathrin-dependent endocytosis of VE-cadherin. *Mol Biol Cell* 16: 5141-5151.
38. Yin T, Green KJ (2004) Regulation of desmosome assembly and adhesion. *Semin Cell Dev Biol* 15: 665-677.
39. Sobolik-Delmaire T, Katafiasz D, Wahl JK, 3rd (2006) Carboxyl terminus of Plakophilin-1 recruits it to plasma membrane, whereas amino terminus recruits desmoplakin and promotes desmosome assembly. *J Biol Chem* 281: 16962-16970.
40. Schmidt A, Jager S (2005) Plakophilins--hard work in the desmosome, recreation in the nucleus? *Eur J Cell Biol* 84: 189-204.

41. Nekrasova OE, Amargo EV, Smith WO, Chen J, Kreitzer GE, Green KJ (2011) Desmosomal cadherins utilize distinct kinesins for assembly into desmosomes. *J Cell Biol* 195: 1185-1203.
42. Godsel LM, Dubash AD, Bass-Zubek AE, Amargo EV, Klessner JL, Hobbs RP, Chen X, Green KJ (2010) Plakophilin 2 couples actomyosin remodeling to desmosomal plaque assembly via RhoA. *Mol Biol Cell* 21: 2844-2859.
43. Abe K, Takeichi M (2008) EPLIN mediates linkage of the cadherin catenin complex to F-actin and stabilizes the circumferential actin belt. *Proc Natl Acad Sci U S A* 105: 13-19.
44. Pappas DJ, Rimm DL (2006) Direct interaction of the C-terminal domain of alpha-catenin and F-actin is necessary for stabilized cell-cell adhesion. *Cell Commun Adhes* 13: 151-170.
45. Bonne S, Gilbert B, Hatzfeld M, Chen X, Green KJ, van Roy F (2003) Defining desmosomal plakophilin-3 interactions. *J Cell Biol* 161: 403-416.
46. Smith EA, Fuchs E (1998) Defining the interactions between intermediate filaments and desmosomes. *J Cell Biol* 141: 1229-1241.
47. Hartsock A, Nelson WJ (2008) Adherens and tight junctions: structure, function and connections to the actin cytoskeleton. *Biochim Biophys Acta* 1778: 660-669.
48. Anastasiadis PZ (2007) p120-ctn: A nexus for contextual signaling via Rho GTPases. *Biochim Biophys Acta* 1773: 34-46.

49. Fang X, Ji H, Kim SW, Park JI, Vaught TG, Anastasiadis PZ, Ciesiolka M, McCrea PD (2004) Vertebrate development requires ARVCF and p120 catenins and their interplay with RhoA and Rac. *J Cell Biol* 165: 87-98.
50. Grosheva I, Shtutman M, Elbaum M, Bershadsky AD (2001) p120 catenin affects cell motility via modulation of activity of Rho-family GTPases: a link between cell-cell contact formation and regulation of cell locomotion. *J Cell Sci* 114: 695-707.
51. Keil R, Wolf A, Huttelmaier S, Hatzfeld M (2007) Beyond regulation of cell adhesion: local control of RhoA at the cleavage furrow by the p0071 catenin. *Cell Cycle* 6: 122-127.
52. Noren NK, Liu BP, Burridge K, Kreft B (2000) p120 catenin regulates the actin cytoskeleton via Rho family GTPases. *J Cell Biol* 150: 567-580.
53. Wolf A, Keil R, Gotzl O, Mun A, Schwarze K, Lederer M, Huttelmaier S, Hatzfeld M (2006) The armadillo protein p0071 regulates Rho signalling during cytokinesis. *Nat Cell Biol* 8: 1432-1440.
54. Anastasiadis PZ, Moon SY, Thoreson MA, Mariner DJ, Crawford HC, Zheng Y, Reynolds AB (2000) Inhibition of RhoA by p120 catenin. *Nat Cell Biol* 2: 637-644.
55. Furukawa C, Daigo Y, Ishikawa N, Kato T, Ito T, Tsuchiya E, Sone S, Nakamura Y (2005) Plakophilin 3 oncogene as prognostic marker and therapeutic target for lung cancer. *Cancer Res* 65: 7102-7110.

56. Koetsier JL, Amargo EV, Todorovic V, Green KJ, Godsel LM (2013) Plakophilin 2 Affects Cell Migration by Modulating Focal Adhesion Dynamics and Integrin Protein Expression. *J Invest Dermatol*.
57. Daniel JM (2007) Dancing in and out of the nucleus: p120(ctn) and the transcription factor Kaiso. *Biochim Biophys Acta* 1773: 59-68.
58. Daniel JM, Reynolds AB (1999) The catenin p120(ctn) interacts with Kaiso, a novel BTB/POZ domain zinc finger transcription factor. *Mol Cell Biol* 19: 3614-3623.
59. Molenaar M, van de Wetering M, Oosterwegel M, Peterson-Maduro J, Godsave S, Korinek V, Roose J, Destree O, Clevers H (1996) XTcf-3 transcription factor mediates beta-catenin-induced axis formation in *Xenopus* embryos. *Cell* 86: 391-399.
60. Hosking CR, Ulloa F, Hogan C, Ferber EC, Figueroa A, Gevaert K, Birchmeier W, Briscoe J, Fujita Y (2007) The transcriptional repressor Glis2 is a novel binding partner for p120 catenin. *Mol Biol Cell* 18: 1918-1927.
61. Kim SW, Park JI, Spring CM, Sater AK, Ji H, Otchere AA, Daniel JM, McCrea PD (2004) Non-canonical Wnt signals are modulated by the Kaiso transcriptional repressor and p120-catenin. *Nat Cell Biol* 6: 1212-1220.
62. Park JI, Kim SW, Lyons JP, Ji H, Nguyen TT, Cho K, Barton MC, Deroo T, Vleminckx K, Moon RT, McCrea PD (2005) Kaiso/p120-catenin and TCF/beta-catenin complexes coordinately regulate canonical Wnt gene targets. *Dev Cell* 8: 843-854.

63. Ilioka H, Doerner SK, Tamai K (2009) Kaiso is a bimodal modulator for Wnt/beta-catenin signaling. *FEBS Lett* 583: 627-632.
64. Spring CM, Kelly KF, O'Kelly I, Graham M, Crawford HC, Daniel JM (2005) The catenin p120ctn inhibits Kaiso-mediated transcriptional repression of the beta-catenin/TCF target gene matrilysin. *Exp Cell Res* 305: 253-265.
65. Park JI, Ji H, Jun S, Gu D, Hikasa H, Li L, Sokol SY, McCrea PD (2006) Frd1 links Dishevelled to the p120-catenin/Kaiso pathway: distinct catenin subfamilies promote Wnt signals. *Dev Cell* 11: 683-695.
66. Daniel JM, Spring CM, Crawford HC, Reynolds AB, Baig A (2002) The p120(ctn)-binding partner Kaiso is a bi-modal DNA-binding protein that recognizes both a sequence-specific consensus and methylated CpG dinucleotides. *Nucleic Acids Res* 30: 2911-2919.
67. Bergman R, Sprecher E (2005) Histopathological and ultrastructural study of ectodermal dysplasia/skin fragility syndrome. *Am J Dermatopathol* 27: 333-338.
68. McGrath JA, McMillan JR, Shemanko CS, Runswick SK, Leigh IM, Lane EB, Garrod DR, Eady RA (1997) Mutations in the plakophilin 1 gene result in ectodermal dysplasia/skin fragility syndrome. *Nat Genet* 17: 240-244.
69. McGrath JA, Mellerio JE (2010) Ectodermal dysplasia-skin fragility syndrome. *Dermatol Clin* 28: 125-129.
70. Sprecher E, Molho-Pessach V, Ingber A, Sagi E, Indelman M, Bergman R (2004) Homozygous splice site mutations in PKP1 result in loss of epidermal plakophilin 1 expression and underlie ectodermal dysplasia/skin

- fragility syndrome in two consanguineous families. *J Invest Dermatol* 122: 647-651.
71. Wessagowit V, McGrath JA (2005) Clinical and molecular significance of splice site mutations in the plakophilin 1 gene in patients with ectodermal dysplasia-skin fragility syndrome. *Acta Derm Venereol* 85: 386-388.
72. Whittock NV, Haftek M, Angoulvant N, Wolf F, Perrot H, Eady RA, McGrath JA (2000) Genomic amplification of the human plakophilin 1 gene and detection of a new mutation in ectodermal dysplasia/skin fragility syndrome. *J Invest Dermatol* 115: 368-374.
73. Awad MM, Calkins H, Judge DP (2008) Mechanisms of disease: molecular genetics of arrhythmogenic right ventricular dysplasia/cardiomyopathy. *Nat Clin Pract Cardiovasc Med* 5: 258-267.
74. Gerull B, Heuser A, Wichter T, Paul M, Basson CT, McDermott DA, Lerman BB, Markowitz SM, Ellinor PT, MacRae CA, Peters S, Grossmann KS, Drenckhahn J, Michely B, Sasse-Klaassen S, Birchmeier W, Dietz R, Breithardt G, Schulze-Bahr E, Thierfelder L (2004) Mutations in the desmosomal protein plakophilin-2 are common in arrhythmogenic right ventricular cardiomyopathy. *Nat Genet* 36: 1162-1164.
75. Grossmann KS, Grund C, Huelsken J, Behrend M, Erdmann B, Franke WW, Birchmeier W (2004) Requirement of plakophilin 2 for heart morphogenesis and cardiac junction formation. *J Cell Biol* 167: 149-160.

76. Hall C, Li S, Li H, Creason V, Wahl JK, 3rd (2009) Arrhythmogenic right ventricular cardiomyopathy plakophilin-2 mutations disrupt desmosome assembly and stability. *Cell Commun Adhes* 16: 15-27.
77. Breuninger S, Reidenbach S, Sauer CG, Strobel P, Pfitzenmaier J, Trojan L, Hofmann I (2010) Desmosomal plakophilins in the prostate and prostatic adenocarcinomas: implications for diagnosis and tumor progression. *Am J Pathol* 176: 2509-2519.
78. Kundu ST, Gosavi P, Khapare N, Patel R, Hosing AS, Maru GB, Ingle A, Decaprio JA, Dalal SN (2008) Plakophilin3 downregulation leads to a decrease in cell adhesion and promotes metastasis. *Int J Cancer* 123: 2303-2314.
79. Schwarz J, Ayim A, Schmidt A, Jager S, Koch S, Baumann R, Dunne AA, Moll R (2006) Differential expression of desmosomal plakophilins in various types of carcinomas: correlation with cell type and differentiation. *Hum Pathol* 37: 613-622.
80. Wolf A, Rietscher K, Glass M, Huttelmaier S, Schutkowski M, Ihling C, Sinz A, Wingenfeld A, Mun A, Hatzfeld M (2013) Insulin signaling via Akt2 switches plakophilin 1 function from stabilizing cell adhesion to promoting cell proliferation. *J Cell Sci* 126: 1832-1844.
81. Carnahan RH, Rokas A, Gaucher EA, Reynolds AB The molecular evolution of the p120-catenin subfamily and its functional associations. *PLoS One* 5: e15747.

82. McCrea PD, Park JI (2007) Developmental functions of the P120-catenin sub-family. *Biochim Biophys Acta* 1773: 17-33.
83. South AP, Wan H, Stone MG, Dopping-Hepenstal PJ, Purkis PE, Marshall JF, Leigh IM, Eady RA, Hart IR, McGrath JA (2003) Lack of plakophilin 1 increases keratinocyte migration and reduces desmosome stability. *J Cell Sci* 116: 3303-3314.
84. Hofmann I, Mertens C, Brettel M, Nimmrich V, Schnolzer M, Herrmann H (2000) Interaction of plakophilins with desmoplakin and intermediate filament proteins: an in vitro analysis. *J Cell Sci* 113 (Pt 13): 2471-2483.
85. Kowalczyk AP, Hatzfeld M, Bornslaeger EA, Kopp DS, Borgwardt JE, Corcoran CM, Settler A, Green KJ (1999) The head domain of plakophilin-1 binds to desmoplakin and enhances its recruitment to desmosomes. Implications for cutaneous disease. *J Biol Chem* 274: 18145-18148.
86. Hobbs RP, Green KJ (2012) Desmoplakin Regulates Desmosome Hyperadhesion. *J Invest Dermatol* 132: 482-485.
87. Roberts BJ, Pashaj A, Johnson KR, Wahl JK, 3rd (2011) Desmosome dynamics in migrating epithelial cells requires the actin cytoskeleton. *Exp Cell Res* 317: 2814-2822.
88. Hofmann I, Casella M, Schnolzer M, Schlechter T, Spring H, Franke WW (2006) Identification of the junctional plaque protein plakophilin 3 in cytoplasmic particles containing RNA-binding proteins and the recruitment of plakophilins 1 and 3 to stress granules. *Mol Biol Cell* 17: 1388-1398.

89. Wolf A, Krause-Gruszczynska M, Birkenmeier O, Ostareck-Lederer A, Huttelmaier S, Hatzfeld M (2010) Plakophilin 1 stimulates translation by promoting eIF4A1 activity. *J Cell Biol* 188: 463-471.
90. Munoz WA, Kloc M, Cho K, Lee M, Hofmann I, Sater A, Vleminckx K, McCrea PD (2012) Plakophilin-3 is required for late embryonic amphibian development, exhibiting roles in ectodermal and neural tissues. *PLoS One* 7: e34342.
91. Schmidt A, Langbein L, Rode M, Pratzel S, Zimbelmann R, Franke WW (1997) Plakophilins 1a and 1b: widespread nuclear proteins recruited in specific epithelial cells as desmosomal plaque components. *Cell Tissue Res* 290: 481-499.
92. Sobolik-Delmaire T, Reddy R, Pashaj A, Roberts BJ, Wahl JK, 3rd (2010) Plakophilin-1 localizes to the nucleus and interacts with single-stranded DNA. *J Invest Dermatol* 130: 2638-2646.
93. Bonne S, van Hengel J, Nollet F, Kools P, van Roy F (1999) Plakophilin-3, a novel armadillo-like protein present in nuclei and desmosomes of epithelial cells. *J Cell Sci* 112 (Pt 14): 2265-2276.
94. Mertens C, Kuhn C, Franke WW (1996) Plakophilins 2a and 2b: constitutive proteins of dual location in the karyoplasm and the desmosomal plaque. *J Cell Biol* 135: 1009-1025.
95. Klymkowsky MW (1999) Plakophilin, armadillo repeats, and nuclear localization. *Microsc Res Tech* 45: 43-54.

96. Beausoleil SA, Jedrychowski M, Schwartz D, Elias JE, Villen J, Li J, Cohn MA, Cantley LC, Gygi SP (2004) Large-scale characterization of HeLa cell nuclear phosphoproteins. *Proc Natl Acad Sci U S A* 101: 12130-12135.
97. Mertens C, Hofmann I, Wang Z, Teichmann M, Sepehri Chong S, Schnolzer M, Franke WW (2001) Nuclear particles containing RNA polymerase III complexes associated with the junctional plaque protein plakophilin 2. *Proc Natl Acad Sci U S A* 98: 7795-7800.
98. Sobolik-Delmaire T, Reddy R, Pashaj A, Roberts BJ, Wahl JK, 3rd Plakophilin-1 localizes to the nucleus and interacts with single-stranded DNA. *J Invest Dermatol* 130: 2638-2646.
99. Schmidt A, Langbein L, Pratzel S, Rode M, Rackwitz HR, Franke WW (1999) Plakophilin 3--a novel cell-type-specific desmosomal plaque protein. *Differentiation* 64: 291-306.
100. North AJ, Bardsley WG, Hyam J, Bornslaeger EA, Cordingley HC, Trinnaman B, Hatzfeld M, Green KJ, Magee AI, Garrod DR (1999) Molecular map of the desmosomal plaque. *J Cell Sci* 112 (Pt 23): 4325-4336.
101. Edgar R, Domrachev M, Lash AE (2002) Gene Expression Omnibus: NCBI gene expression and hybridization array data repository. *Nucleic Acids Res* 30: 207-210.
102. Sklyarova T, Bonne S, D'Hooge P, Denecker G, Goossens S, De Rycke R, Borgonie G, Bosl M, van Roy F, van Hengel J (2008) Plakophilin-3-

- deficient mice develop hair coat abnormalities and are prone to cutaneous inflammation. *J Invest Dermatol* 128: 1375-1385.
103. Papagerakis S, Shabana AH, Depondt J, Gehanno P, Forest N (2003) Immunohistochemical localization of plakophilins (PKP1, PKP2, PKP3, and p0071) in primary oropharyngeal tumors: correlation with clinical parameters. *Hum Pathol* 34: 565-572.
104. Demirag GG, Sullu Y, Gurgenyatagi D, Okumus NO, Yucel I (2011) Expression of plakophilins (PKP1, PKP2, and PKP3) in gastric cancers. *Diagn Pathol* 6: 1.
105. Demirag GG, Sullu Y, Yucel I (2012) Expression of Plakophilins (PKP1, PKP2, and PKP3) in breast cancers. *Med Oncol* 29: 1518-1522.
106. Degnan BM, Degnan SM, Naganuma T, Morse DE (1993) The ets multigene family is conserved throughout the Metazoa. *Nucleic Acids Res* 21: 3479-3484.
107. Karim FD, Urness LD, Thummel CS, Klemsz MJ, McKercher SR, Celada A, Van Beveren C, Maki RA, Gunther CV, Nye JA, et al. (1990) The ETS-domain: a new DNA-binding motif that recognizes a purine-rich core DNA sequence. *Genes Dev* 4: 1451-1453.
108. Laudet V, Niel C, Duterque-Coquillaud M, Leprince D, Stehelin D (1993) Evolution of the ets gene family. *Biochem Biophys Res Commun* 190: 8-14.

109. Liang H, Mao X, Olejniczak ET, Nettesheim DG, Yu L, Meadows RP, Thompson CB, Fesik SW (1994) Solution structure of the ets domain of Fli-1 when bound to DNA. *Nat Struct Biol* 1: 871-875.
110. Sharrocks AD (2001) The ETS-domain transcription factor family. *Nat Rev Mol Cell Biol* 2: 827-837.
111. Hollenhorst PC, McIntosh LP, Graves BJ (2011) Genomic and biochemical insights into the specificity of ETS transcription factors. *Annu Rev Biochem* 80: 437-471.
112. Hart AH, Reventar R, Bernstein A (2000) Genetic analysis of ETS genes in *C. elegans*. *Oncogene* 19: 6400-6408.
113. Hsu T, Schulz RA (2000) Sequence and functional properties of Ets genes in the model organism *Drosophila*. *Oncogene* 19: 6409-6416.
114. Wei GH, Badis G, Berger MF, Kivioja T, Palin K, Enge M, Bonke M, Jolma A, Varjosalo M, Gehrke AR, Yan J, Talukder S, Turunen M, Taipale M, Stunnenberg HG, Ukkonen E, Hughes TR, Bulyk ML, Taipale J (2010) Genome-wide analysis of ETS-family DNA-binding in vitro and in vivo. *EMBO J* 29: 2147-2160.
115. Brass AL, Zhu AQ, Singh H (1999) Assembly requirements of PU.1-Pip (IRF-4) activator complexes: inhibiting function in vivo using fused dimers. *EMBO J* 18: 977-991.
116. de Launoit Y, Baert JL, Chotteau A, Monte D, Defossez PA, Coutte L, Pelczar H, Leenders F (1997) Structure-function relationships of the PEA3 group of Ets-related transcription factors. *Biochem Mol Med* 61: 127-135.

117. Greenall A, Willingham N, Cheung E, Boam DS, Sharrocks AD (2001) DNA binding by the ETS-domain transcription factor PEA3 is regulated by intramolecular and intermolecular protein.protein interactions. *J Biol Chem* 276: 16207-16215.
118. Bojovic BB, Hassell JA (2001) The PEA3 Ets transcription factor comprises multiple domains that regulate transactivation and DNA binding. *J Biol Chem* 276: 4509-4521.
119. Lin JH, Saito T, Anderson DJ, Lance-Jones C, Jessell TM, Arber S (1998) Functionally related motor neuron pool and muscle sensory afferent subtypes defined by coordinate ETS gene expression. *Cell* 95: 393-407.
120. Arber S, Ladle DR, Lin JH, Frank E, Jessell TM (2000) ETS gene Er81 controls the formation of functional connections between group Ia sensory afferents and motor neurons. *Cell* 101: 485-498.
121. Laing MA, Coonrod S, Hinton BT, Downie JW, Tozer R, Rudnicki MA, Hassell JA (2000) Male sexual dysfunction in mice bearing targeted mutant alleles of the PEA3 ets gene. *Mol Cell Biol* 20: 9337-9345.
122. Hagedorn L, Paratore C, Brugnoli G, Baert JL, Mercader N, Suter U, Sommer L (2000) The Ets domain transcription factor Erm distinguishes rat satellite glia from Schwann cells and is regulated in satellite cells by neuregulin signaling. *Dev Biol* 219: 44-58.
123. Flames N, Hobert O (2009) Gene regulatory logic of dopamine neuron differentiation. *Nature* 458: 885-889.

124. Chen Y, Hollemann T, Grunz H, Pieler T (1999) Characterization of the Ets-type protein ER81 in *Xenopus* embryos. *Mech Dev* 80: 67-76.
125. Shin S, Oh S, An S, Janknecht R (2013) ETS variant 1 regulates matrix metalloproteinase-7 transcription in LNCaP prostate cancer cells. *Oncol Rep* 29: 306-314.
126. Fuchs B, Inwards CY, Janknecht R (2003) Upregulation of the matrix metalloproteinase-1 gene by the Ewing's sarcoma associated EWS-ER81 and EWS-Fli-1 oncoproteins, c-Jun and p300. *FEBS Lett* 553: 104-108.
127. Oh S, Shin S, Janknecht R (2012) ETV1, 4 and 5: an oncogenic subfamily of ETS transcription factors. *Biochim Biophys Acta* 1826: 1-12.
128. Aho S, Levansuo L, Montonen O, Kari C, Rodeck U, Uitto J (2002) Specific sequences in p120ctn determine subcellular distribution of its multiple isoforms involved in cellular adhesion of normal and malignant epithelial cells. *J Cell Sci* 115: 1391-1402.
129. Gu D, Tonthat NK, Lee M, Ji H, Bhat KP, Hollingsworth F, Aldape KD, Schumacher MA, Zwaka TP, McCrea PD Caspase-3 cleavage links delta-catenin to the novel nuclear protein ZIFCAT. *J Biol Chem*.
130. Paulson AF, Mooney E, Fang X, Ji H, McCrea PD (2000) Xarvcf, *Xenopus* member of the p120 catenin subfamily associating with cadherin juxtamembrane region. *J Biol Chem* 275: 30124-30131.
131. Ciesiolka M, Delvaeye M, Van Imschoot G, Verschuere V, McCrea P, van Roy F, Vleminckx K (2004) p120 catenin is required for morphogenetic

- movements involved in the formation of the eyes and the craniofacial skeleton in *Xenopus*. *J Cell Sci* 117: 4325-4339.
132. Schneider S, Herrenknecht K, Butz S, Kemler R, Hausen P (1993) Catenins in *Xenopus* embryogenesis and their relation to the cadherin-mediated cell-cell adhesion system. *Development* 118: 629-640.
133. DeMarais AA, Moon RT (1992) The armadillo homologs beta-catenin and plakoglobin are differentially expressed during early development of *Xenopus laevis*. *Dev Biol* 153: 337-346.
134. Mo YY, Reynolds AB (1996) Identification of murine p120 isoforms and heterogeneous expression of p120cas isoforms in human tumor cell lines. *Cancer Res* 56: 2633-2640.
135. Keirsebilck A, Bonne S, Staes K, van Hengel J, Nollet F, Reynolds A, van Roy F (1998) Molecular cloning of the human p120ctn catenin gene (CTNND1): expression of multiple alternatively spliced isoforms. *Genomics* 50: 129-146.
136. Munchberg SR, Steinbeisser H (1999) The *Xenopus* Ets transcription factor XER81 is a target of the FGF signaling pathway. *Mech Dev* 80: 53-65.
137. de Nooij JC, Doobar S, Jessell TM (2013) Etv1 inactivation reveals proprioceptor subclasses that reflect the level of NT3 expression in muscle targets. *Neuron* 77: 1055-1068.
138. Abe H, Okazawa M, Nakanishi S (2011) The Etv1/Er81 transcription factor orchestrates activity-dependent gene regulation in the terminal maturation

- program of cerebellar granule cells. *Proc Natl Acad Sci U S A* 108: 12497-12502.
139. Gallicano GI, Bauer C, Fuchs E (2001) Rescuing desmoplakin function in extra-embryonic ectoderm reveals the importance of this protein in embryonic heart, neuroepithelium, skin and vasculature. *Development* 128: 929-941.
140. Cho K, Vaught TG, Ji H, Gu D, Papasakelariou-Yared C, Horstmann N, Jennings JM, Lee M, Sevilla LM, Kloc M, Reynolds AB, Watt FM, Brennan RG, Kowalczyk AP, McCrea PD (2010) *Xenopus* Kazrin interacts with ARVCF-catenin, spectrin and p190B RhoGAP, and modulates RhoA activity and epithelial integrity. *J Cell Sci* 123: 4128-4144.
141. Paratore C, Brugnoli G, Lee HY, Suter U, Sommer L (2002) The role of the Ets domain transcription factor Erm in modulating differentiation of neural crest stem cells. *Dev Biol* 250: 168-180.
142. de Launoit Y, Audette M, Pelczar H, Plaza S, Baert JL (1998) The transcription of the intercellular adhesion molecule-1 is regulated by Ets transcription factors. *Oncogene* 16: 2065-2073.
143. Ray-Gallet D, Mao C, Tavitian A, Moreau-Gachelin F (1995) DNA binding specificities of Spi-1/PU.1 and Spi-B transcription factors and identification of a Spi-1/Spi-B binding site in the c-fes/c-fps promoter. *Oncogene* 11: 303-313.
144. Chi P, Chen Y, Zhang L, Guo X, Wongvipat J, Shamu T, Fletcher JA, Dewell S, Maki RG, Zheng D, Antonescu CR, Allis CD, Sawyers CL

- (2010) ETV1 is a lineage survival factor that cooperates with KIT in gastrointestinal stromal tumours. *Nature* 467: 849-853.
145. Bosc DG, Goueli BS, Janknecht R (2001) HER2/Neu-mediated activation of the ETS transcription factor ER81 and its target gene MMP-1. *Oncogene* 20: 6215-6224.
146. Cai C, Hsieh CL, Shemshedini L (2007) c-Jun has multiple enhancing activities in the novel cross talk between the androgen receptor and Ets variant gene 1 in prostate cancer. *Mol Cancer Res* 5: 725-735.
147. Gu D, Tonthat NK, Lee M, Ji H, Bhat KP, Hollingsworth F, Aldape KD, Schumacher MA, Zwaka TP, McCrea PD (2011) Caspase-3 cleavage links delta-catenin to the novel nuclear protein ZIFCAT. *J Biol Chem* 286: 23178-23188.
148. Achtstatter T, Fouquet B, Rungger-Brandle E, Franke WW (1989) Cytokeratin filaments and desmosomes in the epithelioid cells of the perineurial and arachnoidal sheaths of some vertebrate species. *Differentiation* 40: 129-149.
149. Funayama N, Fagotto F, McCrea P, Gumbiner BM (1995) Embryonic axis induction by the armadillo repeat domain of beta-catenin: evidence for intracellular signaling. *J Cell Biol* 128: 959-968.
150. Klaus A, Birchmeier W (2008) Wnt signalling and its impact on development and cancer. *Nat Rev Cancer* 8: 387-398.
151. Clevers H (2006) Wnt/beta-catenin signaling in development and disease. *Cell* 127: 469-480.

152. Hong JY, Park JI, Cho K, Gu D, Ji H, Artandi SE, McCrea PD (2010) Shared molecular mechanisms regulate multiple catenin proteins: canonical Wnt signals and components modulate p120-catenin isoform-1 and additional p120 subfamily members. *J Cell Sci* 123: 4351-4365.
153. Israely I, Costa RM, Xie CW, Silva AJ, Kosik KS, Liu X (2004) Deletion of the neuron-specific protein delta-catenin leads to severe cognitive and synaptic dysfunction. *Curr Biol* 14: 1657-1663.
154. Sive HL, R.M. Grainger, and R.M. Harland (2000) Early Development of *Xenopus laevis* - a Laboratory Manual. Cold Spring Harbor: Cold Spring Harbor Laboratory Press.
155. McMillan JR, Haftek M, Akiyama M, South AP, Perrot H, McGrath JA, Eady RA, Shimizu H (2003) Alterations in desmosome size and number coincide with the loss of keratinocyte cohesion in skin with homozygous and heterozygous defects in the desmosomal protein plakophilin 1. *J Invest Dermatol* 121: 96-103.
156. Green KJ, Simpson CL (2007) Desmosomes: new perspectives on a classic. *J Invest Dermatol* 127: 2499-2515.
157. Snider P, Olaopa M, Firulli AB, Conway SJ (2007) Cardiovascular development and the colonizing cardiac neural crest lineage. *ScientificWorldJournal* 7: 1090-1113.
158. Nolze A, Schneider J, Keil R, Lederer M, Huttelmaier S, Kessels MM, Qualmann B, Hatzfeld M (2013) FMRP regulates actin filament organization via the armadillo protein p0071. *RNA* 19: 1483-1496.

159. Clarke JD, Hayes BP, Hunt SP, Roberts A (1984) Sensory physiology, anatomy and immunohistochemistry of Rohon-Beard neurones in embryos of *Xenopus laevis*. *J Physiol* 348: 511-525.
160. Kuriyama S, Mayor R (2008) Molecular analysis of neural crest migration. *Philos Trans R Soc Lond B Biol Sci* 363: 1349-1362.
161. Christiansen JH, Coles EG, Wilkinson DG (2000) Molecular control of neural crest formation, migration and differentiation. *Curr Opin Cell Biol* 12: 719-724.
162. Basch ML, Bronner-Fraser M (2006) Neural crest inducing signals. *Adv Exp Med Biol* 589: 24-31.
163. Pleger B, Ruff CC, Blankenburg F, Kloppel S, Driver J, Dolan RJ (2009) Influence of dopaminergically mediated reward on somatosensory decision-making. *PLoS Biol* 7: e1000164.
164. Borrmann CM, Mertens C, Schmidt A, Langbein L, Kuhn C, Franke WW (2000) Molecular diversity of plaques of epithelial-adhering junctions. *Ann N Y Acad Sci* 915: 144-150.
165. Hong JY, Park JI, Lee M, Munoz WA, Miller RK, Ji H, Gu D, Ezan J, Sokol SY, McCrea PD (2012) Down's-syndrome-related kinase Dyrk1A modulates the p120-catenin-Kaiso trajectory of the Wnt signaling pathway. *J Cell Sci* 125: 561-569.
166. Miller RK, Hong JY, Munoz WA, McCrea PD (2013) Beta-catenin versus the other armadillo catenins: assessing our current view of canonical Wnt signaling. *Prog Mol Biol Transl Sci* 116: 387-407.

167. Saito-Diaz K, Chen TW, Wang X, Thorne CA, Wallace HA, Page-McCaw A, Lee E (2013) The way Wnt works: components and mechanism. *Growth Factors* 31: 1-31.
168. Mosimann C, Hausmann G, Basler K (2009) Beta-catenin hits chromatin: regulation of Wnt target gene activation. *Nat Rev Mol Cell Biol* 10: 276-286.
169. Brown LA, Amores A, Schilling TF, Jowett T, Baert JL, de Launoit Y, Sharrocks AD (1998) Molecular characterization of the zebrafish PEA3 ETS-domain transcription factor. *Oncogene* 17: 93-104.
170. Oh S, Shin S, Lightfoot SA, Janknecht R (2013) 14-3-3 Proteins Modulate the ETS Transcription Factor ETV1 in Prostate Cancer. *Cancer Res.*
171. Montross WT, Ji H, McCrea PD (2000) A beta-catenin/engrailed chimera selectively suppresses Wnt signaling. *J Cell Sci* 113 (Pt 10): 1759-1770.
172. Cho K, Lee M, Gu D, Munoz WA, Ji H, Kloc M, McCrea PD (2011) Kazrin, and its binding partners ARVCF- and delta-catenin, are required for *Xenopus laevis* craniofacial development. *Dev Dyn* 240: 2601-2612.
173. Bilinski SM, Jaglarz MK, Dougherty MT, Kloc M (2010) Electron microscopy, immunostaining, cytoskeleton visualization, in situ hybridization, and three-dimensional reconstruction of *Xenopus* oocytes. *Methods* 51: 11-19.
174. Wallingford JB (2010) Preparation of fixed *Xenopus* embryos for confocal imaging. *Cold Spring Harb Protoc* 2010: pdb prot5426.

175. Rain JC, Cribier A, Gerard A, Emiliani S, Benarous R (2009) Yeast two-hybrid detection of integrase-host factor interactions. *Methods* 47: 291-297.
176. Hollenhorst PC, Ferris MW, Hull MA, Chae H, Kim S, Graves BJ (2011) Oncogenic ETS proteins mimic activated RAS/MAPK signaling in prostate cells. *Genes Dev* 25: 2147-2157.
177. Miller RK, Canny SG, Jang CW, Cho K, Ji H, Wagner DS, Jones EA, Habas R, McCrea PD (2011) Pronephric tubulogenesis requires Daam1-mediated planar cell polarity signaling. *J Am Soc Nephrol* 22: 1654-1664.
178. Taube JH, Allton K, Duncan SA, Shen L, Barton MC (2010) Foxa1 functions as a pioneer transcription factor at transposable elements to activate Afp during differentiation of embryonic stem cells. *J Biol Chem* 285: 16135-16144.

VITA

William Muñoz was born in Houston, Texas, on July 17th 1985 to Guillermo And Susan Muñoz. After attending Katy High School, he pursued a Bachelor's of Science degree in Biochemistry at The University of Texas at Austin, which he earned in 2007. While pursuing his undergraduate studies he conducted research on the yeast deubiquitinating enzyme Ubp2 at The University of Texas at Austin Institute for Cellular and Molecular Biology. In 2007 William initiated his Doctor of Philosophy studies in Biomedical Science at The University of Texas – Houston Graduate School of Biomedical Sciences. William currently lives with his wife, Jennifer Muñoz, J.D., in Kansas City, Missouri.

Permanent address:

20602 Cascading Brook Ct., Cypress, TX 77433